BERICHTE
aus dem Fachbereich Geowissenschaften
der Universität Bremen

No. 199

Jahn, B.

MID TO LATE PLEISTOCENE VARIATIONS OF MARINE PRODUCTIVITY IN AND TERRIGENOUS INPUT TO THE SOUTHEAST ATLANTIC

Berichte, Fachbereich Geowissenschaften, Universität Bremen, No. 199,
97 pages, Bremen 2002

ISSN 0931-0800

Mid to Late Pleistocene Variations of Marine Productivity in and Terrigenous Input to the Southeast Atlantic

Dissertation
zur Erlangung des
Doktorgrades der Naturwissenschaften

im Fachbereich Geowissenschaften
der Universität Bremen

vorgelegt von
Britta Jahn

Bremen 2002

SUMMARY

During Ocean Drilling Program (ODP) Leg 175, the Sites 1075, 1077, and 1082 were drilled off the western coast of Africa (Congo and Namibia). The goal was to reconstruct the Pleistocene history of the Angola-Benguela Current system (ABC-system) between about 5°S and 22°S. The investigated area is one of the five largest continental margin upwelling systems in the world, with analogues off Peru, California, northwest Africa and in the northeastern Arabian Sea. The ABC-system is characterized by organic-rich sediments that yield an outstanding record of productivity history.

One major goal of the present work is to document fluctuations in marine productivity and terrigenous input in relationship to large-scale climate changes within the Pleistocene, including the onset of the mid-Pleistocene Revolution (MPR) associated to Northern Hemisphere glaciation. The MPR covers the transition from the dominant 41 k.y.-cycle of obliquity during the mid-Pleistocene to the dominant 100-k.y. cycle of eccentricity during the late Pleistocene, that has been observed in many marine paleoclimatic records.

In order to improve the knowledge about paleoclimatic events in the ABC-system we used X-ray fluorescence (XRF) Core Scanner analyses of Fe as a proxy for terrigenous input in combination with total organic carbon mass accumulation rates (TOC MAR) and $\delta^{13}C_{org}$-isotope values as indicators for marine productivity. Furthermore, we used the alkenone method to evaluate variations in past sea surface temperature (SST).

The investigated sites have high sedimentation rates (~10 cm / 1000 yr), which offers an opportunity to develop detailed paleoceanographic records for 1 to 2 Ma long records.

The northernmost Sites (1075 and 1077) are located in a complex environment dominated by (1) the freshwater input from the Congo River, (2) the seasonal coastal upwelling and associated filaments and eddies moving offshore, and (3) the incursions of open ocean waters. The reconstruction of paleoproductivity and terrigenous signals suggest that both low-latitude (precessional) and high-latitude (ice-mass related) cycles play an important role in the response to insolation forcing in the sediment deposition of the northern Congo Fan region. It seems that glacial-interglacial boundary conditions may have influenced the magnitude of precessional climatic variations in the tropical latitudes of Africa. Before 0.9 Ma, eccentricity modulation of the low-latitude precessional insolation directly influenced the local climate and lead to changes in the southern African monsoon system. After 0.9 Ma, paleoproductivity and terrigenous input is largely controlled by glacial-interglacial cycles with a 100-k.y. oscillation associated to Northern Hemisphere glaciation.

Site 1082 is located on the upper continental margin off Namibia. Accordingly, this site records the variability of wind transport evidenced by the eolian, terrigenous input and changes in marine productivity in the northern Benguela Current. The terrigenous input of eolian dust and paleoproductivity exhibit generally higher amplitude variations from 1.5 to 0.58 Ma. At 0.58 Ma variations in paleoproductivity and wind transport abruptly decreased in their amplitude for the 100-k.y. period. Fe intensity and TOC MAR show strong influences of the 100-k.y. and 41-k.y. periods and support the assumption that strong ice-buildup in the Northern Hemisphere is the domi-

nant trigger for climate changes in the northern Benguela system while Southern Hemisphere insolation plays only a secondary role.

The Benguela Current region were also studied to evaluate variations of sea-surface temperature (SST). For this purpose we used two sediment cores from the upper continental margin off Namibia (Site 1082) and from the deeper continental margin in the Mid Cape Basin (GeoB 1722-1). Alkenone-based SSTs were compared with $\delta^{18}O$ records established on planktonic foraminifera. SST pattern in the northern and southern Benguela Current system are in a good agreement with each other and generally matches the climate variations revealed by the $\delta^{18}O$ records. Alkenone SSTs and $\delta^{18}O$ values show a trend towards negative isotope ratios especially during glacial periods for the past 0.45 m.y., pointing out increasingly warmer sea-surface temperatures during glacials towards the end of the Pleistocene. The late Pleistocene warming in the Benguela Current region over the past 0.45 m.y. is indicated as a response to a weakening in the thermohaline circulation.

ZUSAMMENFASSUNG

Während der Ocean Drillin Program (ODP) Ausfahrt 175 wurden die Lokationen 1075, 1077 und 1082 vor der Westküste Afrikas (Kongo und Namibia) erbohrt. Das Ziel der Ausfahrt war, die Geschichte des Angola-Benguela-Strom Systems ("ABC-System") zwischen 5°S und 22°S zu rekonstruieren. Das Untersuchungsgebiet gehört, neben den Auftriebsgebieten vor Peru und Kalifornien, zu den größten Auftriebsregionen der Welt. Die Sedimente des "ABC-Systems" zeichnen sich durch hohe Gehalte an organischem Material aus und dokumentieren somit die zeitlichen Veränderungen in der Paläoproduktivität.

Ein wichtiger Aspekt dieser Arbeit besteht darin, die Schwankungen in der marinen Produktivität und dem terrigenen Eintrag in Beziehung zu den langanhaltenden Klimaveränderungen des Pleistozäns zu setzen. Ein bedeutender Klimawechsel stellt dabei die Abkühlungsphase im Mittleren Pleistozän dar, die sogennante "mid-Pleistocene Revolution". Dieser Klimaumschwung ist durch den Übergang vom dominanten 41.000-Jahre-Zyklus während des Frühen Pleistozäns, zum dominanten 100.000-Jahre-Zyklus während des Späten Pleistozäns gekennzeichnet und steht im Zusammenhang mit starken Vereisungszyklen in der Nordhemisphäre.

Die mit Röntgen-Fluoreszenz-Analyse ermittelten Fe-Intensitäten im Sediment dienen als Indikator für den terrigenen äolischen Eintrag. Die Massenakkumulationsraten des organischen Kohlenstoffs und $\delta^{13}C_{org}$-Isotope aus den Sedimentablagerungen dienen als Indikatoren der marinen Produktivität. Die Oberflächenwassertemperaturen wurden anhand von Alkenonkonzentrationen im Sediment ermittelt.

Die Bohrlokationen zeichnen sich durch eine relativ hohe Sedimentationsrate aus (ca. 10 cm / 1000 Jahre) und sind deshalb hervorragend für detaillierte paläozeanographische Untersuchungen geeignet.

Die nördlichsten Bohrlokationen 1075 und 1077 werden von folgenden Faktoren geprägt: (1) vom

Süßwassereinfluss des Kongos, (2) von dem saisonalen Küstenauftrieb und den damit verbundenen Filamenten und Verwirbelungen ("Eddies") sowie (3) von den Wassermassen des offenen Ozeans. Die rekonstruierten Schwankungen in der Paläoproduktivität und des terrigenen Eintrags zeigen, dass sowohl die Zyklen der niederen Breiten (Präzession) als auch die Zyklen der höheren Breiten (Vereisungszyklen) eine wichtige Rolle in den Sedimentablagerungen des nördlichen Kongofächers spielen. Es scheint, dass die glazialen-interglazialen Randbedingungen die Stärke der präzessionsgesteuerten Klimavariationen in den tropischen Breiten Afrikas beeinflusst haben könnten. Vor ca. 0.9 Mio. J.v.h. beeinflusste die Modulation der Einstrahlung der niederen Breiten, durch die Ekzentrizität das lokale Klima und führte zu Veränderungen im südlichen afrikanischen Monsun-System. Nach 0.9 Mio. J.v.h. werden die Paläoproduktivität und der terrigene Eintrag weitestgehend über glaziale-interglaziale Zyklen mit einer Periodizität von 100.000 J. in Verbindung mit der Nordhemisphärenvereisung kontrolliert

Die Bohrlokation 1082 liegt am oberen Kontinentalhang vor Namibia. An den Sedimenten dieser Lokation lassen sich die Veränderungen im terrigenen, äolischen Eintrag sowie in der marinen Produktivität rekonstruieren.

Im nördlichen Benguela Strom ist die Amplitudenvariabilität des terrigenen, äolischen Eintrags von Staub und die Paläoproduktivität zwischen 1.5 - 0.58 Mio. J.v.h am stärksten. Ab ca. 0.58 Mio. J.v.h. zeigen beide Indikatoren eine abrupte Verschiebung zu geringeren Amplituden mit einer Periodizität von 100.000 Jahren. Die Sauerstoffisotopenverhältnisse zeigen für die letzten 0.65 Mio. Jahre einen Trend mit zunehmend negativen $\delta^{18}O$-Werten, besonders während der Kaltzeiten an, was auf einen Temperaturanstieg im Oberflächenwasser während der Kaltzeiten hinweist. Die Fe-Intensitäten und die TOC MAR-Daten zeigen einen starken Einfluss der 100.000-Jahre und 41.000-Jahre-Zyklen und unterstützen die Annahme, dass die Nordhemisphärenvereisung der entscheidende Auslöser für die Klimaveränderungen im nördlichen Benguela Strom-System war während die Sonneneinstrahlung auf der Südhemisphäre eine untergeordnete Rolle spielte.

Im Benguela-Strömungssystem wurden auch Abschätzungen in den Variationen der Oberflächenwassertemperaturen (SST) für die letzten 1.2 Mio. Jahre rekonstruiert. Dafür wurden zwei Sedimentkerne, vom oberen Kontinentalrand vor Namibia (Site 1082) und vom tieferen Kontinentalrand aus dem mittleren Kap Becken (GeoB 1722-1) untersucht. Die aus den Alkenonen ermittelten SST-Werte wurden mit den planktischen $\delta^{18}O$-Werten verglichen und zeigen eine gute Übereinstimmung. Die Meeresoberflächentemperaturen und die Sauerstoffisotope zeigen einen Erwärmungstrend für die letzten 0.45 Mio. Jahre, mit wärmeren Temperaturen bzw. leichteren Isotopen vor allem während der Glaziale. Die Erwärmung im Benguela Strömungssystem ist wahrscheinlich auf eine Abschwächung der thermohalinen Zirkulation zurückzuführen.

TABLE OF CONTENTS

1. INTRODUCTION

The ocean's role in climatic change through heat transport and control of CO_2 is increasingly being recognized. This awareness, and the urgency that must be accorded the attempt to understand the mechanisms of climate change, have led to the initiation of large integrated efforts in paleoceanography.

The Angola-Benguela Current needs to be studied because of its importance in the global ocean-carbon cycle. Eastern boundary upwelling is strongly involved in the marine carbon cycle and helps to set the partial pressure of carbon dioxide (pCO_2) by "biological pumping" (removal of carbon from surface waters to deep waters) and by "biological dumping" (removal of organic carbon to the sediments) (e.g., Berger et al., 1989; Boyle and Keigwin, 1987). Changes in the efficiency of biological pumping is a crucial factor for the explanation of short-term fluctuations in the atmospheric CO_2 (Broecker, 1982). Vincent and Berger (1985) have postulated that carbon dumping by coastal upwelling is responsible for rapid changes in the general level of atmospheric pCO_2. They propose climatic preconditioning by upwelling-induced carbon extraction from the ocean-atmosphere system for the beginning of the modern ice-cap dominated world. Their argument is based on the observation that carbon isotopes in deep-sea benthic foraminifers become enriched in ^{13}C when organic-rich phosphatic sediments begun to accumulate around the Pacific margins. In this view, eastern boundary upwelling, and therefore upwelling off Angola and Namibia has global implications for the long-term history of the carbon cycle and climate. If we are to asses the effects of changes in productivity on the CO_2 content of the atmosphere, the interrelationship between ocean circulation, nutrient transport, and the sedimentation of organic compounds must be established for the productivity regions off Angola and Namibia. The enhanced primary production is combined with higher sedimentation rates, which encourage the preservation of organic material.

The coastal carbon enriched sediments contain also terrestrial signals, which reflect the climate and the vegetation of the adjacent continent. The variations of marine and terrestrial sedimentation allow us to reconstruct paleoclimatic and paleoceanographic conditions for the Pleistocene. For this purpose we examined the eolian and fluvial terrigenous input of iron as a proxy for the strength in the southeast trades as well as monsoon intensity and organic carbon as an indicator for paleoproductivity. Variations of sea-surface temperatures were estimated by means of the unsaturation ratio of C_{37} alkenones. With the help of these proxies we are able to get detailed information about the origin and the preservation of the terrestrial and organic material.

This study focus on the interplay between high-latitude and low-latitude Milankovitch forcing (obliquity versus precession), the role of the 100 k.y. oscillation, the effects of the mid-Pleistocene climate step (near 0.9 Ma) on upwelling and African climate, and the implications of changes in productivity for the Pleistocene.

1.1 PALEOCLIMATE AND PALEOPRODUCTIVITY

Previous work in the Congo Fan area for the late Quaternary has clearly demonstrated where sediment records reveal changes not only of the general climatic and oceanographic processes, but also reflect variations based on local features such as coastal or oceanic upwelling, river discharge, and the inflow of surface waters from equatorial or southern ocean sources, in addition to prevailing monsoonal and trade wind forcing (e.g., Gingele et al., 1998; Schneider et al., 1997, 1996, 1994; Jansen, 1985; Jansen et al.,1984). The Congo Fan sediments are characterized by high opal contents (Müller and Schneider, 1993) related to riverine input of silicate and to river-induced estuarine upwelling (van Bennekom, 1996). Schneider et al. (1994) emphasized that major productivity changes off the Congo follow the pattern determined by wind-forcing and oceanic subsurface nutrient supply rather than merely reflecting fertility changes induced by river discharge of nutrients.

Preceding studies of the late Quaternary upwelling history of the northern part of the Benguela upwelling system has been examined in much more detail (e.g., Diester-Haass, 1985a, b, 1988; Diester-Haass et al., 1986, 1990, 1992; Diester-Haass and Rothe, 1987; Dean and Gardner, 1985; Hay and Brock, 1992). Knowledge about the latest Miocene to latest Pliocene history of upwelling is derived from Sites 362 and 532, drilled during Legs 40 and 75, of the Deep Sea Drilling Project (DSDP) (e.g., Diester-Haass et al., 1990, 1992). During Leg 40, shipboard scientists (Bolli, Ryan et al., 1978) and subsequent investigators (Diester-Haass and Schrader, 1979; Siesser, 1980) recognized that the high abundances of diatoms and organic carbon were linked to upwelling and suggested that they reflected the onset and developement of the Benguela upwelling system. The sediments of Leg 75 were interpreted by the shipboard scientists (Hay, Sibuet et al., 1984) to be the result of an expanded or displaced Benguela upwelling system.

A number of studies have reconstructed southwestern African paleoclimate by studying fine-grained terrigenous components, pollen, phytoliths and freshwater diatoms transported to the ocean floor (e.g., Van Zinderen Bakker, 1984; Diester-Haass, 1985; Jansen, 1990; Gingele, 1996; Shi and Dupont, 1997). These studies show that changes in the trade wind system and changes in continental climate of southwestern Africa during the late Quaternary have had large effects on the transport of wind-blown material to the SE Atlantic Ocean. However, there is no consensus on the southwestern African climate history. For example, Van Zinderen Bakker (1984) concludes that no significant change in rainfall occurred in southwestern Africa during the past 18 k.y., whereas according to Shi and Dupont (1997) the LGM in this region was characterized by relatively cold and arid conditions. In contrast, Stuut et al. (in press) concluded that the LGM was wetter.

Latest work of ODP Leg 175 (e.g., Dupont et al., 2001; Marlow et al., 2000; Lange et al., 1999) examined several sites between 5° and 30°S (1075, 1081, 1082, 1083, 1084, and 1085). Dupont et al. (2001) occupied palynological records in the northern Congo Fan area (Site 1075) and found evidence for an environmental change in equatorial Africa around 1.05 Ma. Further Dupont et al. (2001) concluded that between 0.9 to 0.6 Ma, interglacials were charaterized by warm and dry conditions and glacial periods were characterized by cool and humid conditions, while during the

past 0.2 m.y. glacials were cold and dry and interglacials warm and humid. Lange et al. (1999) investigated sediments between 20° and 30°S in the Benguela Current within the late Pliocene and early Quaternary. Their investigations indicated a distinct opal maximum (MDM; Matuyama Diatom Maximum) centered from around 2.6 to 2.0 Ma, and followed a rapid increase of diatom deposition near 3.1 Ma. Lange et al. (1999) concluded that the MDM developed during a time of sustained Southern Ocean influence (3.2 to 1.6 Ma), probably reflecting a period of seasonally-pulsed advection of subantartic waters into the Benguela Ocean Current. Marlow et al. (2000) evaluated sea surface temperatures (SST) derived from alkenones in the Benguela upwelling system (Site 1084) for the past 4.5 m.y. They documented that temperatures in the region have declined by about 10°C since the past 3.2 m.y. and records of paleoproductivity suggested that this cooling was associated with an increase in wind-driven upwelling tied to a shift from relatively stable global warmth during the mid-Pliocene to the high-amplitude glacial-interglacial cycles of the late Quaternary. Other studies (e.g., Schefuss et al., 2001; Güntner, 2000) focussed on geochemical signals as indicators for paleoclimatic and paleoceanographic conditions in the northern Congo Fan area for the late Quaternary. Güntner (2000) suggested that increased mass accumulation rates of marine biomarkers in the sediments of the northern Congo Fan area indicated an increase of marine productivity during glacial periods. Simultaneously, increased concentrations of long-chain n-alkanes and n-alcohols indicated enhanced terrigenous input within glacial periods.

The introduced studies of the Angola-Benguela-Current system give a short overview about the work who was already done. Apparently, most of the authors investigated the plaleoclimatic and paleoceanographic changes during the late Quaternary and/or within the Pliocene/Pleistocene boundary but less work was used on investigations during the mid-Pleistocene.

1.2 MAIN OBJECTIVES

The aim of this study is to reconstruct the history of the Angola-Benguela Current system for the Pleistocene. Changes in marine productivity and the terrigenous input by eolian and fluvial transport of Fe are supposed to reflect changes in regional land climate. The emphasis of this studies lies on the reconstruction of geochemical proxies ($\delta^{18}O$, Fe intensity, organic carbon, $\delta^{13}C_{org}$, and SSTs derived from C_{37} alkenones).

The main objectives in the Congo fan area are:

* to reconstruct the changing influence of the Congo River and marine contributions to the dynamics of the region for the Pleistocene
* to evaluate orbital frequencies of productivity and the fluvial terrigenous input in comparison with monsoonal forcing and Northern Hemisphere climate changes

The main objectives in the Walvis Bay area off Namibia are:

* to reconstruct the changing influence of the southeast trades, and paleoproductivity in the northern Benguela Current for the Pleistocene
* to estimate variations in sea surface temperatures derived from sedimentary alkenones in the northern Benguela Current system for the Pleistocene
* to evaluate orbital frequencies of productivity and wind transport in comparison with Northern Hemisphere climate changes and Southern Hemisphere insolation forcing

The research that was conducted to answer these questions resulted in the preparation of three manuscripts. These manuscripts will be submitted to international journals.

I. Jahn, B., Donner, B., Müller, P.J., Röhl, U., Schneider, R.R., and Wefer, G. **Terrigenous Climatic Signals And Changes In Marine Productivity From Sediments Of The Congo Fan Region For The Last 1.7 m.y.**

The aim of this study was to reconstruct the changing influence of the Congo River in sediments of the northern Congo Fan area. For this issue we used iron (Fe intensity) as a proxy for variations in the fluvial supply of the Congo River and total organic carbon mass accumulation rates (TOC MAR) as an indicator for variations in marine productivity. We utilized $\delta^{13}C_{org}$ isotopes of the organic matter to give an idea about the estimated share of marine and terrestrial organic carbon content. Filter experiments show the results of our proxy records related to high- and low-latitude (obliquity versus precession) Milankovitch frequencies and the influence of the 100 k.y. oscillation.

II. Jahn, B., Donner, B., Müller, P.J., Röhl, U., Schneider, R.R., and Wefer, G. **Variability Of**

Terrestrial Input And Marine Productivity In The Northern Benguela Current Associated With Orbital Cycles Over The Last 1.5 m.y.
(Submitted to Palaeogeography, Palaeoclimatology, Palaeoecology)

This study was conducted in order to reconstruct variations in the terrestrial eolian input and marine productivity in the northern Benguela Current for the Pleistocene (past 1.5 m.y.). We used Fe-intensity values as a proxy for terrigenous eolian transport from the Namib Desert in relation to variations of the southeast trade winds. Further we applied total organic carbon mass accumulation rates (TOC MAR) as an indicator for changes in paleoproduvtivity. We used band-pass filter to examine the evolution of the Milankovitch cycles over the time and compare our proxy data in relation to Northern Hemisphere glaciation (ODP 659 $\delta^{18}O$ record) and to Southern Hemisphere winter insolation. Under modern conditions, southeast trade winds in the eastern South Atlantic are strogest during austral winter and are due to variations in the atmospheric constellation of high pressure troughs over the African continent. Therefore, trade wind intensities may also be linked to orbital variations in Southern Hemisphere winter insolation during the Pleistocene when the southeast trade winds are strongest.

III. Jahn, B., Müller, P.J., Schneider, R.R., von Storch, I., and Wefer, G. **Mid To Late Pleistocene Temperature Variability In The Benguela Current system Derived From Alkenones**

In this study we evaluate variations of sea surface temperatures (SST) derived from alkenones in the Benguela Current region for the past 1.2 m.y. For this purpose we examined sediments of two cores from the upper continental margin off Namibia and from the deep sea of the mid Cape Basin. We compared the alkenone-based SSTs with the planktonic $\delta^{18}O$ values of both sediment cores. Both SST records are in a good agreement with each other and generally match the climatic pattern revealed by oxygen isotopes. Furthermore, we wanted to evaluate the influence of the relatively warm Agulhas Current to the Benguela Current system over long-term periods. We also discussed a warming of the eastern South Atlantic as a respnse to a weakening of the cross-equatorial heat transport from the South to the North Atlantic.

1.3 MILANKOVITCH THEORY

Milankovitch theory posits that summer insolation in high northern latitudes is the crucial factor in allowing the buildup of ice sheets, or else forcing their removal. What we now call Milankovitch theory made its public debut in the writings of Köppen and Wegener (1924) and Milankovitch (1930) and more recently by Berger (1988). An excellent account of the way in which this hypothesis developed into a crucial theory in paleoclimatology is given by Imbrie and Imbrie (1979).
Acceptance of Milankovitch theory came as a result of the discovery of cyclic sedimentation in deep-sea sediments (Arrhenius, 1952), especially within oxygen isotope records (Emiliani, 1955), which are closely tied to variations in ice mass.
Variations in insolation have occurred related to the degree of orbital eccentricity around the Sun, in the axial tilt (obliquity) of the Earth from the plane of the ecliptic, and in the timing of the perihelion (the Earth is closest to the Sun) with respect to seasons of the Earth (precession of the equinoxes) (Fig. 1).

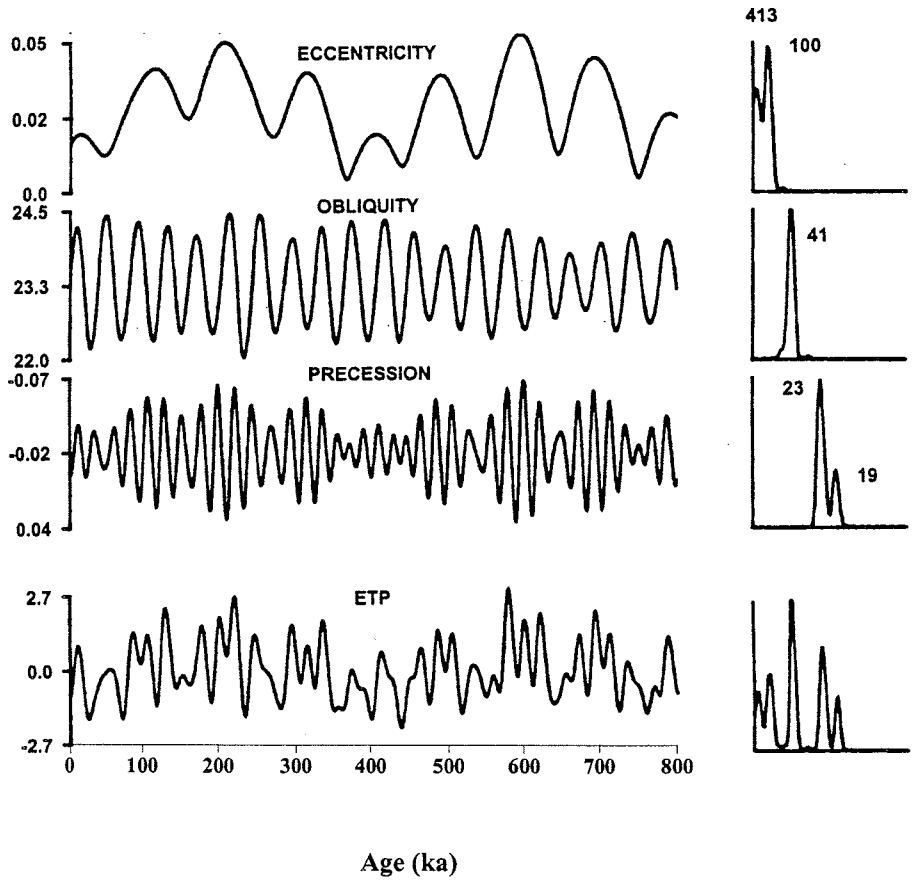

Figure 1: Variations of eccentricity, obliquity, precession, and the combination of all three factors (ETP) over the last 800 k.y. with their principal periodic characteristics indicated by the power spectrum to the right of each time series (modified after Imbrie et al., 1993).

Variations in orbital eccentricity are quasi-periodic with an average period length of ~95.8 k.y. over the past 5 m.y. Eccentricity variations affect the relative intensities of the seasons, which implies an opposite effect in each hemisphere. Changes in axial tilt are periodic with a mean period of 41 k.y. The angle of inclination has varied from 21.8° to 24.4° and defines the latitudes of the polar circles (Arctic and Antarctic). Changes in obliquity have relatively little effect on radiation receipts at low latitudes but the effect increases toward the poles. As obliquity increases, summer radiation receipts at high latitudes increase. Changes in the seasonal timing of perihelion and aphelion (the Earth is farthest away from the Sun) result from a slight wobble in the Earth's axis of rotation as it moves around the Sun (Fig. 2).

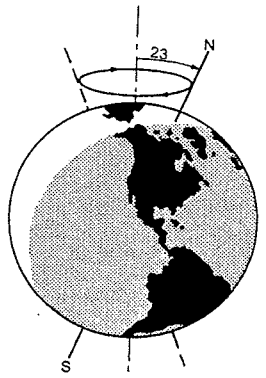

Figure 2: The Earth wobbles slightly on its axis (due to the gravitational pull of the Sun and Moon on the equatorial bulge of the Earth). In effect, the axis moves slowly around a circular path and completes one revolution every 23 k.y. This effect is independent of changes in the angle of tilt (obliquity) of the Earth (from Imbrie & Imbrie, 1979).

The effect of the wobble (which is independent of variations in axial tilt) is to change the timing of the solstices and equinoxes relative to the extreme positions the Earth occupies on its elliptical path around the Sun (precession of the equinoxes) (Fig. 3). Clearly, the effects of precession of the equinoxes on radiation receipts will be modulated by the variations in eccentricity. The solar radiation receipts of low latitudes are affected mainly by variations in eccentricity and precession, whereas higher latitudes are affected mainly by variations in obliquity.

The periods mentioned for each orbital parameter (95.8 k.y., 41 k.y., and 21.7 k.y. for eccentricity, obliquity and precession, respectively) are averages of the principal periodic terms in the equations used to calculate the long-term changes in orbital parameters. For the precessional parameter the mean period is 21.7 k.y., but some paleoclimatic records show the principal ~19- and ~23 k.y. periods separately (Hays et al., 1976). Similarly, the mean period of changes in eccentricity is 95.8 k.y. but it may be possible to detect separate periods of 95- and 123 k.y. in long-resolution marine records (Wigley, 1976). Eccentricity also has a longer-term periodicity of ~412 k.y. (Imbrie et al., 1993). Furthermore the relative importance of all these periods and the climatic response may have changed over time. For example, the 19 k.y. precessional and 100 k.y. eccentricity cycles were more significant in the forcing prior to 600 ka BP (Imbrie et al., 1993). During the last one million years the 100-k.y. period in geological records increased in amplitude yet over the same interval the main period associated with eccentricity shifted to lower frequencies (~412 k.y.).

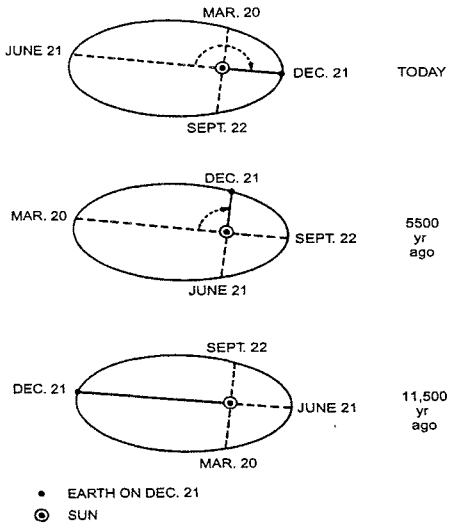

Figure 3: As a result of a wobble in the Earth's axis the position of the equinox (March 20 and September 22) and solstice (June 21 and December 21) change slowly around the Earth's elliptical orbit, with a period of 23 k.y. Thus 11 ka ago the Earth was at perihelion at the time of the summer solstice whereas today the summer solstice coincides with aphelion (from Imbrie & Imbrie, 1979).

1.4 THE MID-PLEISTOCENE CLIMATE SHIFT

The early Quaternary is characterized by roughly equally spaced sinusoidal variations, with a period of ca. 41 k.y. The late Quaternary shows seemingly less regular fluctuations, with larger amplitudes and a period near 100 k.y. The mid-Quaternary switch in climatic variability from an obliquity-dominated mode to an eccentricity-dominated one dated around 0.9 Ma (Berger and Jansen, 1994; Raymo et al., 1997). The so called mid-Pleistocene Revolution (MPR after Berger and Jansen, 1994) or mid-Pleistocene transition (MPT after Raymo et al., 1997) represents one of the major puzzles in Quaternary research (e.g., Ruddiman et al., 1986; 1989; Ruddiman and Raymo, 1988; De Blonde and Peltier, 1991; Berger and Jansen, 1994; Mudelsee and Stattegger, 1997; Raymo et al., 1997). Questions arising concern the appearence of the transition, as well as its dynamics: The first is the cause of the 100-k.y. periodicity of eccentricity, which is by far the weakest insolation forcing, and the second is why this dominance over the stronger precession and obliquity cycles began relatively suddenly after 0.9 Ma. These observations, and their lack of satisfactory explanation, are referred to the "100K problem". A condensed history of work on the 100K problem is presented in Imbrie et al. (1993). This work together with other recent studies (e.g., Saltzman and Maasch, 1991; DeBlonde and Peltier, 1991; Saltzman and Verbitsky, 1994; Berger and Jansen, 1994; Raymo et al., 1997) focus on the role played by large ice sheets in amplifying the weak eccentriccity forcing.

According to Berger and Jansen (1994) the MPR is similar to the onset of the ice ages, which may be understood as a threshold phenomenon. A long-term cooling trend, from orogenesis and uplift, reaches a point where ice sheets can grow in high northern latitudes (Ruddiman and Raymo, 1988). The result is a "sudden" onset of ice-buildup (trough albedo amplification, largely), from a "gradual" shift in boundary conditions (Berger and Jansen, 1994). During the growth of large, and therefore, unstable ice sheets to a long-term secular decrease in atmospheric CO_2 levels, driven by internal tectonic processes.

In this study, we focus on the transition from a world dominated by the 41-k.y. obliquity (tilt) cycle (Prell, 1982; Raymo et al., 1989) to the more familiar 100-k.y. world of the late Pleistocene. Previous studies of the MPR have focused almost exclusively on the constraints provided by oxygen isotope records of global ice volume and temperature (e.g., Saltzman and Verbitsky, 1994; Berger and Jansen, 1994). Here we present and discuss constraints provided by records of oxygen isotopes, marine paleoproductivity, fluvial and eolian terrigenous Fe input, ocean and terrestrial carbon chemistry, as well as alkenone-derived sea-surface temperature. We try to find an answer of the following questions: 1.) What was the history of the surface circulation in the southeast Atlantic Ocean across this important climate transition? 2.) Does the magnitude of marine production and wind intensity over the Pleistocene vary lineary with the ice volume? Using new geological records from ODP sites 1075 and 1082, we reexamine this conclusion and adress how the atmospheric and oceanic circulation changed associated with Northern Hemisphere glaciation along southwest Africa over the last 1.7 m.y.

1.5 THE INVESTIGATION AREA

TOPOGRAPHY

The Cape and Angola Basins which comprise the abyssal plain in the southeast Atlantic are separated by the Walvis Ridge, which runs from its abutment with the coast at about 20°S in a southwesterly direction for more than 2500 km towards the Mid-Atlantic Ridge (Fig. 4). The Walvis Ridge forms a barrier to the northward and southward flow of water below a depth of 3000 m and exerts a major influence on the deep-sea circulation in the southeast Atlantic (Shannon, 1985).
The western coast of southern Africa forms the eastern boundary of the Angola-Benguela Current system ("ABC-system"). The bathymetry of the western continental margin of southern Africa is variable (20 to 140 km wide). The Walvis Shelf is relatively deep on average, with the shelf break being about 350 m on average (Birch et al. 1976). Double shelf breaks are, however, common off the west coast (Siesser et al., 1974). The Congo Fan comprises an area of around 250 000 km². It begins in a water depth of 3000 m at the foot of the Congo-Canyon and covers the abyssal plain of the Angola Basin to a water depth of 5600 m and 1000 km far from the coast. Most of the sediment supply flows through a 200 to 700 m deep canyon, which cuts in to the river mouth more than 30 km from the coast. To the west the Congo-Canyon extends to a water depth of 3500 m (Jansen et al., 1984).
The Benguela system is characterized by a relatively narrow coastal plain. Much of the coastal region is arid. The Namib Desert extends between about 14°S and 31°S (Ward et al., 1983). The major part of the coastal belt is characterized by sand dunes, with occasional rocky outcrops (Lancaster, 1988).

PRESENT CLIMATE

Precipitation in central Africa is seasonal and coupled to the African monsoon. Sensible and latent heating over central Africa during boreal summer drive the inflow of moisture-laden air from the adjacent eastern Atlantic. The summer monsoon precipitation nourishes the vegetation of central Africa. Atmospheric circulation reverses in boreal winter. NE trade winds blow over north and central Africa and supply eolian dust to the adjacent eastern Atlantic.
The prevailing winds over the Benguela region are determined by the South Atlantic high pressure system (anticyclone), the pressure field over the adjacent subcontinent, and by eastward moving cyclones across the southern part produced by perturbations on the subtropical jet stream (Nelson and Hutchings, 1983; Fig. 5). The pressure over the African subcontinent changes from a well-developed low during summer to a weak high in winter as the continental heat low and the Intertropical Convergence Zone moves northwards, and the pressure gradient along the western coast is seasonally variable.
The winds along the western coast of southern Africa are predominantly southerly and induce

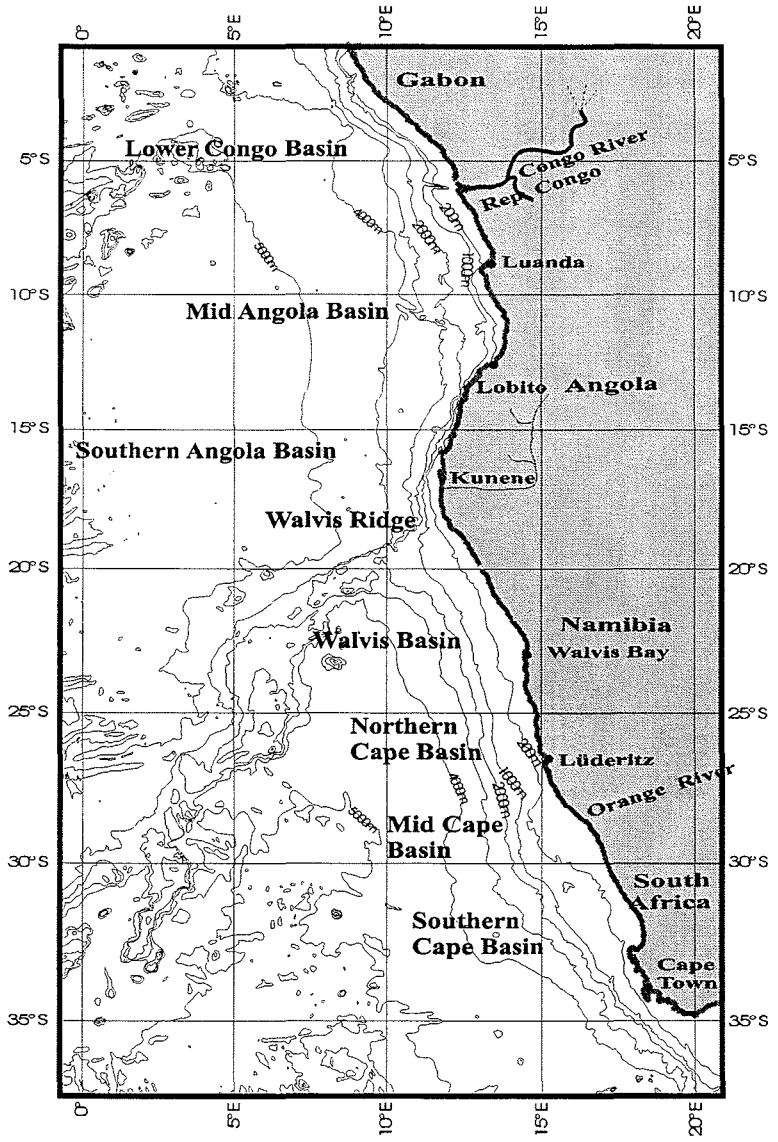

Figure 4: Bathymetric map of the investigation area (after Wefer et al., 1998).

upwelling and are responsible for the eolian transport of terrigenous material from the Namib and the Kalahari Deserts into the northern Cape Basin. In the northern Benguela system along the coast of Namibia seasonality in winds is less evident, and upwelling is perennial, with a spring-summer maximum and an autumn minimum.

OCEANOGRAPHY

The "Benguela Current" was defined by Hart and Currie (1960) as the name applying"..... to the region of cool upwelled coastal water along the southward coast of Africa. The Benguela Current is divided into the main Benguela Ocean Current (BOC), flowing in a northwest direction and the smaller Benguela Coastal Current (BCC), a northward stream parallel to the coast (Fig. 6).

The prevailing southeast trades cause coastal upwelling along the coast of SW-Africa (Shannon, 1985). The cold and nutrient-rich upwelled surface water comes from a water depth of 200 to 400 m, a depth where the South Atlantic Central Water (SACW) predominates.

The northern part of the subtropical anticyclone forms the westward streaming South Equatorial Current (SEC). The eastward flowing South Equatorial Counter Current (SECC) marks the boundary of the SEC. The SECC is divided into a northern directed current and into the southward flowing Angola Current (AC).

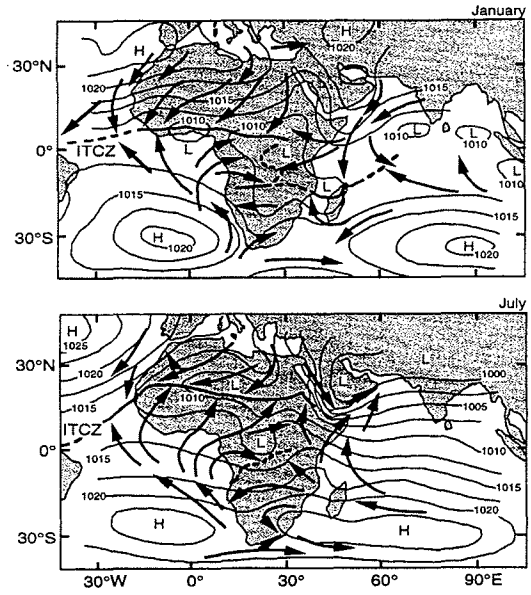

Figure 5: January (above) and July (below) atmospheric circulation and pressure distribution (hPa) in tropical and subtropical latitudes (redrawn from Mpounza and Samba-Kimbata, 1990)

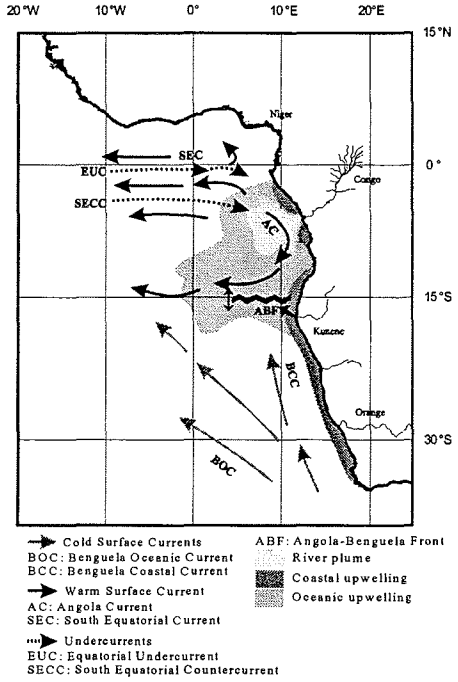

Figure 6: Oceanography of the investigation areas (surface currents: AC, SEC, SECC, ABF, BOC, and BCC etc.; modified from Schneider et al., 1997).

The AC and the BOC converge at the Angola Benguela front (ABF) (Fig. 6). This front is most intense within 250 km off the coast and in the upper 50 m of the water column. The ABF is a permanent feature and is maintained throughout the year within a narrow latitudinal band of 14 to 17°S. Its average position migrates seasonally over 2° of latitude, the front being farthest north in austral winter (August) and south in the late summer (March) (Shannon, 1987).

1.6 MATERIAL AND METHODS

During ODP Leg 175, thirteen sites were drilled in a north-south transect off the western coast of Africa (Congo, Angola, Namibia, and South Africa). The occupied sites were drilled from the RV *JOIDES Resolution* (Wefer et al., 1998) by using the advanced hydraulic piston coring and the extended core barrel method. For this study sediments from the Sites 1075, 1077, and 1082 were investigated.

Sediments at Site 1075 consist of one lithostratigraphic unit composed entirely of greenish-gray diatomaceous clay. The sediments are bioturbated and have overall low calcium carbonate contents. Site 1075 represents a continuous record for the Quaternary.

Sediments from Site 1077 form a lithostratigraphic unit of greenish-gray diatom- and nannofossil-rich clay. Most of the sediment is strongly bioturbated. The calcium carbonate content varies between 0.8 and 13.2 wt%.

Site 1082 recovered a continuous hemipelagic sedimentary section spanning the upper Miocene to Holocene (5.8 - 0 Ma). The sediment consists of olive to black clays, which contain varying abundances of diatoms, nannofossils, foraminifers, and radiolarians.

ISOTOPES AND STRATIGRAPHY

The planktonic foraminiferal species *Globogerinoides ruber* pink was used for stable oxygen ($\delta^{18}O$) isotope measurements at ODP Site 1077. For ODP Site 1082 we used the planktonic foraminiferal species *Globigerina inflata* for stable oxygen isotope measurements. A Finnigan MAT 251 micromass-spectrometer equipped with a Kiel automated carbonate preparation was used to analyze the samples. The stratigraphic framework of ODP Site 1077 was derived from graphic correlation with the benthic *Cibicides wuellerstorfi* isotope record of ODP Site 677 (Shackleton et al., 1990) from the Pacific. At ODP Site 1075 there was no carbonate available to produce an oxygen isotope stratigraphy. Therefore, a time scale was established by correlating the magnetic susceptibility of Site 1075 to that of ODP Site 1077.

The age model of ODP Site 1082 is based on the correlation of the $\delta^{18}O$ record of the planktonic foraminifera *G. inflata* to the benthic foraminifera *C. wullerstorfi* $\delta^{18}O$ record of ODP Site 659 from the Cape Verde Plateau off northwest Africa (Tiedemann et al., 1994). For the graphic correlation of the oxygen isotope records we used the software package *AnalySeries 1.0* of Paillard et al. (1996). Sedimentation rates were calculated on the basis of the linear interpolation between stratigraphic tie-points.

X-RAY FLOURESCENCE CORE SCANNING

High-resolution X-ray fluorescence (XRF) data were obtained on the undisturbed archive halves of

the cores in 2 cm steps through the XRF Core Scanner of Bremen University (Röhl and Abrams, 2000). The scanner allows a semiquantitative analysis of element intensities in counts per seconds (cps) from potassium through strontium in the periodic system of chemical elements (Jansen et al., 1998). The sediment surface is animated by a molybdenum X-ray tube (20 kV) and fluorescent radiation is measured by a Peltier cooled PSI detector (KEVEXtm) with a 125 µm Beryllium window and a multi channel analyzer with a 20 eV spectral resolution. Test runs resulted in the definition of 30-second counting time and an X-ray current of 0.087 mA as the optimal configuration for obtaining high-quality and statistically significant intensity data for the elements of interest (e.g., K, Ca, Fe, Ti, Mn, Sr). In this study only the Fe counts are presented for our interpretations.

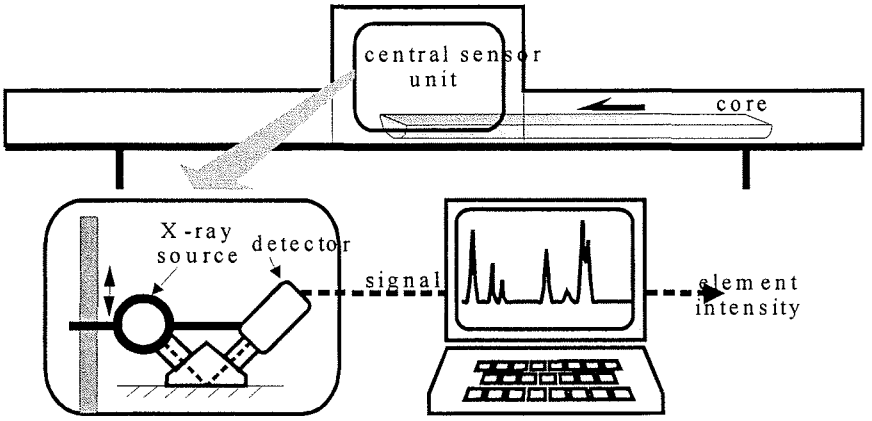

Figure 8: Schematic construction of the XRF Core Scanner (modified from Arz, 1998).

ORGANIC CARBON

Organic carbon in marine sediments is widely used as a paleoproductivity indicator especially in continental margin areas (Müller and Suess, 1979; Sarnthein et al., 1987; Rühlemann et al., 1999). The export of organic carbon to the deep-sea sediments is proportional to its production in the euphotic zone. During settling through the water column and within the sediments organic matter is partly remineralised. The degree of preservation is a function of the amount of organic matter exported to the sea floor, of the exposure time of the biogenic matter to the oxygenated water column (seasonality of flux, water depth, oxygenation of bottom water, sedimentation rate), of the fate of the organic matter (freshly produced or reworked, marine or terrestrial origin), and probably on the surface area of the mineral grains of the sediments (Müller and Suess, 1979).

Organic carbon concentration reported in this thesis were measured using a Heraeus CHN-O-Rapid elemental analyzer. Freeze-dried and homogenized samples were combusted at temperatures above 1000°C. Total carbon was measured on raw samples while organic carbon was measured after removal of carbonate with hydrochloric acid. Samples were placed in tin boats for total carbon analysis and in silver boats for organic carbon analysis.

STABLE CARBON ISOTOPE RATIO

Next to the biogenic carbon fixed in the marine environment, terrestrial organic matter may contribute to the particulate organic carbon in marine sediments. Especially in the vicinity of large rivers, terrestrial particles are the major source of the sedimentary organic carbon (Schlünz et al., 1999). In the Congo Fan area, riverine input is of major importance.

The stable carbon isotope ratio of the organic matter ($\delta^{13}C_{org}$) is widely used as an indicator of the marine or terrestrial origin of sedimentary organic matter. Terrigenous organic matter derived from C_3-plants reveal low $\delta^{13}C_{org}$ (Tyson, 1995). If high amounts of the terrestrial organic matter is derived from C_4-plants (mainly grasses of the savanna) the terrestrial organic matter is opposingly enriched in ^{13}C. Despite of these uncertainties, sedimentary $\delta^{13}C_{org}$ has been sufficiently used to quantify the relative portion of terrestrial organic matter on the sedimentary organic carbon (e.g., Schneider et al., 1996).

The stable isotope ratio of carbon was measured using a Heraeus Delta Plus CHN analyzer coupled with a Finnigan MAT mass spectrometer. Samples were combusted at 1050°C with excess oxygen. $\delta^{13}C_{org}$ was measured on carbonate free samples. In order to remove the carbonate, samples were acidified in silver boats with 6M HCl.

TEMPERATURE ESTIMATES USING C_{37} ALKENONES

Application of alkenone as paleothermometer for past sea-surface temperature (SST) is based on the ratio of di- and tri-unsaturated C_{37} alkenones that changes as a function of temperature (e.g., Brassell et al., 1986; Prahl and Wakeham, 1987). The growth temperature of alkenone producing algea, mainly *Emiliania huxleyi* and *Gephyrocapsa oceanica* (Volkman et al., 1980), can be estimated by determining this ratio expressed by the keton-unsaturation index $U_{37}^{k'}$ (Prahl et al., 1988):

$$U_{37}^{k'} = ([37:2] / [37:3 + 37:2])$$

The $U_{37}^{k'}$ index is then to be converted into temperatures applying an empirical function after e.g. Müller et al. (1998):

$$SST\ (°C) = ([U_{37}^{k'} - 0.044] / 0.033)$$

TIME SERIES ANALYSES

The time series analysis (band-pass filter synthesis approach from the *AnalySeries* package, Paillard et al., 1996) allows to examine climate records in order to evaluate stationary of the system (Imbrie et al., 1993). We started by extracting the Fe-intensity and MAR TOC records for their harmonic components associated with the 23-k.y. (precession), 41-k.y. (obliquity), and 100-k.y. (eccentricity) band-pass filters (*AnalySeries* package, Paillard et al., 1996).

The reconstruction of the Fe phase diagram is performed by an evolutionary spectra to investigate changes of phasing with respect to precession forcing over the time. Statistical analysis was based on the SPECMAP standard methods (Jenkins and Watts, 1968; Imbrie et al., 1984).

Changes in eccentricity, obliquity and precession index were calculated after Berger & Loutre (1991) using the *AnalySeries* package (Paillard et al., 1996), normalized and summed in an orbital record referred to as ETP (Imbrie et al., 1989).

2. MANUSCRIPTS

2.1 Manuscript I:

Terrigenous Climatic Signals And Changes In Marine Productivity From Sediments Of The Congo Fan Region For The Last 1.7 m.y.

Britta Jahn, Barbara Donner, Peter J. Müller, Ursula Röhl, Ralph R. Schneider, and Gerold Wefer

Department of Geosciences, University Bremen, Postbox 330440, D-29334 Bremen, Germany

ABSTRACT

Organic geochemical and terrestrial records covering the last 1.7 m.y. are presented for the northern Congo Fan from Ocean Drilling Program (ODP) Site 1075, and are discussed with regard to the development of marine productivity and terrigenous African paleoclimate. For this purpose, detailed records of total organic carbon accumulation rate (TOC MAR) and stable carbon isotope composition of the sediment ($\delta^{13}C_{org}$), as well as XRF core-scanner analyses of Fe intensity are considered. Elevated TOC MAR and Fe intensities are observed predominantly during interglacial periods when the African monsoon was most intensive. Band-pass filter results of TOC MAR show distinct precessional power, indicating that African climate was largely controlled by low-latitude insolation variations due to orbital precession. The TOC MAR filter also displays a dominant 100-k.y. oscillation for the last 0.6 m.y., an interval characterized by increased climatic contrast between glacial and interglacial conditions in the Northern Hemisphere. Variations in the terrestrial input off the Congo indicate eccentricity forcing well before the Northern Hemisphere ice caps dramatically increased in size between 0.9 and 0.6 Ma. Obliquity cycles in the Fe signal are strongly expressed for the last 0.9 m.y. The highest precessional amplitudes in the Fe-intensity cycles were produced when the amplitudes in the 100-k.y. oscillation increased. The evolutionary phase diagram shows a constant shift in phase between the terrestrial Fe signal and the precession cycles. The terrestrial record suggests that eccentricity modulation of the low-latitude insolation directly influenced the equatorial African monsoon system. Low-latitude climate forcing and response in the tropics might have played an important role in the initiation of the 100-k.y. cycle.

INTRODUCTION

Studies of African terrestrial paleoclimate recorded in marine proxies provide evidence for high-latitude glacial-interglacial forcing of African aridity-humidity cycles (Clemens et al., 1990; Anderson and Prell, 1993; deMenocal et al., 1993; Dupont and Leroy, 1995) and for responses to direct low-latitude orbital insolation variations (Clemens et al., 1991; deMenocal et al., 1993). Late Quaternary maxima in boreal summer insolation caused stronger monsoonal flow and, thus, greater precipitation rates over tropical Africa via increased thermal contrast between the South Atlantic and the air and moisture on the African continent. This led to increased vegetation on land and enhanced river transport in response to precession-related insolation changes (Dupont et al., 1999; Schneider et al., 1997; Gingele et al., 1998). It has been established that, for the past 200 k.y., the influence of precession-modulated seasonal insolation has been especially strong in the tropical regions (Schneider et al., 1994, 1996, 1997) when the zonal intensity of the trades and associated ocean upwelling was weakened (e.g., McIntyre et al., 1989; deMenocal et al., 1993). Previous work (Schneider, 1991; Schneider et al., 1994, 1996, 1997) has concluded that paleoproductivity variations off the Congo were induced by changes in trade-wind intensity and advection of the nutrient-rich Benguela Current subsurface waters. Conditions of strong advection resulted in a shallowing of the thermocline in the oceanic upwelling area off the Congo and increased oceanic nutrient transport via the subsurface Benguela Current into the eastern Angola Basin (Schneider et al., 1997;

Jansen & Van Iperen, 1991).

ODP Site 1075 provides an opportunity to investigate climate variations in marine paleoproductivity and terrestrial input off the coast of Congo, and thus the development of African paleoclimate during the Pleistocene (1.7 Ma). One major question is the influence of high- and low-latitude processes on paleoclimatology: how sensitive was low-latitude climate to the glacial-interglacial climate signal beginning at high latitudes? In contrast to high –latitudes, where temperature is the dominant climate signal, low-latitude terrestrial responses can often be characterized in terms of changes in precipitation. Therefore, it is of great importance to examine low-latitude insolation changes, which modulate monsoonal precipitation at 23- to 19-k.y. periodicities.

In this study we used records of total organic carbon mass accumulation rates (TOC MAR) and $\delta^{13}C_{org}$ isotope values as productivity indicators and to estimate the relative proportions of terrigenous and marine organic carbon (Schneider, 1991) in the northern Congo Fan area for the last 1.7 m.y. The predominant source of Fe transported into the study area is fluvial input by the Congo River (Gingele et al., 1998). Relative variations in high-resolution terrigenous Fe content are taken as an indicator for changes in the composition of the Congo River sediment load (Zabel et al., 2001).

With our proxy variables we seek a better understanding of the deep-sea fan sedimentation dynamics in relation to the river discharge and productivity. In particular, we examine differences in the influence of glacial-interglacial cycles with periods of 100 k.y. and 41 k.y., and monsoonal variations with periods near 23 k.y. Berger et al. (1998) used the red/blue ratio of Site 1075 as a proxy for paleoproductivity, and the results indicated strong precessional cycles, especially for the last 0.6 m.y. when the 100-k.y. cycle has dominated climate change. We therefore filtered the TOC MAR and Fe records to the Milankovitch frequencies and examined the evolution of the TOC MAR and Fe amplitude variability in correlation with the filtered 100-k.y. (eccentricity), 41-k.y. (obliquity), and 23-k.y. (precession) cycles for the last 1.7 m.y.

MODERN CONDITIONS

The freshwater outflow of the Congo River at 6°S is detectable by reduced surface-water salinity as far as 800 km offshore during austral summer, when monsoonal circulation and precipitation reach their maximum seasonal intensities (van Bennekom and Berger, 1984). The rapid freshwater outflow, forced by a narrow estuary, induces upwelling of subsurface oceanic waters rich in phosphate and nitrate within the estuary and the inner plume area. The river plume broadens in a narrow meridional zone 150 to 200 km offshore. Here, high rates of primary production are assumed to be the result of nutrient input from the river and of river-induced upwelling. Outside this highly productive plume, elevated primary production depends entirely on oceanic mixing of nutrients from subsurface into surface waters within frontal systems and geostrophic upwelling.

As a result of the oceanic and river-induced upwelling, as well as the supply of nutrients by the river, modern primary productivity is very high, with values of 90 to 125 g C $m^{-2}yr^{-1}$ (Berger and Wefer, 1991) in the surface waters off the Congo Fan (gray shaded area, Fig. 1). Existing data indicate that biogenic silica production in the oceanic surface waters surrounding the central Congo plume account for 40 to

60% of the total phytoplankton carbon productivity (van Bennekom and Berger, 1984). Opal contents are relatively high off the coast of Congo (6°S) where diatoms are the predominant component (van Iperen et al., 1987).

The major processes contributing to the clay mineral assemblage (Kaolinite, Smectite, Illite, and Chlorite) of the Congo Fan are: a) sediment input by the Congo River, b) dust supply by southeast (northeast) trades, and 3) erosion of the exposed shelf areas during times of lowered sea level (e.g., Petschick et al., 1996; Van der Gaast and Jansen, 1984; Pastouret et al., 1978; Eisma et al., 1978). Illites are the clay

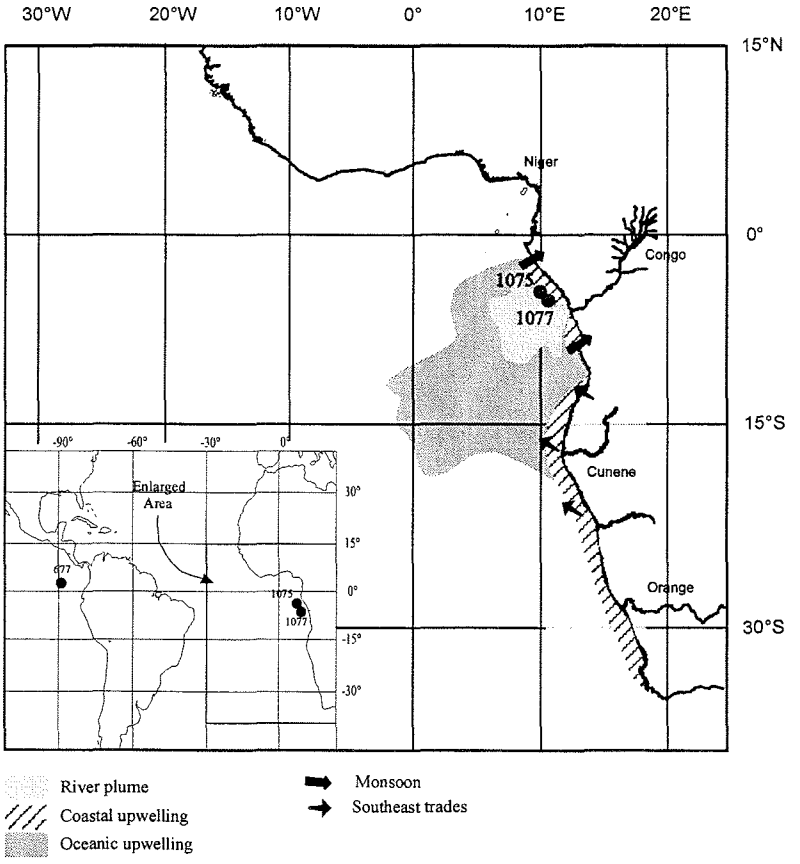

Figure 1: Oceanographic setting of the study area (modified from Schneider et al., 1997).

mineral group that are Mg- and Fe-rich, and are products of mechanical abrasion in the absence of water (Petschick et al., 1996).

MATERIAL AND METHODS

Core Location, Lithology and Stratigraphy

We investigated sediments of ODP Sites 1075 and 1077. During ODP Leg 175 three holes were drilled at each site (1077A, 1077B, 1077C and 1075A, 1075B, 1075C) with the advanced hydraulic piston corer to a maximum depth of 205.1 m and 207.2 m below sea floor, respectively. Continuous sequences

of hemipelagic sediments spanning the upper Pliocene and the entire Pleistocene were recovered. ODP Site 1075 was drilled at 4° 47'S, 10° 4'E at a water depth of 2995 m at the northern edge of the Congo River plume (Fig. 1; Wefer et al., 1998). Sediments at Site 1075 are dominated by greenish-gray diatomaceous, partially carbonate-bearing clays (Wefer et al., 1998). ODP Site 1077 was recovered at 5°10'S, 10°26'E from a shallower position (2382 m water depth) on the same transect. Sediments from Site 1077 form a lithostratigraphic unit of greenish-gray diatom- and nannofossil-rich clay. Most of the sediment is strongly bioturbated. Sampling was mainly performed on cores from Holes 1075A and 1077A. Additional samples were collected from Holes 1077B and 1077C at certain depth intervals to cover coring gaps in the A-Holes. Core depths are reported in meters composite depth (mcd) according to Wefer et al. (1998).

Bulk Organic Carbon

Samples for determination of organic carbon content and its carbon isotopic composition were collected at intervals of 50 cm. Total carbon (TC) values were obtained by sediment combustion at 1050°C using a HERAEUS CHN-O-Rapid elemental analyzer following standard procedures described in Müller et al. (1994). The TOC (Total Organic Carbon) content is reported in dry weight percent. The relative precision of the measurements is based on duplicates and control analysis of a laboratory internal reference sediment sample (WST 2). We calculated TOC MAR (Mass Accumulation Rates) after van Andel (1975) using the following equation:

$$MAR_{total} = SR * DBD$$

$$TOC\ MAR = MAR_{total} * TOC\ wt\ \% * 100^{-1}$$

where:

MAR_{total} = Mass accumulation rate of the total sediment ($g*cm^{-2}*k.y.^{-1}$),

TOC MAR = Total organic carbon mass accumulation rate ($g*cm^{-2}*k.y.^{-1}$),

SR = Sedimentation rate ($cm * k.y.^{-1}$),

DBD = Dry Bulk Density ($g * cm^{-3}$), and

TOC wt % = weight of total organic carbon of the total sediment (wt %).

To determine the isotopic signature of bulk organic carbon in the Congo Fan sediments, we measured the stable organic carbon isotope ratio ($\delta^{13}C_{org}$). Before analysis of $\delta^{13}C_{org}$, the carbonate component was removed by treatment with 1M HCl. Samples were filtered on a cellulose acetate filter and dried at 50°C. 10 mg of sediment was weighed in tin crucibles, mixed with copper oxide, and combusted at 950° C in a HERAEUS CHN-Rapid elemental analyzer. The isotope measurements were obtained with a FINNIGAN MAT delta E micromass spectrometer. The overall analytical precision ($\pm 1\sigma$, based on repeated analyses

of the laboratory-internal WST 2 standard) was better than 0.1 ‰. The $\delta^{13}C_{org}$ values are reported in the (δ) standard notation relative to PDB.

X-ray Flourescence Iron Counts

High-resolution XRF measurements were performed at 2-cm intervals on undisturbed core surfaces with an X-ray flourescence (XRF) core scanner developed at the Netherlands Institute for Sea Research. The system configuration allows a semiquantitative non-destructive determination of relative changes in elemental concentrations expressed in counts per second (cps) (e.g., Jansen et al., 1998, Röhl and Abrams, 2000). The sediment surface is stimulated by a molybdenum X-ray source (3 to 50 kV) and X-ray fluorescence is measured with a Peltier cooled PSI detector (KEVEXTM) with a 125 µm Beryllium window and a multi-channel analyzer with a 20 eV spectral resolution. The X-ray current was 0.087 mA and the integration time was 30 sec.

Magnetic susceptibility (MS) wastaken from shipboard measurements (Wefer et al., 1998) and is a measure of the concentration of magnetic grains in a sample, which correlates with Fe content. It was measured continuously with a pass-through loop sensor on whole, unsplit core sections in the shipboard laboratory (Wefer et al., 1998).

Time-Series Analyses

The statistical methods used to achieve the frequency domain (spectra) and the time domain (filters) were carried out with the *AnalySeries* software package (Paillard et al., 1996).

Band-pass filter

According to Berger et al. (1998) productivity and terrigenous records show significant variance in all orbital frequency bands (e.g., 1/100 k.y., 1/41 k.y., and 1/23 k.y.). However, relative proportions of variance are highly variable for each orbital frequency over the last 1.7 m.y. Therefore, we have filtered the TOC MAR and Fe-intensity records for orbital frequencies. This was done by applying an appropriate band-pass filter (Jenkins and Watts, 1968). These filtered records make visible the changing importance of individual orbital cycles in the records (Fig. 6 and 7).

Cross-spectral analysis

We used the Blackman-Tukey method of cross-spectral analysis (linear detrend, no prewhitening, Bartlett window, and one-half lag) to identify those periods where significant variance is concentrated (Blackman and Tukey, 1958). When similar periodicities are present in any two signals, cross-spectral analysis is employed to define the level of coherency at these periods (Jenkins and Watts, 1968). Coherency (k) is a measure of the degree to which two signals are linearly related to a zero-phase correlation coefficient. Cross-spectral analyses between TOC MAR and the terrigenous concentrations were conducted. Positive phase values indicate a lagging while negative values denote a leading.

Evolutionary phase diagram

Reconstruction of the phase diagram of terrigenous Fe is performed by an evolutionary spectrum. Statistical analysis was based on the SPECMAP standard methods (Jenkins and Watts, 1968; Imbrie et al., 1984).

After interpolating the Fe-intensity record to a constant time interval (1 ka.), we calculated the coherency and the phase spectra of Fe against the eccentricity, obliquity, and precession record (ETP) to show the extent to which the local and ETP signals are linearly correlated in each frequency band. We used a configuration for time series analysis that considered high confidence but low spectral resolution, applying a setup using a Bartlett window. From the amplitude-density spectra of 150-k.y. windows with 50-k.y. overlap, we calculated the phase differences for precessional forcing at coherent 23-k.y. cycles and summarized this information in a phase diagram.

Stratigraphy

At Site 1075 there were insufficient amounts of calcareous foraminifera available to produce an oxygen-isotope stratigraphy. A time scale was therefore established by correlating the magnetic susceptibility of Site 1075 to that of ODP Site 1077. The age model for Site 1077 is based on the correlation of $\delta^{18}O$ measurements of *G. ruber* (pink) with a benthic isotope record of ODP Site 677 (Shackleton et al., 1990) from the deep Pacific. Ages for the two sites are supported by magneto- and biostratigraphy (Fig. 2; Dupont et al., 2001). Sites 1075 and 1077 underlie the same hydrographic conditions and show similar variations in magnetic susceptibility (Fig. 2). Isotopic events identified at Site 1077 are tagged with ages from the Shackleton et al. (1990) ODP 677 record (Dupont et al., 2001), thus providing the age scale also for Site 1075. Sedimentation rates were calculated by linear interpolation between age control points. The oxygen-isotope chronology we have developed matches the age provided by the last major reversal in the Earth's magnetic field (Brunhes/Matuyama boundary at 0.78 Ma) for Sites 1075 and 1077.

The oxygen-isotope curve for Site 1077 reveals two distinct periods, from 1.7 to 0.9 Ma and 0.6 to 0.5 Ma, where the temporal resolution is restrained by limited abundances of foraminifera. Nevertheless, the Site 1077 age model shows a good match between the amplitude fluctuations in orbital obliquity and the 41-k.y. filter of magnetic susceptibility variations for the last 1.7 m.y. (Fig. 3a). At Sites 1077 and 1075, The phase relationships of magnetic susceptibility to changes in obliquity of the Earth's axis are strong throughout the Pleistocene. From visual inspection of the isotope and susceptibility curves for Site 1077, it is evident that the magnetic susceptibility signal leads the isotope signal at most of the abrupt glacial-interglacial transitions of the last 0.7 Ma, the so called Terminations (Broecker, 1984) (Fig. 3). The exceptions are Terminations III and VI. Magnetic susceptibility is also high during older glacial-interglacial transitions, those of MIS's 22 to 21 and 20 to 19. We attribute the early rise in magnetic susceptibility to erosion and transport of additional terrigenous material from the shelf during sea-level low stand and sea-level rise, which would allow for a somewhat larger shift than the estimate of 6 k.y. by Berger et al. (1998).

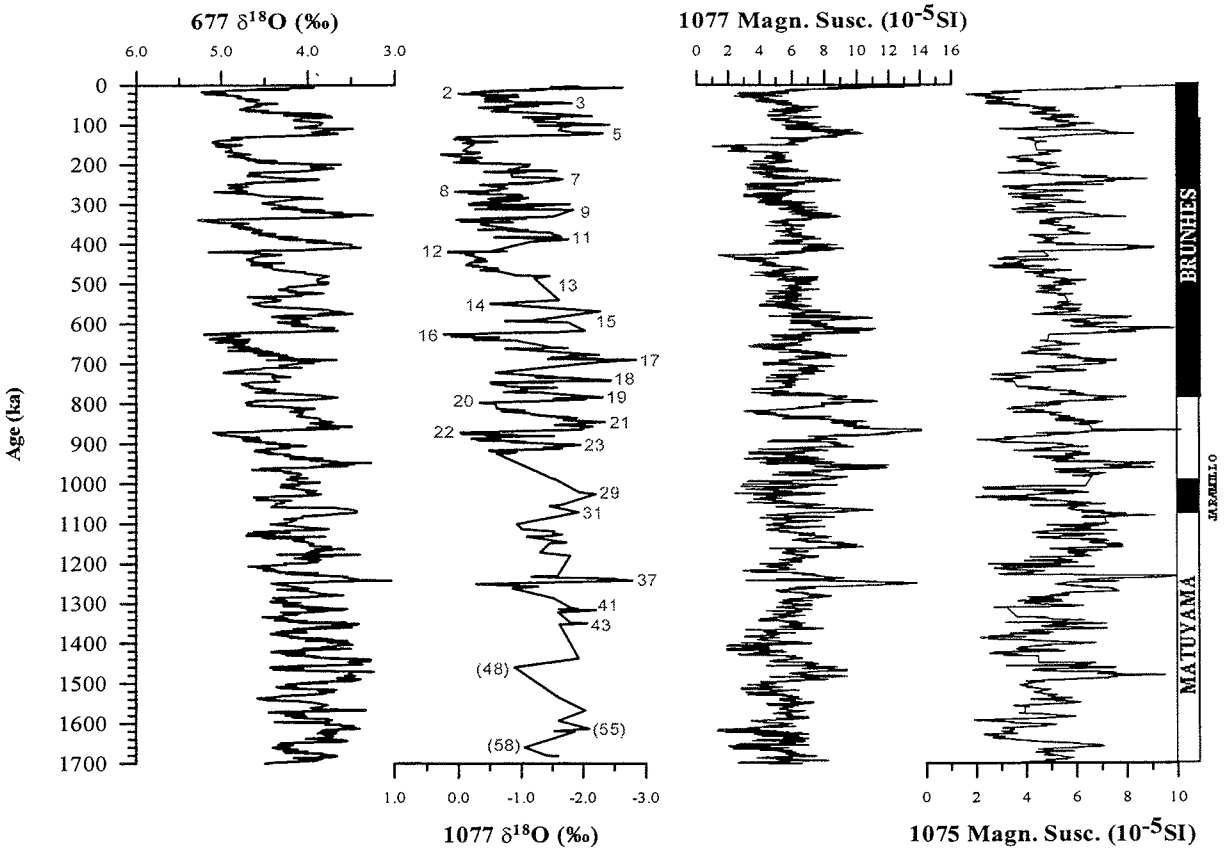

Figure 2: Left: Site 677 (Shackleton et al., 1990) $\delta^{18}O$ record of benthic foraminifera and Site 1077 $\delta^{18}O$ record of planktonic foraminifera labeled with Marine Isotope Stages. Right: Magnetic susceptibility from ODP Sites 1077 and 1075.

RESULTS AND INTERPRETATION

Records of organic matter in the northern Congo Fan area

TOC MAR values at Site 1075 range from 0.05 to 0.25 g/cm²*k.y. with maximum TOC MAR values recorded for stages 15, 9, and 7. Minimum TOC MAR values are exhibited during MIS 37/36, 25, 8, and 7/6. High TOC MAR variability is observed from 0 to 0.7 Ma. Before 0.7 Ma, lower TOC MAR variability is characteristic, except for the intervals from 1.5 to 1.3 Ma and 1.2 to 1.0 Ma (Fig. 4). The TOC MAR record indicates that in the northern Angola Basin organic sedimentation has been relatively high for the last 1.7 m.y. Within the Brunhes Chron, from 0.45 to 0 Ma (Fig. 5), peaks in TOC MAR values are indicated during several cold interglacial substages (11.4, 11.2, 9.2, 7.4, 5.4, 5.2, and 3.2). Exceptions to this pattern are exhibited by high TOC MAR during late glacial stage 8, early glacial stage 4, and glacial stage 2.

Furthermore, we employed $\delta^{13}C_{org}$ isotopes of the organic matter to obtain basic information about the relative proportions of marine and terrestrial organic carbon content. $\delta^{13}C_{org}$ values for TOC in the northern Congo Fan area ranged between -23 ‰ and -19 ‰, while $\delta^{13}C_{org}$ values for terrestrial organic material

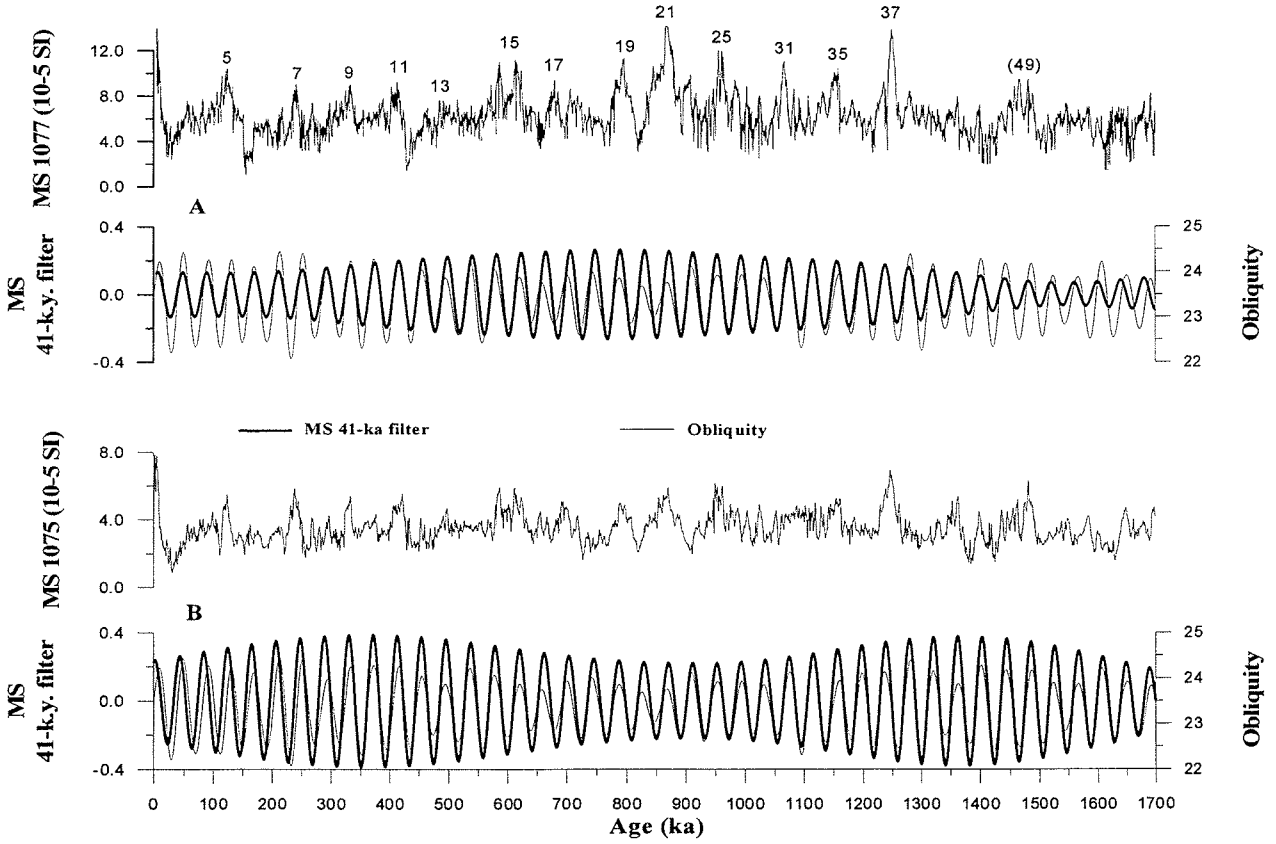

Figure 3: Above: Magnetic susceptibility data of Site 1077 and the 41-k.y. band-pass filter in comparison with obliquity forcing. Below: Magnetic susceptibility data of Site 1075 and the 41-k.y. band-pass filter in comparison with obliquity forcing. Note the very good coherence of magnetic susceptibility and obliquity forcing.

varied from -28 ‰ to -26 ‰, and for marine organic material from -24 ‰ to -18 ‰ (Schneider et al., 1996; Jansen et al., 1984). It appears that the amount of marine organic matter has increased stepwise over the last 1.7 m.y. In this respect the $\delta^{13}C_{org}$ record can be separated into three intervals (Fig 4). The interval from 1.7 to 1.1 Ma exhibits the lowest $\delta^{13}C_{org}$ values, between -23 ‰ and -21.5 ‰. From 1.1 to 0.3 Ma, the $\delta^{13}C_{org}$ values gradually increase, ranging from -22.5 ‰ to -20 ‰. In the youngest interval (0.3 to 0 Ma), $\delta^{13}C_{org}$ ranges between -22 ‰ and -19 ‰ (except for one exceptionally low value in stage 5). The highest values are observed during late MIS 7, early MIS 6, and MIS 3 to 2. The lowest values occur within the interglacial stages 7 and 5, and the Holocene.

Records of iron and magnetic susceptibility in the Congo Fan area

Fe intensity and magnetic susceptibility (Fig. 4) elicit similar temporal patterns, showing a well developed glacial-interglacial cyclicity with higher values during interglacial times. In general, Fe patterns are congruent with the MS record. Average Fe intensities vary around 5000 cps. The highest Fe intensities (8000 to 10000 cps) are recorded during interglacial marine oxygen isotope stages (MIS) 47, 39, 37, 35, 31, 29, 21, and 19, and at glacial-interglacial boundaries 26/25 and 16/15 (Fig. 4). Exceptionally low Fe values of

around 3500 cps were measured at 1.62 Ma, from 1.42 to 1.38 Ma, at 1.2 Ma, between 0.44 to 0.36 Ma, and during glacial MIS 2. Fe, in particular, reflects the typical saw-tooth shape of the $\delta^{18}O$ record for the late Quaternary.

Magnetic susceptibility at Site 1075 (MS; Wefer et al., 1998) is generally low compared to other MS records from the equatorial Atlantic, ranging from 2.5 to 7.5 * 10^{-5} SI. The highest MS peaks occur during MIS's 49, 43, 37, 31, 25, 21, 15, 11, 9, 7, and 5. Generally, the peaks of the Fe-intensity record match those of the MS record, indicating that both are dominated by terrestrial input.

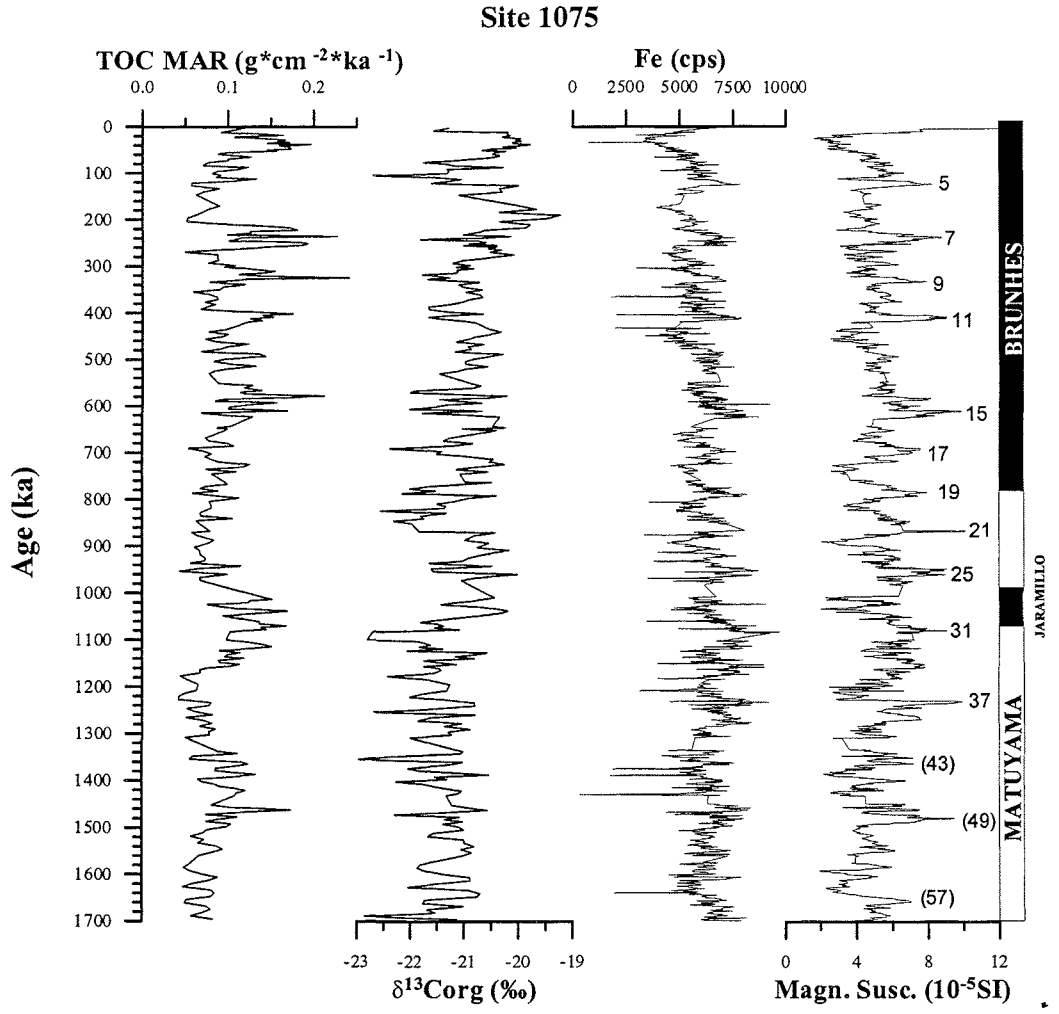

Figure 4: Comparison of TOC MAR (left), $\delta^{13}C_{org}$ isotopes, and Fe intensity (center) with magnetic susceptibility (right) for Site 1075. Note the very good coherence of Fe-intensity and magnetic susceptibility.

Variations in paleoproductivity and terrestrial input in comparison with summer insolation

Terrestrial input to the northern Congo Fan is predominantly driven by the Congo River discharge. Variations in the African monsoon are attributed to changes in insolation intensity, with increased precipitation on the African interior corresponding to insolation maxima. Higher rates of marine paleoproductivity, on the other

hand, are associated with insolation minima, when the monsoon is reduced but stronger SE-trades promote coastal upwelling (Schneider et al., 1997). In the next step, we want to examine the sources of organic matter in the northern Congo Fan area. For that reason, we compare the TOC MAR, $\delta^{13}C_{org}$, and Fe-intensity records with the summer insolation (August) at 10°N (Berger and Loutre, 1991) for the last 0.45 m.y (Fig. 5).

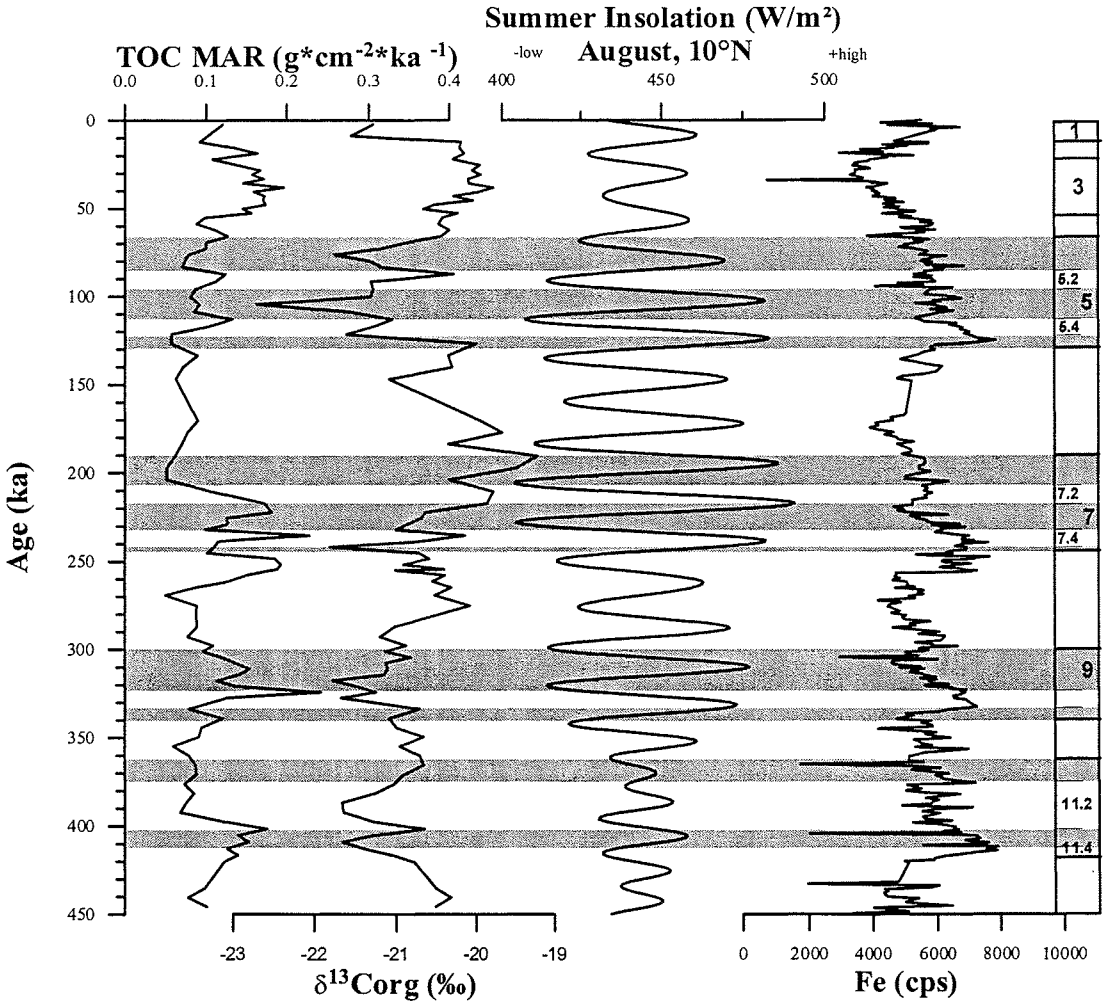

Figure 5: TOC MAR, $\delta^{13}C_{org}$ isotopes (left), and Fe-intensity (right) of Site 1075 in comparison with the summer insolation at 10°N (center) for the last 0.45 m.y. Gray shaded fields mark the Marine Isotope Stages.

In the interval from 0.45 to 0.25 Ma, peaks in TOC MAR values occur together with heavier $\delta^{13}C_{org}$ values, and contemporaneously with low summer insolation and high Fe-intensities (MIS boundaries 11.3/ 11.2, 9.2/9.1, and at the end of glacial stage 8). This result could be explained by shelf erosion during sea-level rise, causing the input of additional terrestrial material (mainly from C_3 plants) to the northern Congo Fan. In contrast, from 0.24 to 0.15 Ma, high TOC MAR and heavy $\delta^{13}C_{org}$ values occurred when summer insolation was high and the terrestrial input (Fe) decreased (MIS 7.4 and at the end of MIS 7.3). Organic

sedimentation in the northern Congo Fan was influenced either by greater marine productivity or increased influx of C_4 plant material, enhancing the TOC MAR and the $\delta^{13}C_{org}$ signal (Holtvoeth et al., 2001). For the last 0.15 m.y. we observe highs in TOC MAR with heavy $\delta^{13}C_{org}$ values contemporaneous with reduced terrigenous input during insolation minima, indicating stronger marine productivity. This result is in agreement with investigations of Schneider et al. (1997) who concluded that increased marine productivity off the coast of Congo occurred during periods of enhanced zonal intensity of the southeast trades and a corresponding weak southeast monsoon over the eastern South Atlantic for the last 0.2 m.y.
In general, we infer that, for the last 1.7 m.y., the terrestrial input of the Congo River discharge is associated with variations in monsoonal precipitation, influencing organic sedimentation in the northern Congo Fan region. The terrestrial input off the coast of Congo was high from 1.7 to 0.15 Ma. For the last 0.15 m.y., the impact of coastal upwelling induced by stronger southeast trades has increased in the area, enhancing marine productivity while monsoon activity was reduced.

DISCUSSION

Looking closely at our results, an important question arises: What are the potential forcing mechanisms for variations of TOC MAR and Fe intensity in the northern Congo Fan region? To evaluate the relative influences of high-latitude forcing (obliquity-related and ice-mass-related cycles) and low-latitude forcing (precession), we filtered our proxy records at orbital frequencies with a periodicity of 100-k.y., 41-k.y., and 23-k.y. cycles (Figs. 6 and 9).

Variations of marine paleoproductivity in the northern Congo Fan

The low-amplitude variability of the TOC MAR_{100} filter (Fig. 6A) from 1.7 to 0.6 Ma indicates a long period of relatively low paleoproductivity, except for two short periods (stages 49 to 43, and stages 35 to 29) that show slightly enhanced values. During the last 0.6 m.y., the TOC MAR_{100} filter exhibits a high-amplitude variability with a strong 100-k.y. character. The enhanced marine productivity is attributed to intensification of coastal upwelling due to stronger SE trades in the northern Congo Fan area. From 1.7 to 1.2 Ma, the TOC MAR_{100} filter is more or less in phase with eccentricity. The filtered records are out of phase for the interval from 1.2 to 0.6 Ma. For the last 0.6 m.y., the TOC MAR_{100} filter lags eccentricity. The amplitude variability of the TOC MAR_{41} filter is high from 1.7 to 0.95 Ma, but then decreases in the period from 0.95 to 0.5 Ma (Fig. 6B). During the last 0.5 m.y., the TOC MAR_{41} filter increases again to a high-amplitude variability. The phase relationship between the TOC MAR_{41} filter and obliquity varies over the last 1.7 m.y. From 1.7 to 1.4 Ma, the TOC MAR_{41} filter and obliquity are out of phase. In the next period, from 1.4 to 1.15 Ma, the TOC MAR_{41} filter lags obliquity. From 1.15 to 0.95 Ma, the TOC MAR_{41} filter and obliquity are more or less in phase. This is followed by a period, lasting until about 0.6 Ma, when the TOC MAR_{41} filter and obliquity are again out of phase. The TOC MAR_{41} filter leads obliquity in the short interval from 0.6 to 0.5 Ma. During the last 0.5 m.y., the TOC MAR_{41} filter and obliquity are again in phase.

The amplitude variability of the TOC MAR_{23} filter is generally low for the interval from 1.7 to 0.7 Ma, but this is interrupted by slightly enhanced amplitudes in the periods from 1.45 to 1.3 Ma and 1.05 to 0.95 Ma (Fig. 6C). The highest amplitudes of the TOC MAR_{23} component occur over the last 0.7 m.y. A comparison of the phase relationship between the TOC MAR_{23} filter and precession indicates that, in general, they are in phase over long periods, except for the intervals from 1.7 to 1.5 Ma, around 1.3 Ma, around 1.1 Ma, around 0.9 Ma, around 0.75 Ma, around 0.6 Ma, and from 0.25 to 0.15 Ma. For the most part, the TOC MAR_{23} filter shows high TOC MAR when the influence of the precessionally modulated seasonal insolation is especially strong. The precessional effect is commonly attributed to the competing influences of monsoon winds and trade winds (Schneider et al., 1996). This competition extends across the equator, with the North African monsoon interfering with the SW trades. Enhanced heating of the North African land masses by a nearby sun in the northern summer (June, July, or August perihelion) weakens the trades off NW Africa as well as those in the South Atlantic (Kutzbach and Liu, 1997). Relevant land masses being much smaller in the south, the reverse effect (monsoon over southern Africa) is much less pronounced. Thus, the precessional tone of the forcing is preserved in the organic sediments of the Congo Fan and is in phase with northern summer monsoon maxima and minima (Berger et al., 2001). Filtering analyses of Site 1075 show that TOC MAR in the northern Congo Fan area is driven by both low-latitude monsoonal precipitation (precessional) and high-latitude (obliquity-related and ice-mass-related) cycles. Prior to 0.6 Ma, fluctuation in organic sedimentation occurred primarily at precessional periodicities (23-19 k.y.), indicating that African monsoonal precipitation was largely controlled by low-latitude insolation variations due to orbital precession. For the last 0.6 m.y., high-latitude forcing with glacial-interglacial cycles of 100 k.y. has influenced the TOC MAR content and enhanced the competitive effects between the monsoon and trade winds. Uliana et al. (2001) have investigated diatom assemblages in sediments of the adjacent Site 1077 in the Congo Fan. They proposed increased monsoonal rains in the northern parts of the drainage area at times when perihelia occurred during the monsoon season (precession effect), as well as changes in current direction offshore, which may have redirected the freshwater outflow off the Congo to the area of the northern Congo plume.

Organic matter content in the northern Congo Fan also shows a change at the time of the mid-Pleistocene climate shift. Both low-latitude (precessional) and high-latitude (obliquity- and ice-mass-related) cycles contracted after the shift at 0.9 Ma. On entering the Milankovitch Chron (at 0.65 Ma), however, the amplitudes of the low- and high-latitude cycles expanded again. From the increased variation in productivity-related indices, Berger et al. (2001) concluded that the sensitivity of the Congo upwelling system to precessional forcing increased at the time of the mid-Pleistocene climate shift, indicating that strong precession will be modulated by the variations in eccentricity. Dupont et al. (2001), studying pollen and dinoflagellate cysts from Site 1075, found that the variation of river discharge increased after 0.94 Ma, suggesting larger contrasts in amounts of rainfall between glacial and interglacial periods in the African interior. A rise of *Podocarpus* pollen at 1.05 Ma suggests a cooling event, which occurred in synchrony with distinct changes in the dinoflagellate record. While the dinoflagellate cysts indicate a reduction in river discharge at this time, the contrast between pollen spectra of glacial and interglacial periods increased after 1.05 Ma. Thus, the expansion in the fluctuation of organic sedimentation at Site 1075 occurred more or less parallel with changes in the vegetation cover in the interior of the continent.

In summary, the enhanced presence of organic material in the northern Congo Fan area at Site 1075 is observed predominantly during interglacial periods, when precession-related insolation was strongest. During these periods the African monsoon increased andthe associated higher levels of precipitation over Africa enhanced the Congo River discharge.

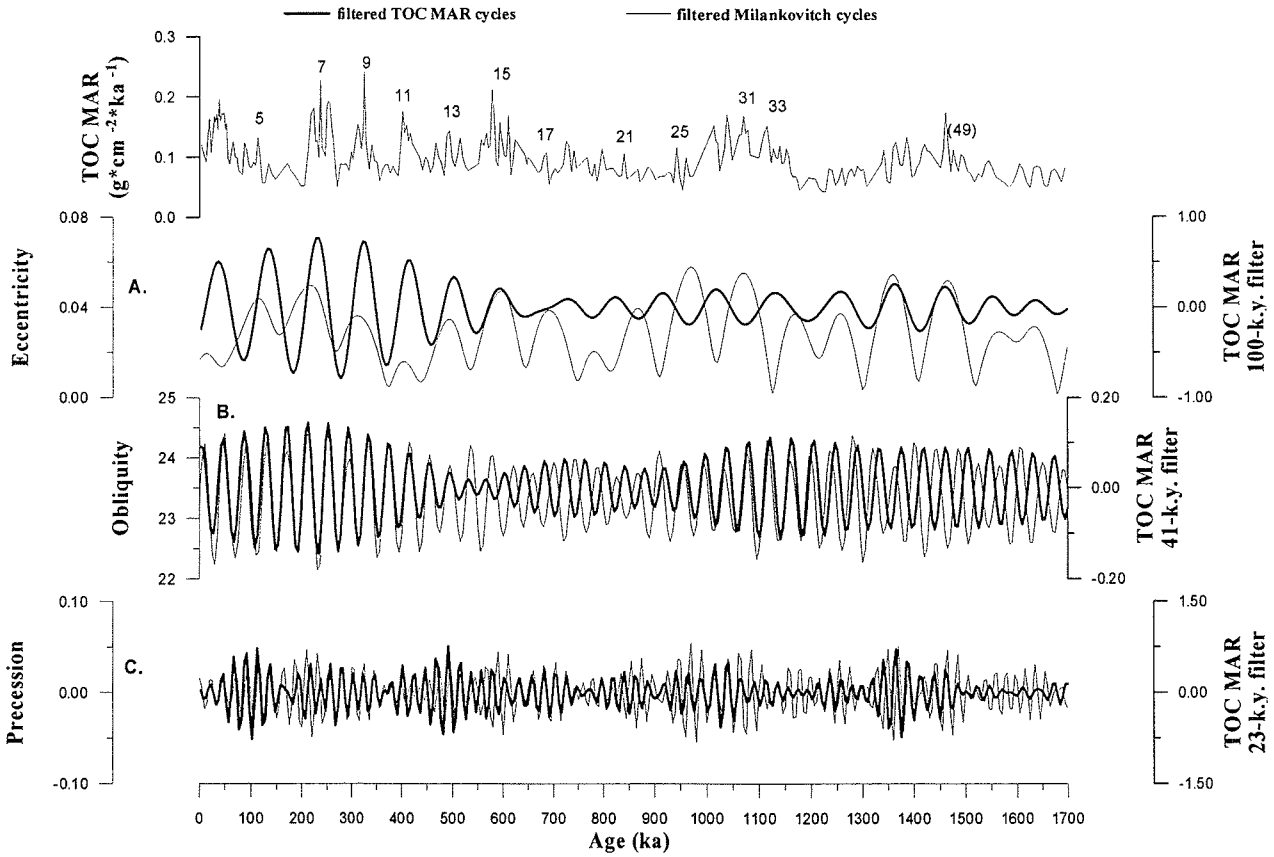

Figure 6: Filtered TOC MAR signal of Site 1075 for the last 1.7 m.y. **A.** The TOC MAR_{100} filter versus eccentricity (with central frequency = 0.01 cycles/k.y. and bandwidth = 0.001 cycles/k.y.). **B.** The TOC MAR_{41} filter versus obliquity (with central frequency = 0.024 cycles/k.y. and bandwidth = 0.001 cycles/k.y.). **C.** The TOC MAR_{23} filter versus precession (with central frequency = 0.043 cycles/k.y. and bandwidth = 0.009 cycles/k.y.).

During glacial periods the NE trades became more important because aridity on the North African continent increased and more dust from the Sahara Desert was transported into the equatorial Atlantic (deMenocal et al., 1993). In contrast, the African monsoon intensity decreased during glacial periods. Therefore, the temporal pattern of organic sedimentation in the equatorial Atlantic should constrast that of the Congo Fan. To investigate this, we used a TOC MAR record of ODP Site 663 (Wagner, 2000) and compared it with the TOC MAR record of Site 1075 (this study). Site 663 is located in the equatorial Atlantic (1°S, 11°W) at a water depth of 3708 m (Ruddiman et al., 1989) and shows strong power at the eccentricity and obliquity bands, indicating a close response of tropical organic sedimentation to the climatic evolution at high latitudes (Wagner, 2000; Fig. 7). In his study, Wagner proposed that enhanced dust supply in

glacial times and surface-water mixing were primary controls for the deposition of organic carbon.

The Milankovitch parameters in the TOC MAR records of Sites 1075 and 663 have been extracted by band pass filtering. We compared the evolution of the Milankovitch parameters between the two TOC MAR records for the last 0.9 m.y. (Fig. 7). The amplitude modulation of the 1075 TOC MAR_{100} filter for the most part agrees with the 663 TOC MAR_{100} filter for the last 0.9 m.y. (Fig. 7A). The TOC MAR_{100} ice volume components of the two sites are out of phase with each other from 0.9 to 0.2 Ma, with interglacial periods characterized by higher TOC MAR amplitudes at Site 1075 simultaneous with lower TOC MAR amplitudes of Site 663. During the last 0.2 m.y., the 100 k.y. filter curve for TOC MAR at Site 1075is in phase with that of Site 663, indicating that the Congo River discharge weakened associated with decreased monsoonal precipitation, while marine productivity attributed to stronger wind-driven upwelling increased. The amplitudes of the TOC MAR_{41} filter at Site 663 are much lower than those of the 1075 TOC MAR_{41} component (Fig. 7B). However, the phase relationship between the two TOC MAR_{41} filters shows a contrasting trend to that of the TOC MAR_{100} filters. From 0.9 to 0.6 Ma, the two TOC MAR_{41} filters are

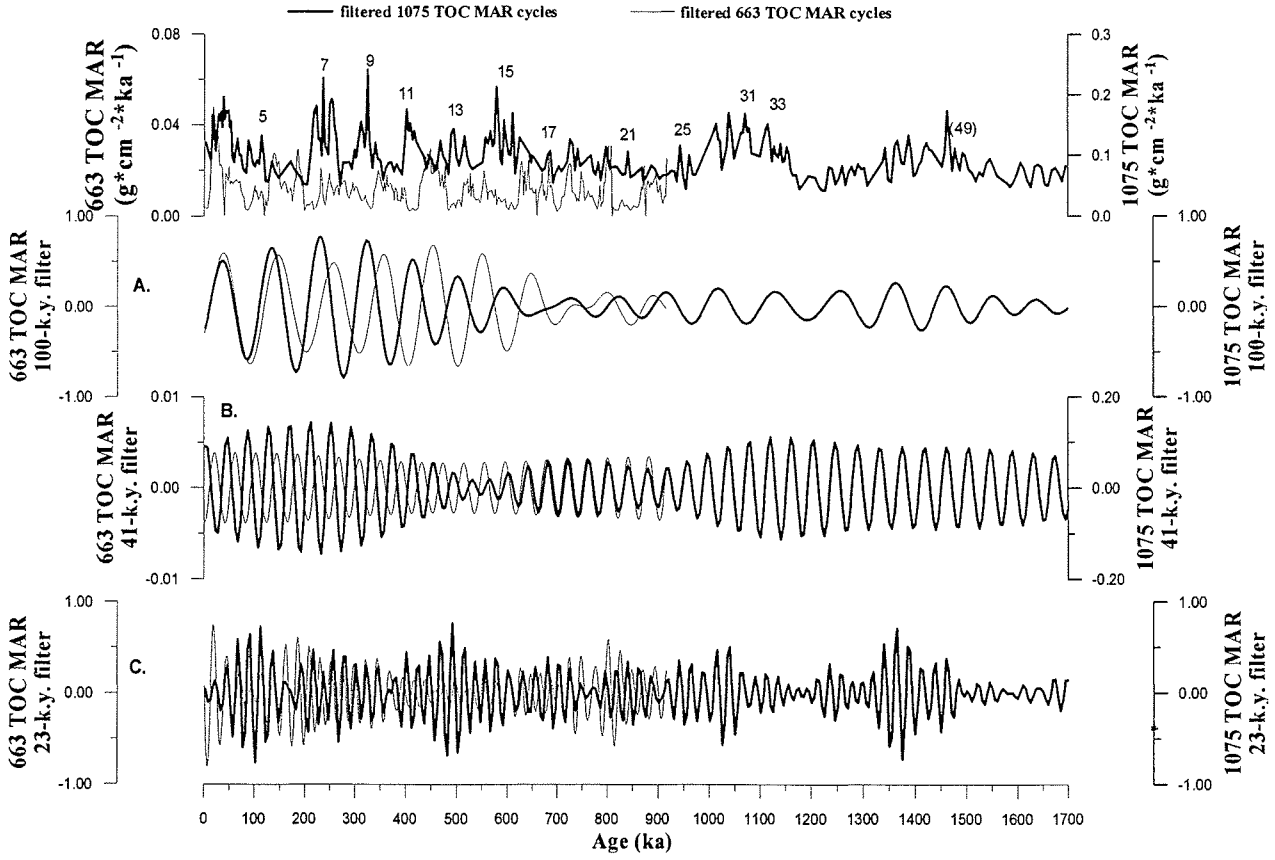

Figure 7: The TOC MAR record of Site 1075 in comparison with the TOC MAR record of ODP Site 663 (Wagner, 2000) for the last 0.9 m.y. **A.** Comparison of the TOC MAR_{100} component of the two sites (with central frequency = 0.01 cycles/k.y. and bandwidth = 0.001 cycles/k.y.). **B.** Comparison of the TOC MAR_{41} filter of the two sites (with central frequency = 0.024 cycles/k.y. and bandwidth = 0.001 cycles/k.y.). **C.** Comparison of the TOC MAR_{23} filter of the two sites (with central frequency = 0.043 cycles/k.y. and bandwidth = 0.009 cycles/k.y.). Note the phase reversal in the amplitudes for the 100 and 41-k.y. components.

in phase but then move out of phase for the last 0.6 m.y. No clear trend is observed in the comparison of amplitude variability of the TOC MAR_{23} component of Site 1075 with that of Site 663 over the last 0.9 m.y. (Fig. 7C). It appears that the amplitudes of the 1075 TOC MAR_{23} filter generally increased when the amplitudes of the 663 TOC MAR_{23} filter decreased and vice versa. The TOC MAR_{23} components are in phase over long periods. Exceptions are the intervals from 0.9 to 0.8 Ma, 0.7 to 0.6 Ma, 0.5 to 0.35 Ma, and 0.25 to 0.15 Ma when the amplitudes of TOC MAR are more or less out of phase. In order to examine the relationship in the frequency domain of the TOC MAR records for the two sites we performed a cross-spectral analysis between TOC MAR for Site 663 and Site 1075. The cross-spectral analysis was calculated for the 0-900 ka interval. The phasing results are illustrated in Figure 8, and demonstrate that the TOC MAR record of Site 663 has a negative correlation with the record of Site 1075 for the 100-k.y., 41-k.y., and 23-k.y. cycles.

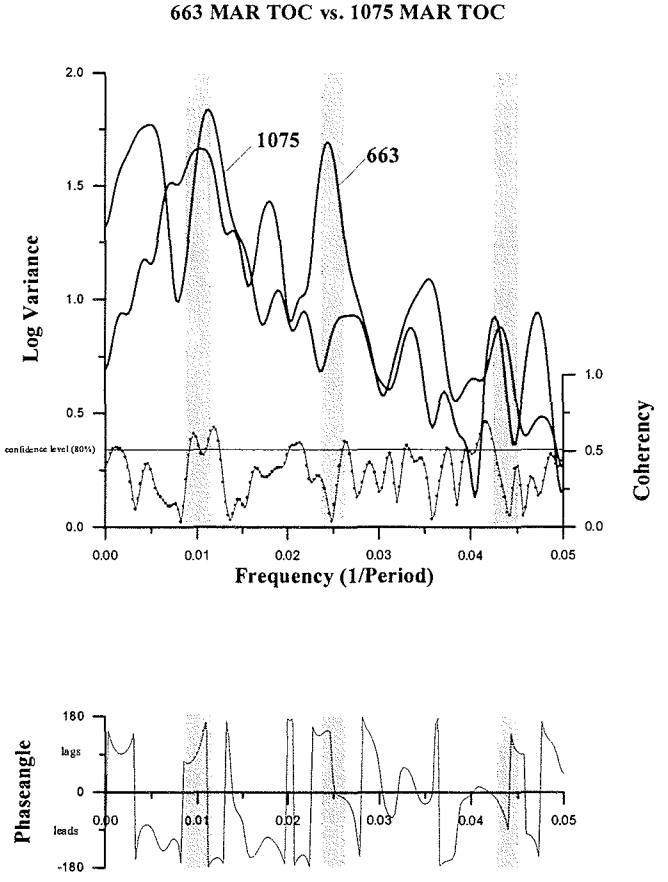

Figure 8: Cross-spectral results for the Site 663 TOC MAR record (Wagner, 2000) relative to the Site 1075 TOC MAR record.

Our filter and cross-spectral results of Sites 663 and 1075 support the hypothesis that organic sedimentation in the northern Congo Fan area is regulated by variations of precession-driven monsoonal precipitation. Strong precession will be modulated by variations in eccentricity. The 100-k.y. cycle might be ice-sheet driven, and in that case associated with high-latitude climatic change. During glacial periods monsoon

activity was reduced, the northward migration of the ITCZ was limited, the pressure gradient over the eastern South Atlantic and North Africa weakened, and the NE trades over the northern African continent were enhanced. Therefore, we can state that the accumulation of organic material in the northern Congo Fan has been, for the most part, relatively low during glacial periods, as evidenced at Site 663 over the past 0.9 m.y. and at Site 1075 for the past 1.7 m.y. During interglacial periods the ITCZ moved yearly to a more northerly position, strengthening the African monsoon and weakening the NE trades. Thus, enhanced terrestrial material from the Congo River, and consequently higher TOC MAR, occurred in the Congo Fan sediments during interglacials, while TOC MAR in the eastern equatorial Atlantic decreased.

Variations in terrigenous Fe input into the northern Congo Fan

Our filter results from the Fe-intensity record at Site 1075 are illustrated in Figure 9. High-amplitude variability of the Fe_{100} filter (Fig. 9A) is observed between 1.5 and 0.9 Ma and from 0.65 to 0.2 Ma. Between 0.9 and 0.65 Ma, the amplitudes of the Fe_{100} filter are subdued. Raymo et al. (1997) and Berger and Jansen (1994) proclaimed that the mid-Pleistocene transition (MPT) around 0.9 Ma was a climate step leading to late Pleistocene ice ages with increased mean ice volume and a dominant 100-k.y. cycle. Before 0.9 Ma, they maintained, the 41-k.y. cycle of Earth's obliquity was dominant over the 100-k.y. band. The strong 100-k.y. component in Fe content at Site 1075 between 0.65 and 0.2 Ma might be attributed to the growth of Northern Hemisphere glaciation. However, our Fe_{100} filter also shows high-amplitude variability prior to the MPT which cannot be easily explained by the ice effect. The amplitude variability pattern of the Fe_{100} filter raises the question of what forcing mechanism could cause such high amplitudes in the Fe_{100} filter between 1.5 and 0.95 Ma. A comparison of the Fe_{100} filter and eccentricity forcing indicates that they are more or less in phase from 1.5 to 0.9 Ma and for the last 0.4 m.y. For the periods from 1.7 to 1.2 Ma and 0.9 to 0.5 Ma, the Fe_{100} filter leads eccentricity. Eccentricity forcing tends to break down at times of maximum variability in the Fe_{100} filter (near 1.2 and 0.4 Ma).

Rutherford and D'Hondt (2000) reported the onset of 100-k.y. glacial cycles as early as 1.2 Ma in the oxygen isotope record of Site 659 from the tropical Atlantic. They concluded that the tropics played a major role in the initiation and maintenance of the 100-k.y. cycles, suggesting that increased heat flow across the equator or from the tropics to higher latitudes strengthened the semiprecession cycle in the Northern Hemisphere, triggering the transition to sustained 100-k.y. glacial cycles. According to Shackleton (2000), the 100-k.y. cycle does not arise from ice-sheet dynamics; instead, he says, it is probably the response of the global carbon cycle that generates the eccentricity signal by causing changes in atmospheric carbon dioxide concentration. An alternate explanation for strong 100-k.y. fluctuation at times when no large ice sheets existed is given by Mudelsee and Stattegger (1997). They also observed an interval of stronger climate fluctuations in the 100-k.y. amplitude around 1.2 Ma and speculated that this interval was a first, but unsuccessful "attempt" of the climate system to attain a nonlinear "late Pleistocene ice ages" state.

Compared to the Fe_{100} filte, somewhat lower amplitudes are observed for obliquity in the Fe-intensity record (Fig. 9B). The amplitude variability of the Fe_{41} filter has generally increased over the last 1.7 m.y., with persistently low amplitudes from 1.7 to 1.1 Ma slowly increasing to high amplitudes over the past 1.1

m.y. The increase of obliquity variations in the Fe counts might indicate an increasing influence of sea-level fluctuations on the sedimentation of terrestrial material in the northern Congo Fan. Precessional amplitudes in Fe intensity at Site 1075 follow the amplitudes of orbital forcing in many respects (Fig. 9C). For example,

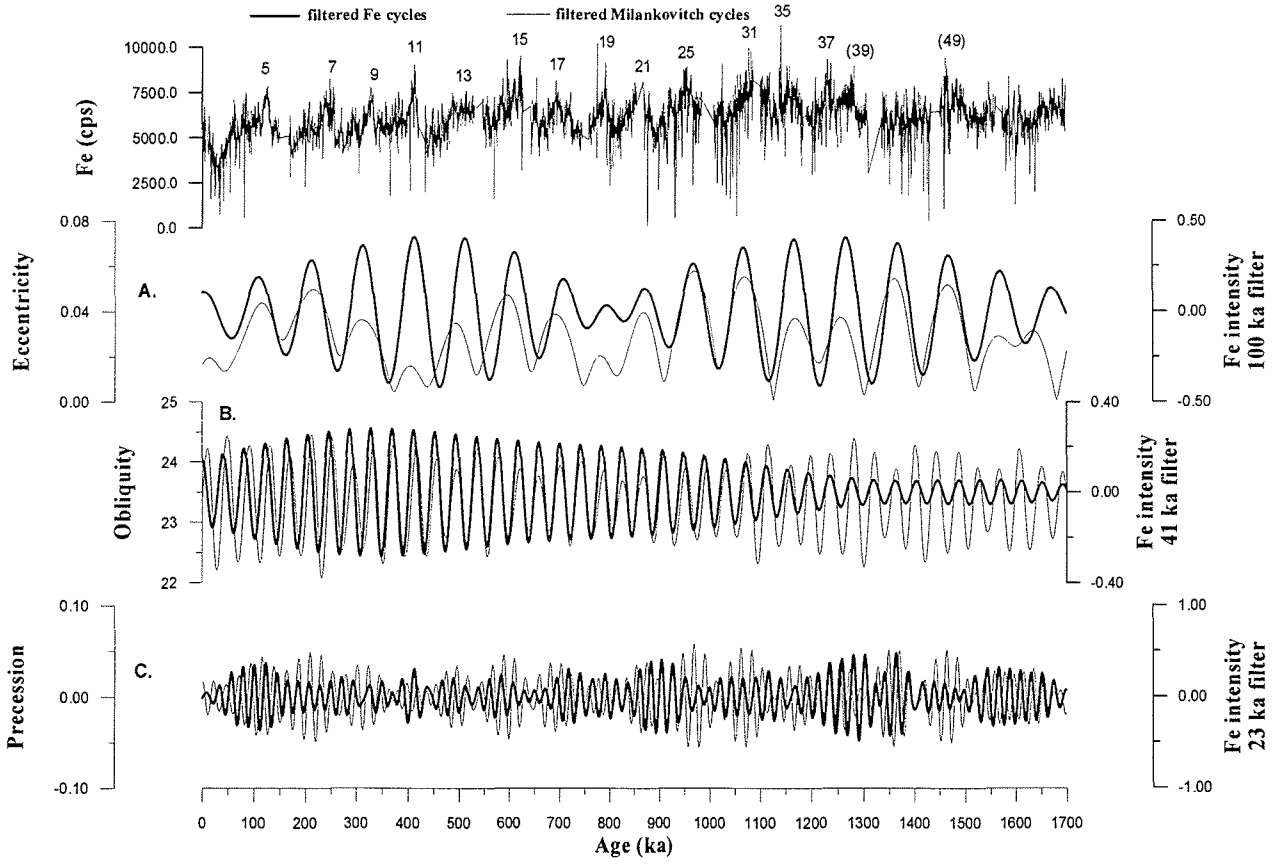

Figure 9: Filtered Fe-intensity signal from Site 1075 for the last 1.7 m.y. **A.** The Fe_{100} filter versus eccentricity (with central frequency = 0.01 cycles/k.y. and bandwidth = 0.001 cycles/k.y.). **B.** The Fe_{41} filter versus obliquity (with central frequency = 0.024 cycles/k.y. and bandwidth = 0.001 cycles/k.y.). **C.** The Fe_{23} filter versus precession (with central frequency = 0.043 cycles/k.y. and bandwidth = 0.009 cycles/k.y.).

we see large amplitudes around 1.6, 1.3, 0.9, and 0.1 Ma. These are to be expected because the amplitudes in the Fe_{100} component are also high. However, the match is not so good for some other intervals. Probably the most striking mismatches are around 1.45, 1.15, 1.0, and from 0.6 to 0.2 Ma, when the Fe_{100} filter is strong, and yet the response of the system is quite suppressed. This would mean that perhaps the sensitivity of the system did not change as a function of conditions provided by the 100-k.y. oscillation. It is apparent that the highest precessional amplitudes in the Fe-intensity cycles are expressed when orbital forcing reached an average position. The phase relationship between the precessional amplitudes in Fe intensity and orbital forcing is not constant, rather it shifts from nearly in phase to an antiphase state and back again. A closer inspection of how the phase relationship of the 23-k.y. precession cycle of Fe intensity evolved over time is illustrated in Figure 10. Moving up from the bottom of the hole, the phasing of the 23-k.y. precession

cycle related to Fe changes continuously, completing a full 360° shift in ca. 800 k.y. The same phase pattern is repeated for the interval from 0.8 to 0 Ma. The phase diagram (Fig. 10) for Site 1075 shows the same trend in the phase shift as reported in the phase-coupled precession and semiprecession cycles of Sites 607 and 659 from 1.5 to 0.5 Ma (Rutherford and D'Hondt, 2000), supporting the assumption that the onset of the 100-k.y. cycle was initiated in the tropics. The eccentricity amplitudes of the Fe record are greatest when the phase shift between Fe and precession is near zero, and smallest when the phase shift reaches 180° (opposite phase angles). Eccentricity forcing was reduced at around 1.25 and 0.4 Ma as shown by maximum amplitude variability of the Fe_{100} filter (Figure 10, vertical lines), and where the Fe_{23} filter is in phase with precession (Fig. 10; horizontal line). It is difficult to identify a logical mechanism that could be responsible for the linkage of the specific processes. One line of reasoning could suggest that a continuous shift in the annual onset of the African monsoon leads to a reinforcement in the amplitudes of the Fe_{100} filter at the time when the Fe_{23} filter and precession are in phase. Obviously, there is a correlation between eccentricity forcing and the Fe_{100} component as well as between precessional forcing and the Fe_{23} filter. Eccentricity shows a strong 400-k.y. cyclicity, whereas the Fe_{100} component implies two strong 800-k.y. cycles.

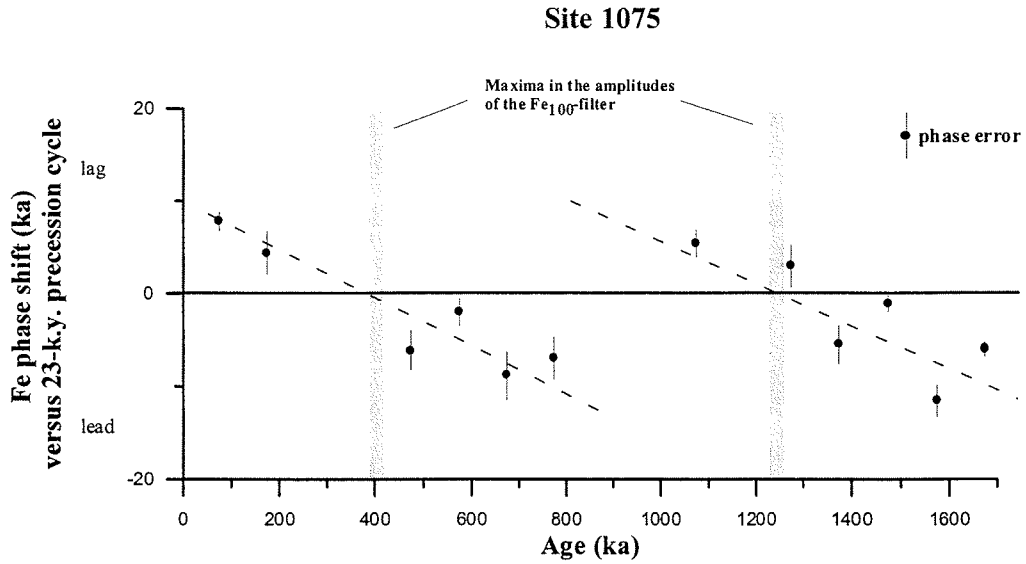

Figure 10: Phase diagram of Site 1075 Fe intensity with respect to orbital precession of the 23-k.y. cycle. Cross-spectral analyses obtained using the *AnalySeries* software package (Paillard et al., 1996).

Recapitulating, iron transport into the northern Congo Fan has been primarily driven by the Congo River load, with a lesser contribution by the SE-trades. The Fe-intensity record shows that enhanced iron input occurred predominantly during interglacial periods when the African monsoon was strengthened and therefore associated with higher precipitation over central Africa. The increased erosion on land is attributed to intensified monsoon rainfall, causing an enrichment of the Fe-rich clays into the Congo River and consequently leading to an increased concentration of Fe in the sediments of the Congo Fan area. From

our filter results we conclude that prior to the MPT high amplitudes in the Fe_{100} filter reflect the envelope of the Fe_{23} component, so that the effects in the Fe_{23} filter are modulated by variations of the Fe_{100} filter. This would support the proposition of Rutherford and D'Hondt (2000) that the tropics played a major role in the initiation and the maintenance of the 100-k.y. cycle and that the effects of low-latitude insolation will be modulated by eccentricity forcing, influencing the local climate and leading to changes in the African monsoon. From 0.65 to 0.2 Ma, the high-amplitude variability in the Fe_{100} component is primarily attributed to the ice buildup in the Northern Hemisphere within glacial-interglacial cycles. During glacial periods the ITCZ moved to a southerly position, weakening monsoon intensity and strengthening the trades, while during interglacials the ITCZ moved northward, intensifying the monsoon winds and weakened the trades. Our investigations bring us to conclude that terrigenous Fe in the northern Congo Fan area is predominantly driven by low-latitude forcing (precession modulated by eccentricity).

In contrast to the northern Congo Fan region, eolian material from the Sahara Desert into the equatorial Atlantic is mainly driven by the NE trades, which are more intense during glacial periods. According to deMenocal et al. (1993), terrigenous records in the equatorial Atlantic vary predominantly at 100 and 41-k.y. periodicities. They propose that high-latitude forcing could be related to cool North Atlantic sea-surface temperatures, which in turn promote African aridity and enhance dust-transporting wind speeds. Therefore, we assume that terrigenous signals in the equatorial Atlantic should be significant during glacial periods when Northern Hemisphere glaciation increased, which would support our theory that the Fe input into the northern Congo Fan is mainly driven by precession-related monsoonal precipitation. To verify this idea we collated the calculated terrigenous material of ODP Site 663 (deMenocal et al., 1993) from the eastern equatorial Atlantic with the Fe-intensity record of ODP Site 1075 (this study) for the last 0.9 m.y. For this we filtered the Site 663 terrigenous record on orbital parameters and compared it with the filtered 1075 Fe-intensity data. Our filter results are shown in Figure 11. The terrigenous content and the Fe-intensity data show the well-documented increasing amplitude of the 100 k.y. component since about 0.9 m.y. (Raymo et al., 1997; Berger and Jansen, 1994), reflecting particularly strong values during the last 0.65 m.y. (Fig. 11A). During the last 0.9 m.y., Fe and terrigenous content are out of phase, indicating higher Fe in the northern Congo Fan during interglacials concurrent with lower terrigenous concentration in the eastern equatorial Atlantic. For the 41-k.y. component, both the 1075 Fe and the 663 terrigenous content increased in their amplitudes over the last 0.9 m.y. Fig. 11B). The two parameters are out of phase over the entire period. The $terrigenous_{23}$ filter shows, in general, somewhat higher amplitudes compared to the Fe_{23} filter (Fig. 11C). However, the two parameters exhibit a good correlation in their amplitude modulation. The 23-k.y. filters of the 1075 Fe and the 663 terrigenous content are out of phase for the most part over the last 0.9 m.y., with exceptions at two short intervals from 0.8 to 0.75 Ma and from 0.25 to 0.2 Ma, when they are in phase. Our filter results confirm the assumption that Fe in the northern Congo Fan area and terrigenous content in the equatorial Atlantic are dominated by strong 100 and 41-k.y. variations, whereby the 1075 Fe content is most sensitive to high-latitude forcing during full interglacial periods when the ITCZ moved to a more northerly position, strengthening the precession-driven African monsoon. To corroborate the filter analysis we further examined this relationship in the frequency domain and performed a cross-spectral analysis between the terrigenous content of Site 663 and the Fe-intensity content of Site 1075 over the last 0.9 m.y. The cross-spectral analysis is shown in

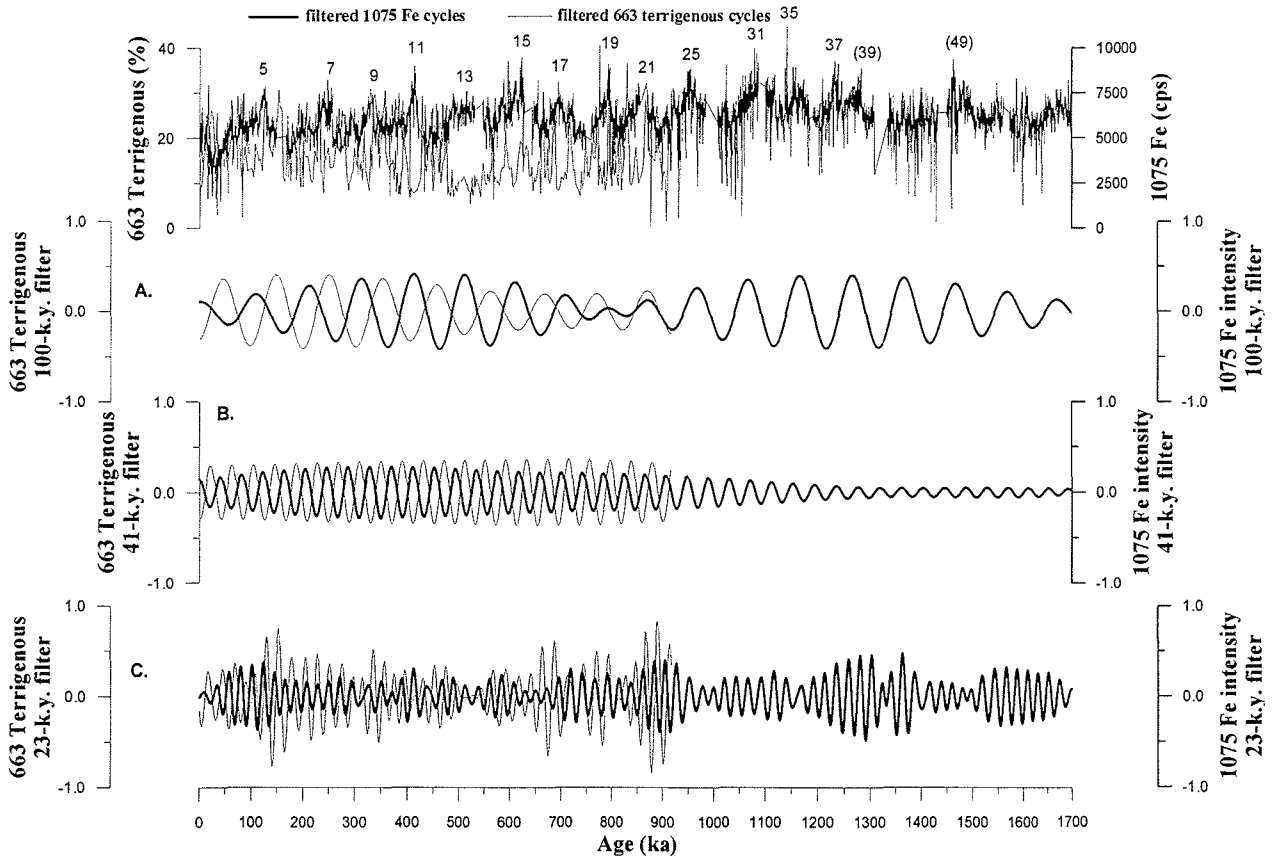

Figure 11: The Fe-intensity record of Site 1075 in comparison with the terrigenous record of ODP Site 663 (deMenocal et al., 1993) for the last 0.9 m.y. **A.** Comparison of the Fe_{100} component with the $terrigenous_{100}$ component (with central frequency = 0.01 cycles/k.y. and bandwidth = 0.001 cycles/k.y.). **B.** The Fe_{41} filter versus the $terrigenous_{41}$ filter (with central frequency = 0.024 cycles/k.y. and bandwidth = 0.001 cycles/k.y.). **C.** Comparison of the Fe_{23} component with the $terrigenous_{23}$ filter (with central frequency = 0.043 cycles/k.y. and bandwidth = 0.009 cycles/k.y.). Note the phase reversal in the amplitudes for the 100 and 41-k.y. components.

Figure 12 and shows significant coherency at the 100-k.y., 41-k.y., and 23-k.y. periodicities. The phasing of the terrigenous content at Site 663 is opposite to that of the Fe-intensity data of Site 1075, confirming our hypothesis based on the filter results. According to Berger et al. (2001) this would indicate that developments in high latitudes (ice buildup) and global cooling (desert development) provided for changes in the responses of tropical systems to (comparatively invariant) astronomical forcing. In turn, the greater sensitivity of the tropical systems would have resulted in increased feedback to the high-latitude ice dynamics.

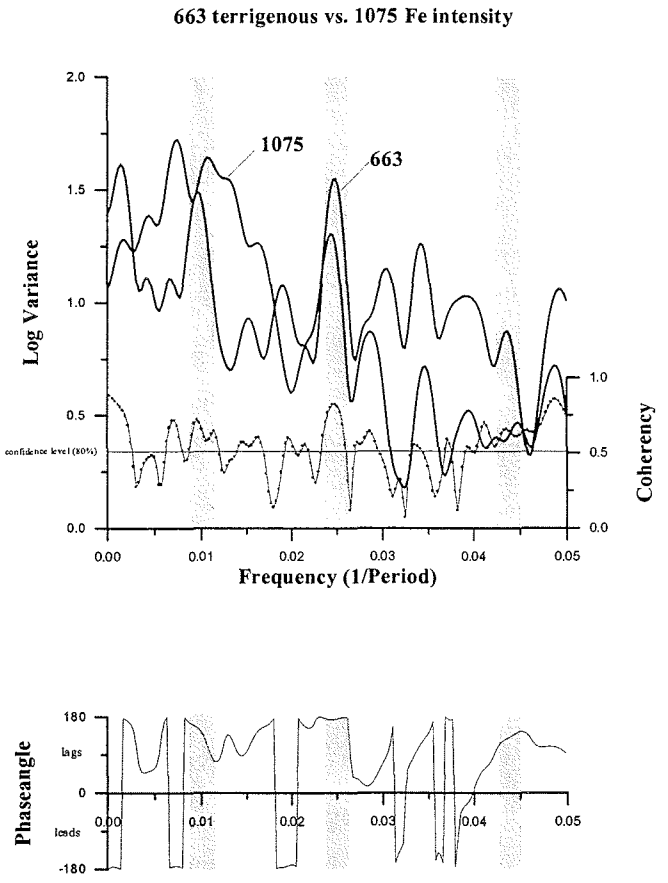

Figure 12: Cross-spectral results for the Site 663 terrigenous content record (deMenocal et al., 1993) relative to the Site 1075 Fe-intensity record.

CONCLUSIONS

1. Variations in organic carbon and terrigenous components in the northern Congo Fan area of site 1075 are used to infer changes in marine paleoproductivity and terrigenous input for the Pleistocene (1.7 Ma).
2. Total organic carbon mass accumulation rate (TOC MAR) and the Fe-intensity record exhibit high contents primarily during interglacial periods.
3. The terrestrial and marine productivity components provide evidence that TOC MAR is influenced by other factors in addition to marine productivity. Organic sedimentation in the northern Congo Fan is a result of various mechanisms, such as the volume of Congo River discharge, erosion of the shelf during low sea-level stands, and the input by C_4 compared to C_3 plants.
4. The iron supply into the northern Congo Fan is predominantly transported via the Congo River and to a lesser extent by the trades, so it is enhanced by increases in monsoonal precipitation.
5. Filtering analyses of the TOC MAR and the Fe-intensity records are dominated by strong 100-k.y. and 41-k.y. variations, implicating high-latitude forcing. Both records strongly exhibit precession variance, and filtering analyses implicate low-latitude forcing (precession), which controls monsoonal precipitation.

6. For the last 0.6 m.y., high amplitudes in variability are observed in the TOC MAR_{100} filter and in the Fe_{100} filter, indicating a stronger influence of Northern Hemisphere glaciation. Prior to 0.9 Ma, high-amplitude variability only occurred in the Fe_{100} filter, reflecting the envelope of the Fe_{23} component and demonstrating that strong precession is modulated by the variations in eccentricity and that the African climate was forced by precessional insolation modulation of monsoon intensity in the absence of significant high-latitude climate variability.

ACKNOWLEDGMENTS

We thank Helge Arz, Lydie Dupont, Eleonora Uliana for their discussions and suggestions. The study was financially supported by the Deutsche Forschungsgemeinschaft (SSP DSDP-ODP). Data are available at www.pangaea.de.

2.2 Manuscript II:

Variability Of Terrestrial Input And Marine Productivity In The Northern Benguela Current Associated With Orbital Cycles Over The Last 1.5 m.y.

Britta Jahn, Barbara Donner, Peter J. Müller, Ursula Röhl, Ralph R. Schneider, and Gerold Wefer

Department of Geosciences, University Bremen, Postbox 330440, D-29334 Bremen, Germany

Submitted to *Palaeogeography, Palaeoclimatology, Palaeoecology*

ABSTRACT

We infer variations in paleoproductivity and eolian input with respect to variations in Earth's orbital Milankovitch cycles over the past 1.5 m.y. For this purpose detailed records of the stable oxygen isotope composition of planktonic foraminifera and total organic carbon mass accumulation rates (TOC MAR), as well as XRF core-scanner analyses of Fe content from ODP Site 1082 (Leg 175) are considered in the Walvis Basin. The most pronounced paleoclimatic changes in the northern Benguela system correspond to the mid-Pleistocene Revolution (MPR), the time interval at about 0.9 Ma, when glacial conditions in the Northern Hemisphere led to the onset of pronounced 100-k.y. glacial-interglacial cycles. We used Fe intensity as a proxy for eolian terrigenous input, and TOC MAR as a paleoproductivity indicator. Paleoproductivity and eolian input show generally higher amplitude variations of glacial-interglacial cyclicity from 1.5 to 0.58 Ma, indicating a strengthening of upwelling-favorable winds in this area. At 0.58 Ma, paleoproductivity and eolian input shifted abruptly to lower amplitude variations with a periodicity of 100 k.y. $\delta^{18}O$ values show a trend toward more negative isotope ratios for the past 0.65 m.y., especially during glacial periods, indicating increasingly warmer sea-surface temperatures during glacials toward the end of the Pleistocene. To evaluate the relative influences of Northern Hemisphere glaciation and Southern Hemisphere insolation as potential forcing mechanisms for variations of eolian input and productivity in the northern Benguela system, we filtered our proxy records at orbital frequencies. The filtered results of Fe intensity and TOC MAR indicate a strong influence of the 100-k.y. and 41-k.y. frequency bands, supporting our assumption that strong ice buildup in the Northern Hemisphere is the dominant trigger for climate changes in the northern Benguela system, while Southern Hemisphere insolation plays only a secondary role.

INTRODUCTION

The Benguela upwelling system is one of the five largest continental margin upwelling systems in the world, with analogues off Peru, California, northwest Africa and in the northeastern Arabian Sea. The development of the Benguela Current system is an important component in the Pleistocene evolution of the Southern Hemisphere climate and of South Atlantic circulation patterns. Our knowledge of the early Pleistocene history of upwelling, productivity, and wind intensity off Namibia is poor (Diester-Haass et al., 1986, 1992; Diester-Haass and Rothe, 1987; Dean and Gardner, 1985; Hay and Brock, 1992), whereas the late Quaternary history of upwelling in the northern part of the Benguela system has been examined in much more detail (e.g., Kirst et al., 1999; Summerhayes et al., 1995; Diester-Haass, 1985a, b, 1988; Diester-Haass et al., 1990). Knowledge of the early Pleistocene history of upwelling in this region is derived mainly from Sites 362 and 532, drilled during Legs 40 and 75 of the Deep Sea Drilling Project (DSDP; e.g., Oberhänsli, 1991).

ODP Site 1082, drilled during Leg 175 off northern Namibia (Fig. 1), allows a more detailed reconstruction of oceanographic and atmospheric processes influencing the Benguela upwelling

system. The coring site is located closer to the coast than the earlier DSDP sites, and is therefore more directly influenced by the northern Namibian upwelling cell, which is driven by prevailing southeast trade winds. The coastal upwelling area and the seaward mixing zone of eddies and filaments of upwelled waters are characterized by high primary production with values of 125-180 gC m^{-2} yr^{-1} (Berger et al., 1987). Compared to DSDP Site 532, which shows evidence of sediment redeposition (e.g., Diester-Haass et al., 1990, 1992), ODP Site 1082 provides a more continuous and less disturbed sequence (Wefer et al., 1998), and thus a new opportunity to determine the variability in related terrigenous input and paleoproductivity during the Pleistocene. Recent investigations in the Cape Basin off northern Namibia have shown that grain-size variations are an excellent indicator for eolian dust and the strength of the southeast trade winds (Stuut et al., in press), and that the organic carbon content of the sediments can be used as a proxy for variations in late Quaternary productivity (Kirst et al., 1999).

The aim of the present study is to reconstruct how the magnitudes of paleoproductivity and eolian terrigenous input have changed in the northern part of the Benguela Current system over the past 1.5 m.y. From such variations we further interpret changes in upwelling trade-wind conditions in connection with orbital parameter variations. Previous work based on DSDP sites, ODP sites, and on gravity and piston cores (e.g., Berger et al., unpublished; Kirst et al., 1999; Summerhayes et al., 1995; Hay and Brock, 1992; Sancetta et al., 1992; and Diester-Haass et al., 1985) has shown that fluctuations in marine productivity and eolian terrigenous input are not related to the classical glacial-interglacial cycles with increased content during glacial periods. Therefore, the intention of this study is to examine long-term variations in the fluctuations of terrigenous input and productivity in the northern Benguela Current. For this purpose we employed the stable oxygen-isotope compositions of planktonic foraminifera, total organic-carbon mass accumulation rates (TOC MAR), and variations of Fe content as determined by X-ray fluorescence. Together, these data provide a set of paleoenvironmental parameters associated with changes in ice volume and temperature inferred from foraminiferal $\delta^{18}O$, paleoproductivity as indicated by TOC MAR, and wind intensity or weathering conditions on land with the amount of Fe as an eolian dust indicator.

REGIONAL CLIMATE AND OCEANOGRAPHIC SETTING

The study area is influenced by the BCC (Benguela Coastal Current) (Fig. 1). The BCC is the northward-flowing coastal branch of the BC (Benguela Current) (Martin, 1981). The splitting of the BC into the westerly (main) and easterly (weaker) branches starts north of 30°S. The northward-flowing BCC converges with the southward-flowing Angola Current (AC) at 18°S, but the AC may penetrate as far as 23°S, the latitude of Walvis Bay (Moroshkin et al., 1970). Where the BCC and AC meet, the Angola Benguela Front (ABF) develops (Fig. 1). The ABF is characterized by eddies with nutrient-rich upwelled water (Hagen et al., 1981). There is a link between the position of the ABF and the atmospheric South Atlantic Anticyclone (SAA) (Shannon et al., 1987). During austral summer and autumn when the SAA moves southward, the flow of warm AC is at its maximum, so

and the ABF is located farthest south and is widest at this time. During austral winter and early spring, when the SAA moves northward, the ABF also shifts to the north, becoming narrower and weaker (Meeuwis and Lutjeharms, 1990), allowing greater amounts of cold BC water to flow into the Angola Basin.

The location of atmospheric high- and low-pressure systems over the South Atlantic is influenced by the position of the Intertropical Convergence Zone (ITCZ; Fig. 1), the convergence zone of the trade wind systems of the Northern and Southern Hemispheres over the Equatorial Atlantic. This pattern induces more meridionally directed trades along the southwest African coast and more zonal wind directions farther offshore (Peterson and Stramma, 1991). At present the thermal equator, marking the mean annual position of the ITCZ, averages around 6°N, so that the oceanic convergence occurs north of the equator (Fig. 1).

In the northern Benguela upwelling system, the prevailing trade winds induce coastal upwelling of cold, nutrient-rich water from depth around 300 to 500 m in the south and 150 to 200 m in the northern part of the upwelling area (Simpson, 1971) (Fig.1). The trade winds are strongest during the southern hemisphere winter, when the South Atlantic anticyclone shifts northwards, so that the strongest upwelling occurs from April to November (Shannon, 1985).

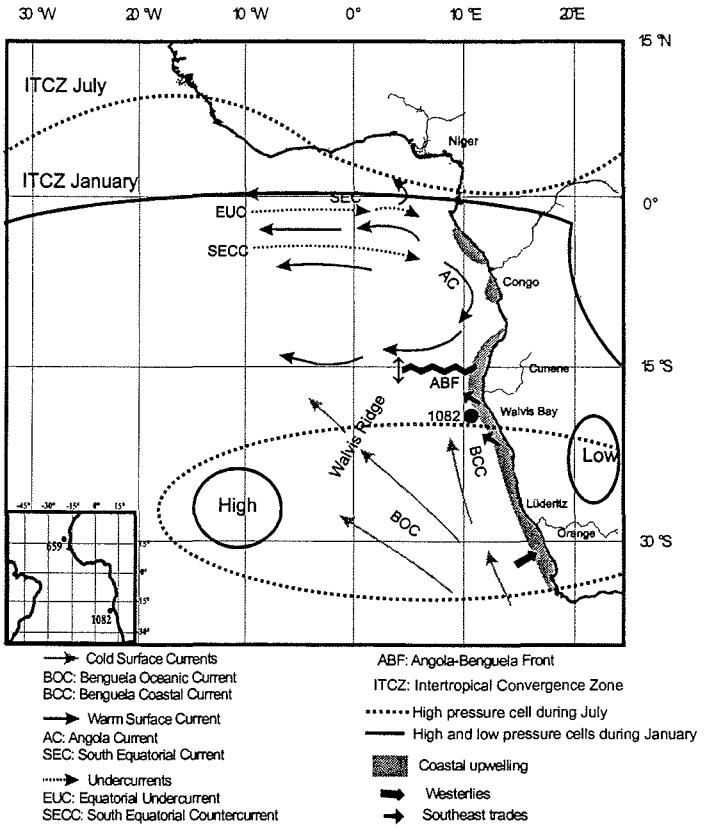

Figure 1: Oceanographic setting of the study area and location of ODP Site 1082.

MATERIAL AND METHODS

Core Location and Lithology

ODP Site 1082 (21.5° S, 11.5° E) was drilled during Leg 175 in 1290 m water depth at the outer edge of the Namibian upwelling cell (Fig. 1; Wefer et al., 1998). The 600 m-long sediment sequence consists of continuous hemipelagic muds spanning the upper Miocene to Holocene (5.8-0 Ma). According to shipboard investigations, the upper 170 meters composite depth (mcd) investigated in this study represent the last 1.5 m.y. and are composed of alternating intervals of bioturbated olive and black muds. The sequence from 0 to 127 mcd is rich in nannofossils and foraminifers, while from 127 mcd downcore the mud is rich in diatoms (Wefer et al., 1998). Within the sequence from 170-0 mcd, small intervals from Holes 1082B and 1082C were used to fill across core breaks in Hole 1082A in order to avoid gaps in our records where the sediment column was disturbed or missed during the coring process. The hole-to-hole correlation is based on magnetic susceptibility and color reflectance data (Wefer et al., 1998).

Analytical Methods

The planktonic foraminiferal species *Globorotalia inflata* was sampled at depth intervals of about 20 cm. For each sample, 15 to 20 specimens were handpicked in the size fraction >150 μm. Stable oxygen isotope ratios were measured on a FINNIGAN MAT 251 micromass spectrometer equipped with a Kiel automated carbonate line. Calibration of the lab internal standard gas to PDB standard scale was achieved using NBS (National Bureau of Standards, Vienna) $CaCO_3$ standards 18, 19, and 20. The analytical precision ($\pm 1\sigma$) based on replicate analyses of an internal calcium carbonate standard was better than 0.07‰ for $\delta^{18}O$.

For total organic carbon (TOC) measurements, samples were taken at depth increments of about 50 cm. TOC was determined by combustion at 1050°C using a HERAEUS CHN-O Rapid elemental analyzer as described in Müller et al. (1994). TOC content is reported in dry weight percent. The relative precision of the measurements based on duplicates and multiple analysis of a reference sediment sample (WST 2) was better than 3%.

High-resolution X-ray fluorescence (XRF) data were obtained by running the undisturbed archive halves of the cores in 2 cm steps through the XRF Core Scanner of Bremen University (Röhl & Abrams, 2000). The scanner provides a semiquantitative analysis of element intensities in counts per second (cps) from potassium through strontium in the periodic table of chemical elements (Jansen et al., 1998). The sediment surface is excited by a molybdenum X-ray tube (20 kV) and fluorescent radiation is measured by a Peltier cooled PSI detector (KEVEXtm) with a 125 μm Beryllium window and a multi-channel analyzer with a 20 eV spectral resolution. Test runs resulted in the definition of a 30-second counting time and an X-ray current of 0.087 mA as the optimal configuration for obtaining high-quality and statistically significant intensity data for the elements of interest (e.g., K, Ca, Fe, Ti, Mn, Sr). In this study only the Fe counts are presented for our interpretations. For

comparison with the Fe record we used measurements of magnetic susceptibility that were made on whole cores from all holes as part of the shipboard routine Multi-Sensor Track (MST) analysis (Wefer et al., 1998).

We employed time-series analysis (band-pass filter synthesis approach *AnalySeries* package, Paillard et al., 1996) to partition each climatic record into its dominant frequency components in the 23-, 41-, and 100-k.y. bands. This makes it possible to examine each of the three major cycles separately and to obtain evidence about the way in which the system responds to the forcing in each band (Imbrie et al., 1993). This is achieved by applying an appropriate band-pass filter, using, in our case, a Tukey filter (Jenkins and Watt, 1968). We started by extracting the filter components from the records of Fe intensity and TOC MAR associated with the 23-k.y. (precession; central frequency = 0.043 cycles/k.y.; bandwidth = 0.0024 cycles/k.y.), 41-k.y. (obliquity; central frequency = 0.024 cycles/k.y.; bandwidth = 0.0024 cycles/k.y.), and 100-k.y. (eccentricity; central frequency = 0.01 cycles/k.y.; bandwidth = 0.0024 cycles/k.y.) band-pass filters. Then we compared our filtered components (Fe intensity and TOC MAR) with those from the Site 659 $\delta^{18}O$ record (Tiedemann et al., 1994) and the winter insolation at 40° south (Berger and Loutre, 1991).

Stratigraphy

As a result of changes in sea water due to the buildup and retreat of glacial polar ice caps, and of changes in water temperature and salinity, the oxygen-isotope record of the planktonic foraminifera *G. inflata* shows the characteristic pattern for marine Quaternary $\delta^{18}O$ records (Fig. 2). *G. inflata* was chosen for isotope stratigraphy, although this species does not occur continuously throughout the investigated sediment sequence at this site. *G. inflata* is absent in MIS (Marine Isotope Stages) 47, 43, 33, and 25 in Site 1082 sediments. The $\delta^{18}O$ record of Site 1082 was visually aligned to the benthic $\delta^{18}O$ record of ODP Site 659 from the Cape Verde Plateau off northwest Africa, assuming uniform sedimentation rates between the assigned age control points of Site 659 (Tiedemann et al., 1994; Fig. 2). However, the correlation between our planktonic record and the benthic curve exhibits some difficulties, as the $\delta^{18}O$ record of *G. inflata* shows a less pronounced glacial-interglacial amplitude than the Site 659 benthic record. A reliable determination of the isotope stages from MIS 21 to 17 was therefore difficult. Paleomagnetic data (Wefer et al., 1998) and assigned magnetochrons were employed to help solve the MIS 21 to 17 problem and to identify the well-dated boundaries of Brunhes/Matuyama (0.78 Ma) and the top and bottom of Jaramillo (0.99 and 1.06 Ma). A comparison of the 41-k.y. filter outputs from the $\delta^{18}O$ records between Sites 1082 and 659 shows a good match for the last 1.5 m.y. (Fig. 3) and supports the initial age model and the alignment shown in Fig. 2. Sedimentation rates (SR) were assumed to be linear between the assigned age control points (Fig. 2) and average on the order of 10 cm/k.y. over the past 1.5 m.y. (MIS 48 to 1; Fig. 2). The time interval from 1.0 Ma (MIS 34) to about 0.75 Ma (MIS 18) is characterized by slightly higher SR's of about 15 cm/k.y.

RESULTS

Oxygen isotopes. The 1.5 m.y.-long oxygen-isotope record of *G. inflata* (Fig. 2) can be separated into three distinctive intervals. The interval from 1.5 to 0.78 Ma is characterized by $\delta^{18}O$ values ranging from 2.8 ‰ to 1.2 ‰, and poorly expressed glacial-interglacial cycles. During the second interval, from 0.78 to 0.6 Ma, the onset of pronounced 100-k.y. glacial-interglacial cycles is evident, and oxygen-isotope values approach their highest glacial and interglacial values during MIS 17 and 16, respectively. This interval appears to contain the mid-Pleistocene climatic shift at the MIS 22/20 boundary, a time when the patterns in many marine $\delta^{18}O$ records change from a shorter cyclicity dominated by the 41-k.y. obliquity period to the sawtooth-shaped larger amplitude 100-k.y. cycles characteristic of the late Pleistocene (Mudelsee and Stattegger, 1997). The third interval, from 0.6 Ma to the Recent shows 100-k.y. glacial-interglacial cycles with $\delta^{18}O$ values ranging from 3.7 ‰ to 0.5 ‰. Marine isotope stages 11, 9, and 5, as well as the Holocene, exhibit the lowest $\delta^{18}O$ values of the entire record, indicating that the warmest interglacial conditions occurred during the last 0.5 m.y. of the total investigated 1.5 m.y. Interestingly, the *G. inflata* $\delta^{18}O$ record shows a continuous trend of decreasing glacial values for the last 0.65 m.y. The decrease in mean glacial $\delta^{18}O$ values over this period is about 1 ‰.

Total organic carbon. In the sediments of Site 1082, TOC content ranges from 2 wt% to 13 wt% (Fig. 4). To compensate for dilution by other sediment constituents, we calculated TOC mass accumulation rates (TOC MAR) by multiplying %TOC with linear SR and DBD (Dry Bulk Density). TOC MAR's show a pattern similar to that for %TOC concentrations (Fig. 4). The highest %TOC concentrations occur in interglacial MIS's 17 and 15. In sediments younger than about 0.55 Ma, the highest TOC contents were observed in the interglacials MIS 3, 5, 7, and 9. High-amplitude variations occurred from 1.5 to 0.58 m.y. and low-amplitude variations for the last 0.58 Ma. TOC MAR ranges from 0.1 g/cm²*k.y. during glacials to interglacial values of about 1.2 g/cm²*k.y. Certain intervals are characterized by higher amplitudes (1.5 to 1.3 Ma, 1.1 to 0.58 Ma, and 0.3 to 0.2 Ma), while between these intervals the glacial-interglacial variability in TOC and TOC MAR is relatively low.

Fe intensity. The record of Fe intensities at a temporal resolution of about 200 years can be compared to variations observed in the %TOC and in the TOC MAR records (Fig. 4). From 0.58 to 1.5 Ma we observe a pattern similar to the %TOC and TOC MAR records (although these two parameters exhibit higher amplitude variations than Fe). High Fe intensities, ranging from nearly 3000 cps to a maximum of 5500 cps, are observed both during glacial and interglacial periods, and at the terminations of interglacials (MIS 27, 25, 19/18, 16, 15, 12, 7/6, 5/4, and 3/2). The sediment sequence above 0.58 Ma exhibits variations in Fe ranging from 4500 to 1300 cps. From 0.5 to 0.27 Ma, it shows a rather low amplitude variability in conformity with the %TOC and TOC MAR values. For the last 0.27 Ma, Fe intensities demonstrate a trend to slightly higher values, while %TOC and TOC MAR exhibit increased values only during MIS's 9, 8, and 7. We therefore presume that the parameters indicative of

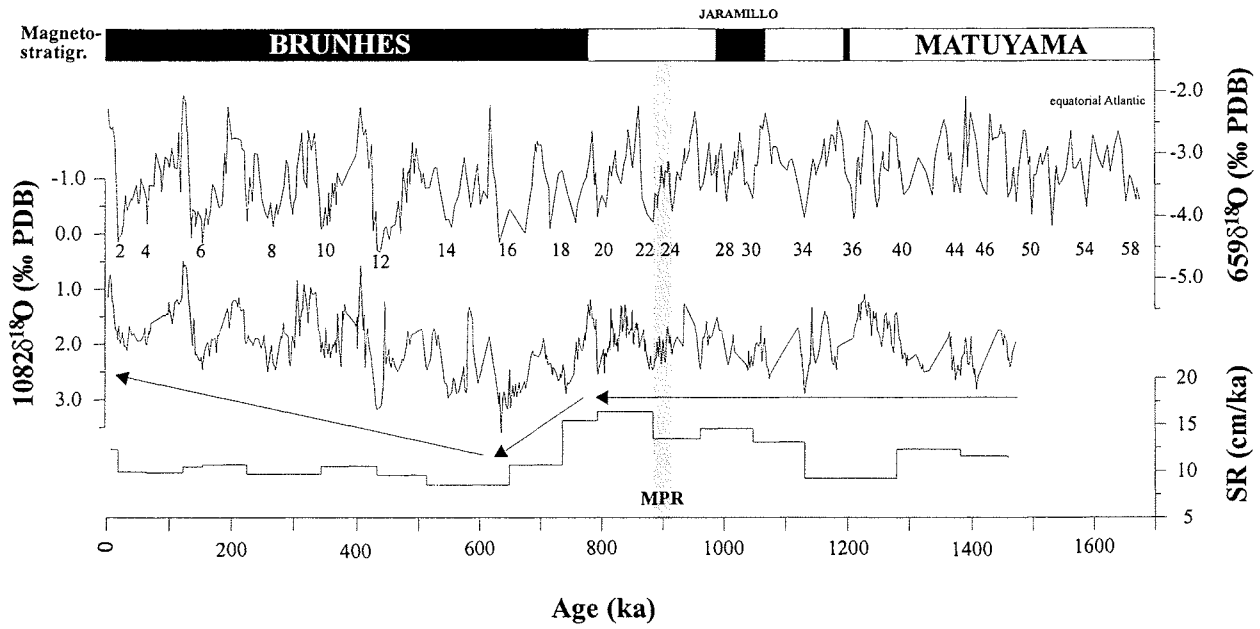

Figure 2: Left: Site 1082 $\delta^{18}O$ record from planktonic foraminifera (bold line) and the associated sedimentation rates. Right: Comparison with Site 659 $\delta^{18}O$ record of benthic foraminifera (Tiedemann et al., 1994). At 0.9 Ma, the mid-Pleistocene Revolution (MPR) indicates the transition from the dominant 41-k.y. cycle before 0.9 Ma to the dominant 100-k.y. cycle throughout the late Pleistocene. Changes in long-term variations of glacial-interglacial cycles are labeled by the arrows.

eolian input and biogenic production can-not be associated unambiguously with either glacial or interglacial conditions.

Magnetic Susceptibility. Shipboard magnetic susceptibility data (MS) (Wefer et al., 1998) vary between 0 and 60 SI*10^{-6}, manifesting again the same pattern as %TOC, TOC MAR, and Fe (Fig. 4). In contrast to the other three proxies, MS displays a continuous high-amplitude variability throughout the core. In the time period from 1.5 to 0.58 Ma, the MS amplitude increases slightly with values between almost 0 and a maximum of 60 SI*10^{-6}. In the interval from 0.58 to 0 Ma, the MS values range from near 0 to 50 SI*10^{-6}.

Filtering the Fe and TOC MAR records. All records show significant variance in all orbital frequency bands (e.g., 1/100 k.y., 1/41 k.y., and 1/23 k.y.). However, relative proportions of variance are highly variable for each orbital frequency over the past 1.5 m.y. Therefore, we have filtered the Fe and TOC MAR records for orbital frequencies. These filtered records elucidate the changing importance of the individual orbital cycles in the records (Fig. 5 and 6).

In general, the sum of filtered orbital signals of the Fe-intensity data compare well with the unfiltered Fe-intensity data in terms of the timing of all major events, except for oxygen-isotope stages 41, 37, 33, 17,

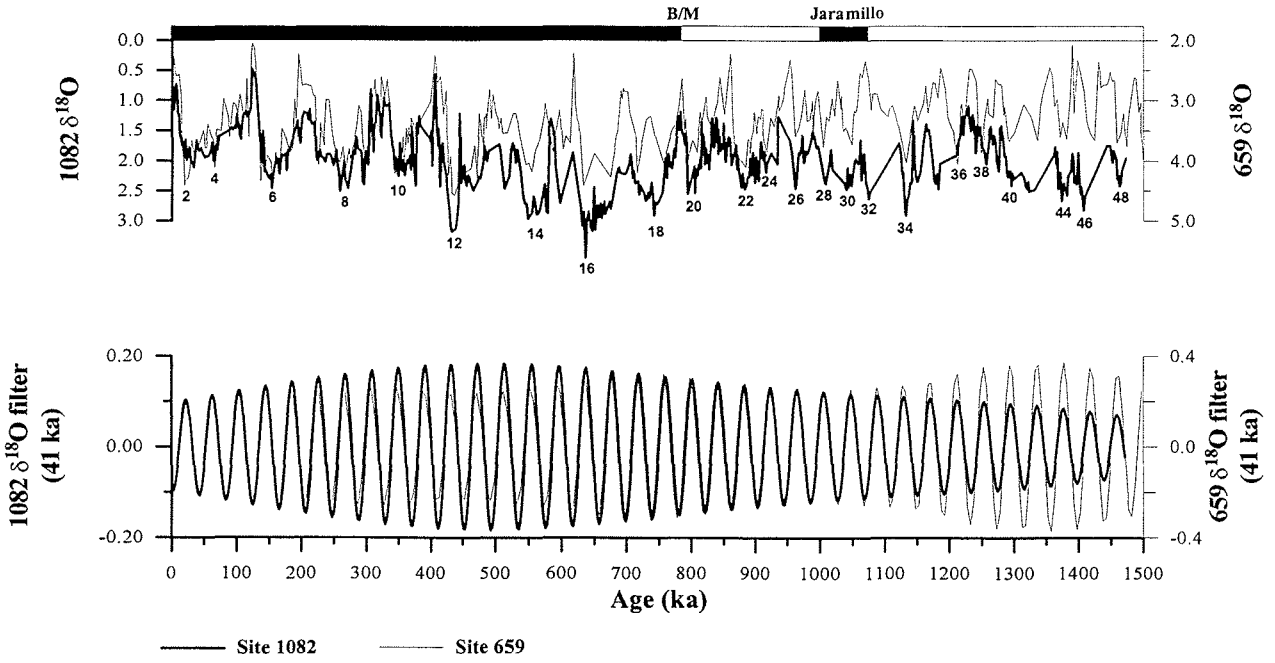

Figure 3: Benthic $\delta^{18}O$ record of Site 659 (thin line above) (Tiedemann et al., 1994) in compared with the planktonic $\delta^{18}O$ record of Site 1082 (thick line above) and their 41-k.y. filter (below). The filters used have a central frequency of 0.024 and a bandwidth of 0.0024 cycle/k.y. for the 41-k.y. band-pass filter.

14, and 6 (Fig. 5). Maximum amplitudes are reflected in the 100-k.y. filter with a strong modulation over the entire record. Low-amplitude signals are the case for the 41-k.y. and 23-k.y. filter. The 41-k.y. filter output demonstrates a shift at around 0.5 Ma from high-amplitude to low-amplitude variability. A decrease in the amplitude of 23-k.y. period is apparent in 23-k.y. filter for the last 0.2 m.y. The sum of filtered orbital signals of the TOC MAR curve closely follows the unfiltered TOC MAR data, except for the last 0.6 m.y. (Fig. 6). The 100-k.y. and 41-k.y. filter results display the highest amplitudes, whereas the 23-k.y. filter shows the lowest amplitudes. Extremely low-amplitude variations are seen in the 100-k.y. and 41-k.y. filters for the last 0.6 Ma, while the 23 k.y. filter shows an increase in amplitude.

DISCUSSION

Terrigenous Supply By Eolian Input

Because Site 1082 is located relatively far (ca. 150 km) from land, we assume that the Fe intensities mainly reflect eolian input along West Africa from the Namib Desert. The Namib Desert is the primary modern source of terrigenous Fe, and has been throughout the Pleistocene (Lancaster, 1981). The terrigenous supply of Fe by eolian transport is influenced by changes in the intensity of the southeast trade winds and

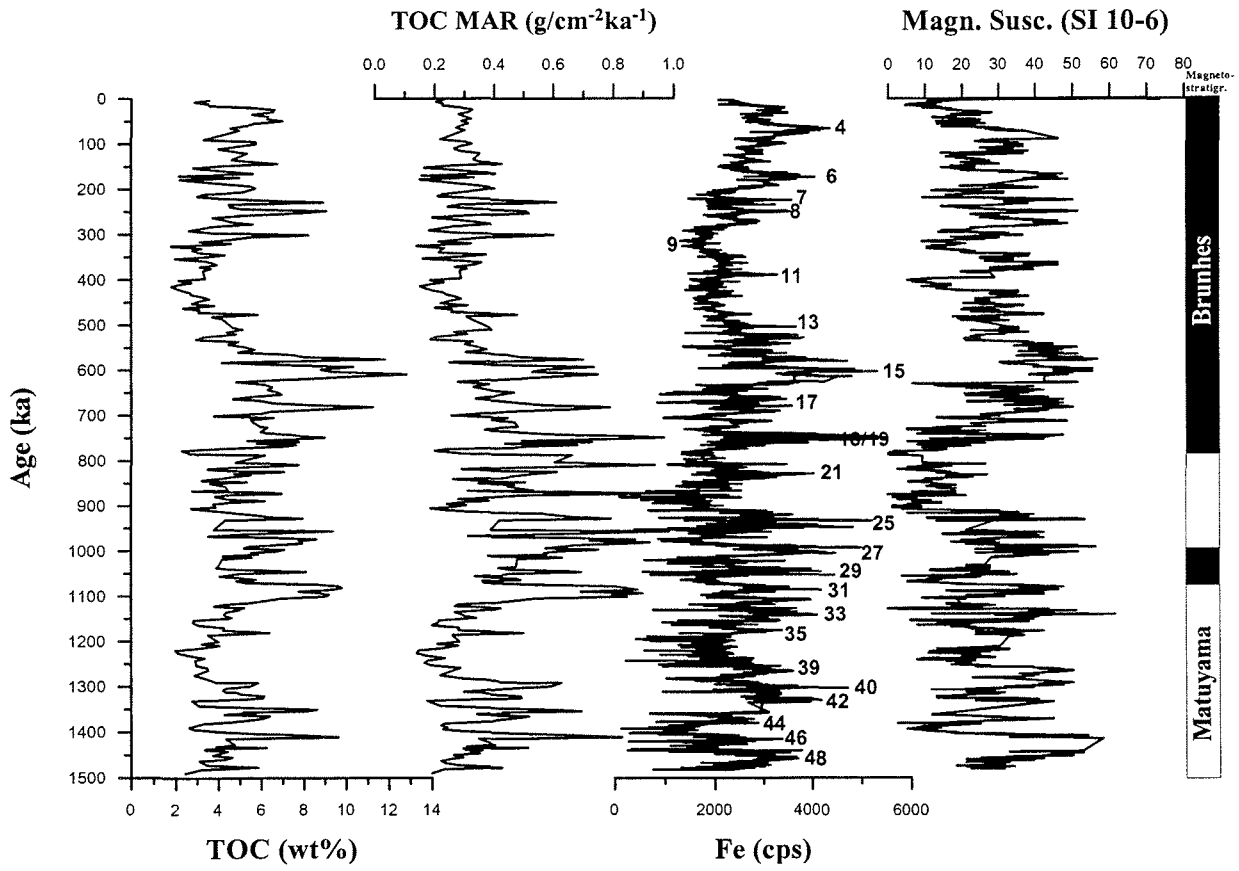

Figure 4: Site 1082 TOC content and TOC MAR (left), Fe intensities (right; thin line) with a smoothed Fe-intensity record (right; thick line) and magnetic susceptibility (right) versus age.

weathering conditions on land. We therefore interpret the amount of Fe in the sediments to reflect the degree of aridity in the eolian source region as well as wind intensity. Because the core is located in the Benguela upwelling system, the greatest changes in surface-water characteristics are expected in response to changes in atmospheric circulation. For that reason, Fe is also a good proxy both for changes in wind stress and for upwelling intensity.

As shown in Fig. 4, terrigenous input of Fe from the Namib Desert is much greater from 1.5 to 0.58 Ma than during the interval from 0.58 Ma to the Holocene. This indicates periods with stronger winds or more intense weathering conditions. At 0.58 Ma, a major change occurred in wind strength or in the humidity conditions related to weathering intensity. This is determined based on a change to low-amplitude variability of Fe intensities related to the 100-k.y. periodicity. Fe intensities between about 0.58 to 0.27 Ma (Fig. 5) indicate a minimum in the amplitude of moderate winds or weathering during the interglacials MIS 13, 11, and 9, and may suggest reduced upwelling intensity in the northern Benguela Current. From 0.27 to 0 Ma, there is a shift to higher Fe values, particularly during MIS 8, 7/6, 4 and 3/2, suggesting another slight increase in wind strength and upwelling intensity. The interpretation of enhanced upwelling and terrigenous supply from the Namib Desert during glacial and interglacial periods

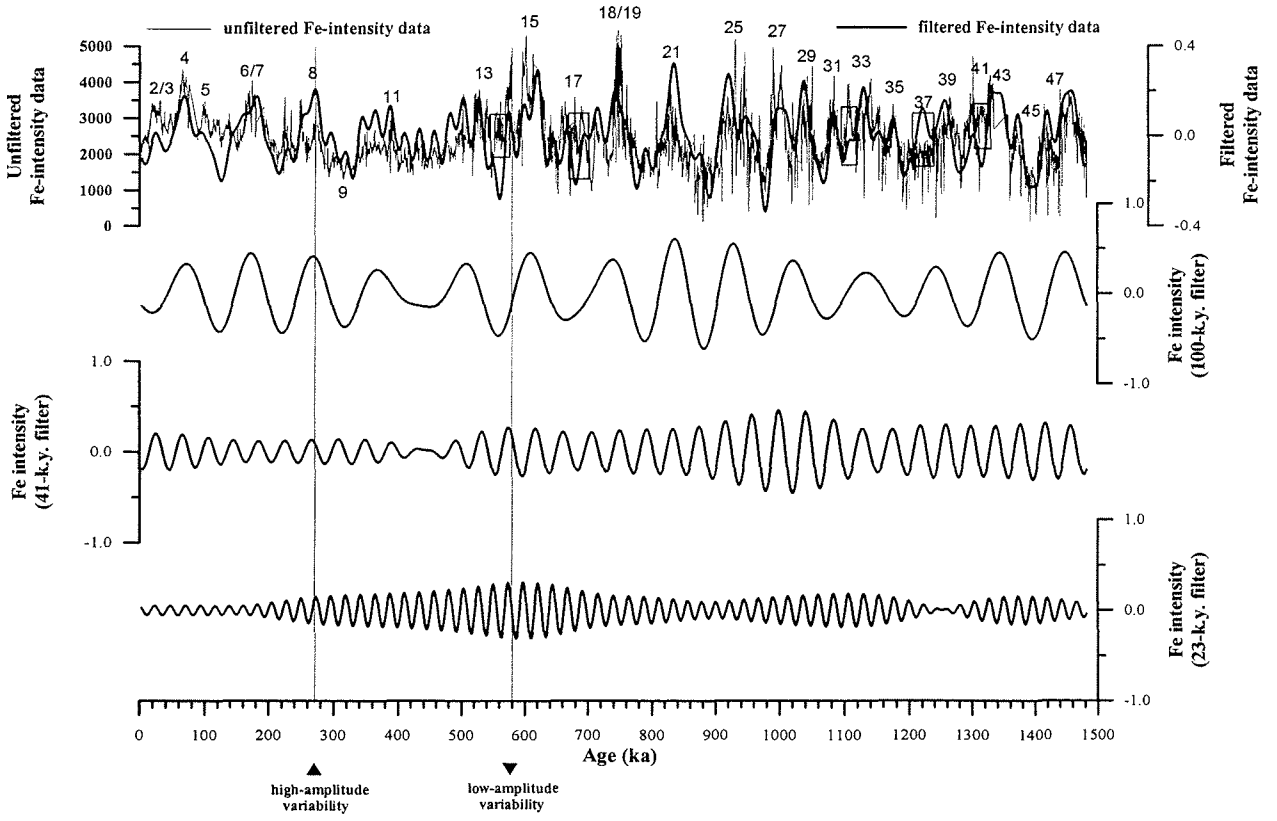

Figure 5: Band-pass filters of Site 1082 Fe-intensity record over time. Below: 23-k.y. filtered precession band (central frequency is 0.043 cycles/k.y. and bandwidth = 0.0024 cycles/k.y.); middle: 41-ka filtered obliquity band (central frequency is 0.024 cycles/k.y. and bandwidth = 0.0024 cycles/k.y.), and 100-ka filtered eccentricity band (central frequency is 0.01 cycles/k.y. and bandwidth = 0.0024 cycles/k.y.). The combination of these three filter components yields the filtered Fe-intensity record (thick line). Vertical lines represent changes in the amplitude variability of the unfiltered Fe-intensity record. Note that filtered and unfiltered Fe data compare well except for MIS 13, 17, 33, 37, and 41.

within the latest Quaternary is in agreement with results of Stuut et al. (in press) who found increased amounts of eolian coarse grain sizes during the interglacial stages 7, 5, and 3, which is attributed to the strength of southeast trades over the Walvis Ridge.

Transport of organic matter to the continental slope

We used TOC MAR as a proxy for paleoproductivity in the northern Benguela Current off Namibia. The seaward transport of organic matter from the shelf in surface waters is achieved through filaments, plumes, and eddies (e.g., Lutjeharms and Shillington, 1992; Lutjeharms and Stockton, 1987). Jahnke and Shimmield (1995) reported that organic matter in upwelling areas is transported across the slope by surface lateral transport. Summerhayes et al. (1995) cocluded that productivity is probably controlled by shelf-edge upwelling related to increased trade wind strength.

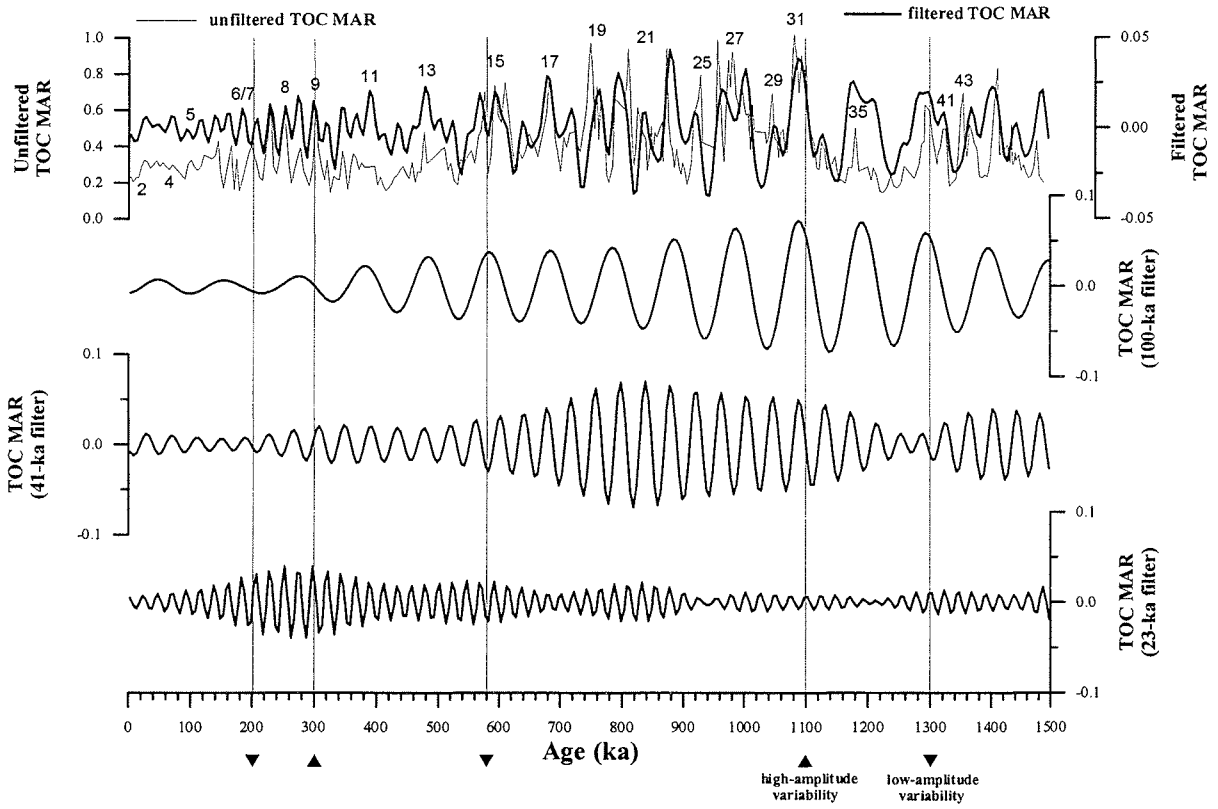

Figure 6: Band-pass filters of Site 1082 TOC MAR record over time. Below: 23 k.y. filtered precession band (central frequency is 0.043 cycles/k.y. and bandwidth = 0.0024 cycles/k.y.); middle: 41 k.y. filtered obliquity band (central frequency is 0.024 cycles/k.y. and bandwidth = 0.0024 cycles/k.y.), and 100 k.y. filtered eccentricity band (central frequency is 0.01 cycles/k.y. and bandwidth = 0.0024 cycles/k.y.). The combination of these three filter components yields the filtered TOC MAR record (thick line). Vertical lines represent changes in the amplitude variability of the unfiltered TOC MAR record. Note that filtered and unfiltered TOC MAR data compare well, except for the last 0.6 m.y.

TOC MAR's at Site 1082 indicate that periods of higher productivity occurred during both glacial and interglacial periods from 1.5 to 0.58 Ma, in contrast to the interval from 0.58 Ma to the Holocene. In general, productivity at Site 1082 from 1.5 to 0.3 Ma reflects a long-term climatic pattern similar to that described for the terrigenous record of Fe intensities. Over the past 0.3 m.y., productivity showed a continuous decrease from higher values during MIS 9, 8, and 7 to lower values towards the Holocene, indicating a reduction in paleoproductivity.

Reconstructing the history of the northern Benguela Current system

Two major questions are raised by the results of our study: (1) What is the cause of the shift at 0.58 Ma from high-amplitude to low-amplitude variability in wind intensity and paleoproductivity, and (2) What is the cause for an increase in wind strength from 0.27 to 0 Ma, while productivity was low?

The long-term variations in upwelling (Fe) intensity and productivity (Fig. 4) suggest that the strength of the Benguela upwelling system may have responded to an increase in Northern Hemisphere glaciation. The growth of the Antarctic ice cap and the onset of Northern Hemisphere glaciation led to changes in the atmospheric circulation that drives ocean currents and upwelling (Flohn, 1984). At the onset of ice buildup in the Northern Hemisphere a general southward migration of the subtropical high and ITCZ occurred in the South Atlantic. The displacement of the ITCZ led to a southward movement of the ABF, and upwelling was more intense south of the ABF (Hay & Brock, 1992). From 1.5 to 0.58 Ma, the amplitudes of glacial-interglacial terrestrial input and productivity in the northern Benguela upwelling system were even stronger than today, indicating a period of strengthened upwelling-favorable winds in this area (Fig. 4). The decline in the glacial-interglacial amplitude of terrestrial input and productivity since 0.58 Ma could either reflect a decrease in upwelling intensity in response to the growth of Northern Hemisphere ice caps, or it may imply that the upwelled water was poor in nutrients due to changes in deep-sea circulation (Hay and Brock, 1992).

Oxygen isotope fluctuations of *G. inflata* at Site 1082 reflect changes in the glacial-interglacial cyclicity at around 0.9 Ma (MIS 24/23) with a change from higher-frequency variations (41 ka) during the early Pleistocene to lower-frequency variations (100 ka) during the late Pleistocene (Fig. 2). This climate adjustment is referred to as the mid-Pleistocene Revolution (MPR; Berger & Jansen, 1994) or the mid-Pleistocene Transition (MPT; Raymo et al., 1997), and represents a fundamental change in the Earth's climate when Northern Hemisphere continental ice sheets increased starting at about 0.9 Ma. From stage 19 to the Holocene, glacial-interglacial cycles with a periodicity of 100 k.y. became dominant. The *G. inflata* $\delta^{18}O$ record suggests that maximum cooling occurred from about 0.8 to 0.6 Ma. Glacial MIS 16 (0.65 Ma) exhibited significantly heavier $\delta^{18}O$ isotopic values than older glacial intervals, which were dominated by the 41-k.y. cycle. Since 0.65 Ma, the glacial-interglacial cyclicity has shown a fully developed 100-k.y. pattern (Fig. 3). Likewise, during this interval of the late Quaternary, relatively lighter $\delta^{18}O$ isotopes are observed, especially related to the glacial periods. The weakening of TOC MAR and Fe-intensity fluctuations at 0.58 Ma was near the time when the 100-k.y. cycle became more significant in the $\delta^{18}O$ curve of many sites in the ocean. Mudelsee and Stattegger (1997) recognized an abrupt increase of the 100-k.y. amplitude in $\delta^{18}O$ time series from ODP Sites 607 and 659 in the North Atlantic at 0.65 Ma. They also identified the climate step at 0.9 Ma, which is characterized by an increase in ice volume due to a decrease in atmospheric CO_2 below a threshold value. The delay interval from 0.9 to 0.65 Ma is described by Mudelsee and Stattegger (1997) as a transition in the climate system to find the two-modal solution (from a principally linear to a complex, nonlinear climate system) after the initial disturbance in the form of increased ice volume. The late Pleistocene ice ages started at about 0.65 Ma with a saw-tooth shaped 100-k.y. cycle and marked glacial and interglacial periods, indicating a climate system with a strong nonlinear character (Mudelsee and Stattegger, 1997). From these considerations we propose that

the decline in terrigenous input and productivity at 0.58 Ma due to the onset of the fully developed 100-k.y. cycle was associated with the growth of the Northern Hemisphere glaciation.

Comparison of orbital frequencies in Fe and TOC MAR with Southern Hemisphere insolation and Northern Hemisphere climate changes

To evaluate the relative influences of Northern Hemisphere glaciation and Southern Hemisphere insolation as potential forcing mechanisms for variations of Fe intensity and TOC MAR in the northern Benguela Current, we filtered our proxy records at orbital frequencies (Figs. 5 and 6). The filtered Fe-intensity and TOC MAR records were than compared with the filtered orbital $\delta^{18}O$-record frequencies for ODP Site 659 (variations in temperature and ice volume), and with filtered orbital frequencies of the insolation at 40°S (differential land-ocean heating) (Figs. 7a,b, and 8a,b). We used the North Atlantic ODP Site 659 $\delta^{18}O$ record to estimate the influence of Northern Hemisphere glaciation on the northern Benguela Current. Southeast trade winds over South Africa are strongest during the winter months (June to August) as the land surface cools relative to the oceans and a broad anticyclonic (high-pressure) circulation prevails (Partridge et al., 1997). For this reason we used the winter insolation at 40°S to evaluate the importance of Southern Hemisphere insolation to the northern Benguela Current system.

Eolian terrigenous input (Fe intensity) and its relation to Northern Hemisphere glaciation

A comparison of the long-term amplitude variations of the unfiltered Fe data (vertical lines) with those of the filtered Fe data show good agreement in the Fe_{100} and Fe_{41} components with high-amplitude variability from 1.5 to 0.58 Ma as well as for the past 0.27 m.y., but low-amplitude variability from 0.58 to 0.27 Ma (Fig. 7a and b).

The amplitude modulation of the $\delta^{18}O_{100}$ filter agrees for the most part with the Fe-intensity variance, except for the periods from 1.5 to 1.2 Ma and from 1.0 to 0.7 Ma, when the amplitudes of the Fe-intensity data increased (Fig. 7a). The filtered $\delta^{18}O_{41}$ components from Site 659 match those of the Fe-intensity record in terms of the amplitude modulation throughout the core. The amplitude variability of the 659 $\delta^{18}O_{23}$ component is equal to that of the Fe-intensity record from 1.5 to 0.5 Ma. For the last 0.5 m.y., the amplitude variability of the 659 $\delta^{18}O_{23}$ component increased, while Fe shows low-amplitude variability. No clear phase relation exists between the $\delta^{18}O_{100}$ filter and the corresponding Fe filter throughout the record, but between 1.2 and 1.0 Ma and for the last 0.3 m.y., it is observed that Fe lags ice volume. The phase relation of the $\delta^{18}O_{41}$ component in ice volume and Fe intensity is threefold: For the early Pleistocene (1.5 to 1.1 Ma), Fe-intensity variance is in phase with the $\delta^{18}O_{41}$ component, suggesting that obliquity forcing was the strongest factor in determining the relative wind strength and timing of strong winds. The middle Pleistocene (1.1 to 0.5 Ma) reflects a transition, as the period of Earth's glacial cycles changed from 41 to 100 k.y., and Fe intensity indicates a small lag compared with the $\delta^{18}O_{41}$ component at the beginning of that period, which increases to a complete phase reversal at its end. For the late Pleistocene (0.5 to 0 Ma), when the 100-k.y. eccentricity

cycle became dominant in global ice-volume changes, Fe variance is again in phase with the $\delta^{18}O_{41}$ component, with slightly increasing amplitude in the 41-k.y. cycle. The $\delta^{18}O_{23}$ component and the Fe_{23} component are in phase for the intervals from 1.2 to 1.1 Ma, and also from 0.45 to 0.16 Ma.

Eolian terrigenous input (Fe intensity) and its relation to Southern Hemisphere winter insolation

Under modern conditions, southeast trade strength in the eastern South Atlantic is not only linked to Northern Hemisphere climate change but also to changes in the atmospheric constellation of high-pressure systems over the subtropical South Atlantic and low-pressure troughs over the African continent. Therefore, trade-wind intensities may also be linked to orbital variations in Southern Hemisphere insolation during the Pleistocene.

In general, a correlation of the amplitude modulation of the filtered insolation components with the filtered Fe-intensity components does not show the same good results as were observed in comparison of the filtered ice-volume components with the filtered Fe-intensity components (Fig. 7b). The $insolation_{100}$ filter and the Fe_{100} filter show no correlation in the amplitude modulation. The amplitude variability of the $insolation_{41}$ filter matches Fe intensity for the interval from 1.5 to 0.9 Ma. During the last 0.9 m.y., the amplitude variability in the Fe_{41} filter decreases, in contrast to that of insolation. The $insolation_{23}$ component exhibits a trend opposite to that of the amplitude variability of the Fe_{23} component. The phase relationship between the Fe_{100} component and the $insolation_{100}$ component at 40°S can be split into four intervals (Fig. 7b): From 1.5 to 1.1 Ma Fe intensity leads insolation. During the mid-Pleistocene (1.1 to 0.7 Ma) a minimum of Fe intensity coincided with an insolation maximum. In the next interval, from 0.7 to 0.5 Ma, a slight lag of Fe is observed with respect to insolation. During the past 0.5 m.y., Fe and insolation are again out of phase. The Fe_{41} and $insolation_{41}$ components at 40°S are out of phase except during the intervals from 1.3 to 1.18 Ma and for the past 0.2 m.y. The Fe_{23} component is out of phase over the large amplitude portion of the $insolation_{23}$ record with the exception of the period from 0.7 to 0.5 Ma.

Paleoproductivity and its relation to Northern Hemisphere glaciation

The amplitude modulations of the filtered TOC MAR data generally reflect the long-term trends of low- and high-amplitude variability in the unfiltered TOC MAR data. The frequency of the filtered components of the Site 659 $\delta^{18}O$ record is ten times higher than those of TOC MAR (Fig. 8a). The $TOC\ MAR_{100}$ and $TOC\ MAR_{41}$ components both show a continuous decrease in amplitude variability towards the Holocene, while the $TOC\ MAR_{23}$ component indicates a gradual increase of the amplitude variability from 1.5 Ma to the Holocene. For the last 0.3 m.y., the amplitudes of the $TOC\ MAR_{100}$ and $TOC\ MAR_{41}$ contributions are substantially smaller than the $\delta^{18}O_{100}$ and $\delta^{18}O_{41}$ components, indicating a decrease in productivity variability with glacial-interglacial cycles. A comparison of the $TOC\ MAR_{23}$ filter with the $TOC\ MAR_{100}$ component shows an opposing trend; high-amplitude fluctuations in the $TOC\ MAR_{23}$ filter occur simultaneously with low-amplitude fluctuations in the $TOC\ MAR_{100}$ component. For the middle Pleistocene (1.5 to 0.85 Ma), the $\delta^{18}O_{100}$ and $TOC\ MAR_{100}$ components exhibit a small phase difference, with TOC MAR leading ice volume (Fig. 8a). At around 0.8 Ma, the

$\delta^{18}O_{100}$ component shows a change in the amplitude, while the TOC MAR_{100} component carries on with a precise period of 100 k.y. for the late Pleistocene. Therefore, it appears that TOC MAR lags ice volume and temperature changes in the north. The $\delta^{18}O_{41}$ and the TOC MAR_{41} components are in phase for the interval from 1.2 to 0.7 Ma (Fig. 8a). Before 1.2 Ma, TOC MAR lags the $\delta^{18}O$ record, indicating that high paleoproductivity occurred during deglaciations. For the late Pleistocene (0.2 to 0 Ma), paleoproductivity leads the $\delta^{18}O$ curve.

Paleoproductivity and its relation to Southern Hemisphere winter insolation

The amplitude modulations of the TOC MAR_{100} component correspond to those of the $insolation_{100}$ component throughout the record. The TOC MAR_{41} and TOC MAR_{23} filters reveal a ten-times

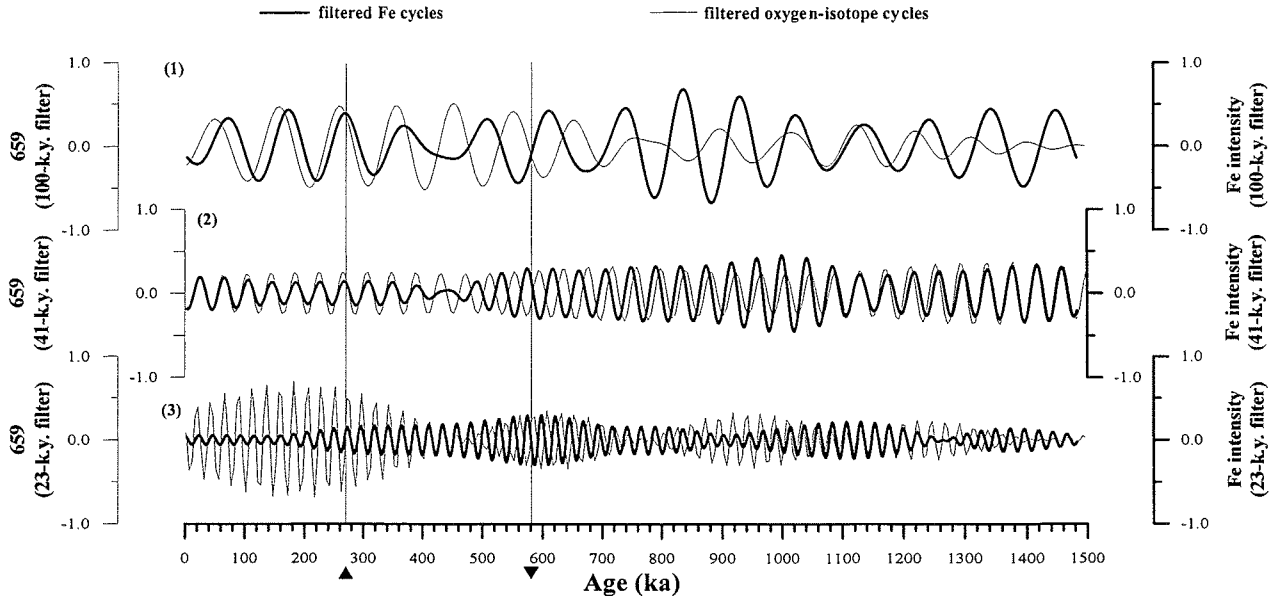

Figure 7a: Fourier components (filters) of potential wind forcing. (1) 100-k.y. component of Site 659 benthic $\delta^{18}O$ record in comparison with those of Site 1082 Fe-intensity record; (2) 41-k.y. component of Site 659 benthic $\delta^{18}O$ record in comparison with those of Site 1082 Fe-intensity record; (3) 23-k.y. component of Site 659 benthic $\delta^{18}O$ record in comparison with those of Site 1082 Fe-intensity record. Vertical lines represent changes in the amplitude variability of the unfiltered Fe-intensity record. Note that the filtered $\delta^{18}O_{41}$ component from Site 659 matches that of the Fe-intensity record both in terms of timing and amplitude modulation.

smaller amplitude modulation than those of the insolation filters. A comparison of the TOC MAR_{41} constituent with the equivalent insolation filter shows a decrease in the amplitude variability of TOC MAR from 1.3 to 1.2 Ma and for the past 0.6 m.y. compared to insolation. The TOC MAR_{23} filter is negatively correlated in its amplitude variability to that of the insolation throughout the core, except for the interval from 0.8 to 0.5 Ma. The phase relation between the TOC MAR_{100} filter and the $insolation_{100}$ filter is threefold: From

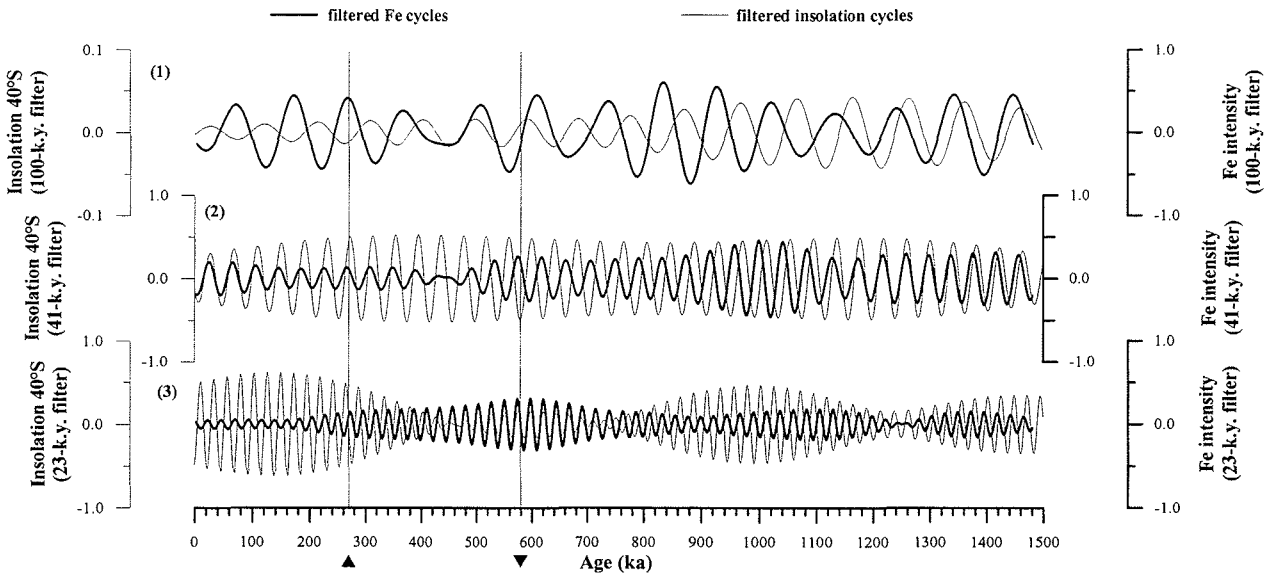

Figure 7b: Fourier components (filters) of the winter insolation at 40° South of potential wind forcing. (1) 100-k.y. component of the insolation record in comparison with that of the Site 1082 Fe-intensity record; (2) 41-k.y. component of the insolation record in comparison with that of the Site 1082 Fe-intensity record; (3) 23-k.y. component of the insolation record in comparison with that of the Site 1082 Fe-intensity record. Vertical lines represent changes in the amplitude variability of the unfiltered Fe-intensity record.

1.5 to 0.7 Ma, TOC MAR leads insolation. They are in phase from 0.7 to 0.6 Ma. During the past 0.6 m.y., TOC MAR lags insolation. The TOC MAR_{41} component is out of phase with the $insolation_{41}$ component from 1.5 to 1.3 Ma. From 1.3 to 0.7 Ma, as well as 0.44 to 0.2 Ma, TOC MAR lags insolation. TOC MAR and insolation are in phase from 0.65 to 0.44 Ma, and for the past 0.2 m.y. A comparison of the TOC MAR_{23} filter with the equivalent insolation is out of phase, except for the short interval from 1.05 to 0.98 Ma.

In summary, our filter results of Site 1082 indicate that strong Northern Hemisphere glaciation during the Pleistocene is the dominant trigger for a southward displacement of the atmospheric and oceanic circulation in the South Atlantic during the last 1.5 m.y. This is confirmed in the 100-k.y. and 41-k.y. frequency bands. Insolation at 40°S plays only a secondary role in the northern Benguela Current.

CONCLUSIONS

Site 1082 is located near the coast off Namibia in a water depth of 1290 m and the sediments reflect the history of the northern Benguela Current system for the past 1.5 m.y. The environmental changes

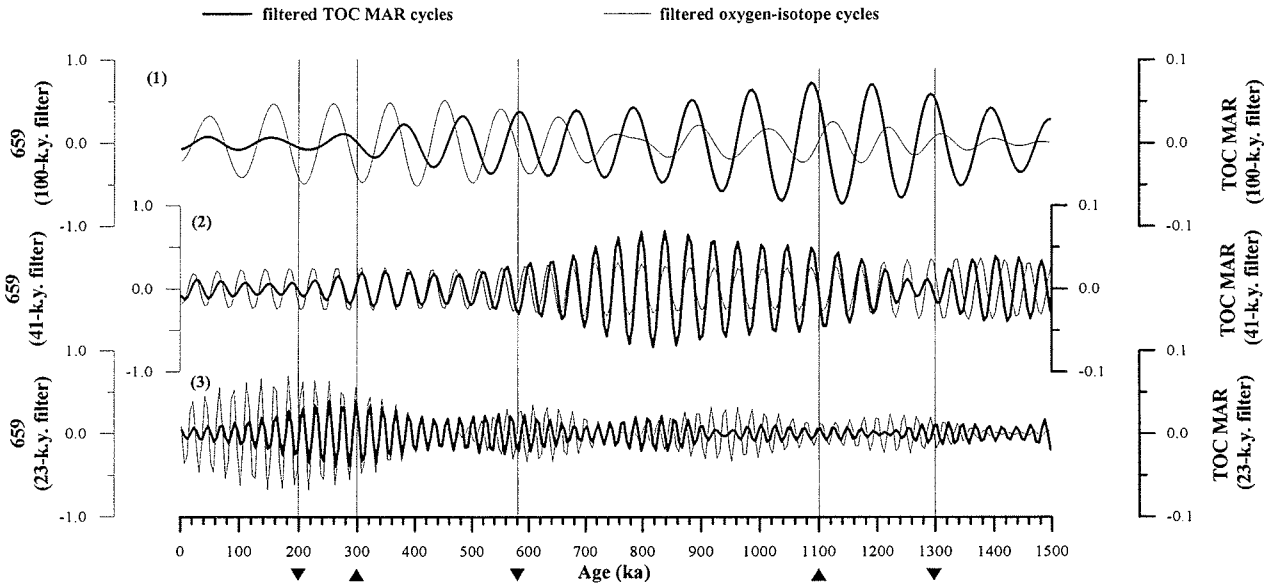

Figure 8a: Fourier components (filters) of potential paleoproductivity forcing. (1) 100-k.y. component of Site 659 benthic $\delta^{18}O$ record in comparison with that of the Site 1082 TOC MAR record; (2) 41-k.y. component of Site 659 benthic $\delta^{18}O$ record in comparison with that of the Site 1082 TOC MAR record; (3) 23-k.y. component of Site 659 benthic $\delta^{18}O$ record in comparison with that of the Site 1082 TOC MAR record. Vertical lines represent changes in the amplitude variability of the unfiltered TOC MAR record.

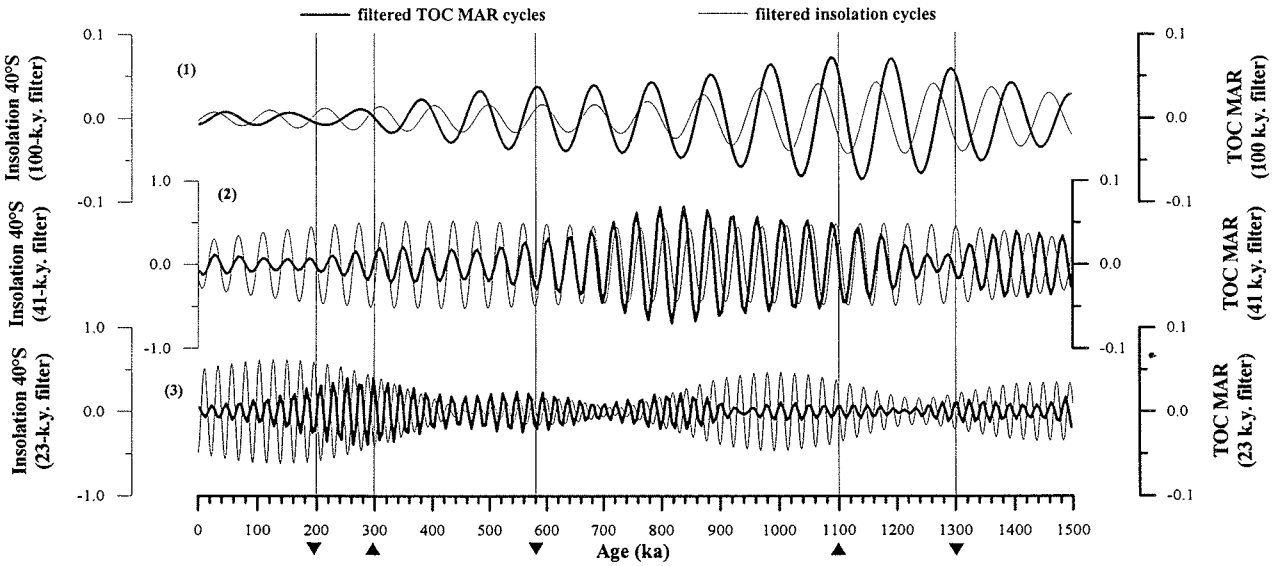

Figure 8b: Fourier components (filters) of the winter insolation at 40° South of potential productivity forcing. (1) 100-k.y. component of the insolation record in comparison with that of the Site 1082 TOC MAR record; (2) 41-k.y. component of the insolation record in comparison with that of the Site 1082 TOC MAR record; (3) 23-k.y. component of the insolation record in comparison with that of the Site 1082 TOC MAR record. Vertical lines represent changes in the amplitude variability of the unfiltered TOC MAR record.

documented in the sediments cover several new aspects of the mid-Pleistocene Revolution in response to Northern Hemisphere glaciation. The proxies we used are $\delta^{18}O$, TOC MAR, and measurements of Fe intensities. Fe intensity is used as an indicator of eolian input from the Namib desert and TOC MAR is taken as a proxy for paleoproductivity. Long-term variations of eolian input and paleoproductivity indicate changes in the strength of upwelling winds in the northern Benguela Current. Filtered results of Fe intensity and TOC MAR confirm our hypothesis that Northern Hemisphere glaciation is the dominant trigger for climate changes in the northern Benguela system.

Acknowledgements

This work was funded by the Deutsche Forschungsgemeinschaft within the DFG-Schwerpunktprogramm DSDP/ODP (We 992/26) "Spätkänozoische Entwicklung des Benguela-Stromsystems in Beziehung zum Klima Zentral- und Südafrikas". We thank H. Buschoff, B. Meyer-Schack, and M. Segl for assistance in the laboratory and H. Arz, L. Dupont, and H. Kuhnert for discussions. Data are available at www.pangaea.de.

2.3 Manuscript III:

Mid to Late Pleistocene Temperature Variability in the Benguela Current System Derived from Alkenones

Britta Jahn, Peter J. Müller, Ralph R. Schneider, Isabel von Storch, and Gerold Wefer

Department of Geosciences, University Bremen, Postbox 330440, D-29334 Bremen, Germany

ABSTRACT

Sediments of two cores, one from the upper continental margin off Namibia (ODP Site 1082; 21.5° S, 1290 m water depth) and the other from the deeper continental margin in the Mid Cape Basin (core GeoB 1722-1; 29.3° S, 3973 m water depth), were studied to evaluate variations of sea-surface temperatures (SST) for the past 1.2 m.y. in the Benguela Current system. SST's were estimated by means of the unsaturation ratio of C_{37} alkenones, and these were compared with the $\delta^{18}O$ records established from planktonic foraminifera. The two SST records are in good agreement and generally match the climatic pattern as revealed by the oxygen isotope records. Two distinct long-term trends mark the alkenone SST records: (1) a decrease in SST by 2°C from 0.8 to about 0.45 Ma and (2) an increase in SST by 2°C, especially during glacial periods, for the last 0.45 m.y. $\delta^{18}O$ isotopes from both sediment cores indicate warming changes of 1‰ (4°C) over the last 0.65 m.y. The most positive $\delta^{18}O$ values (lowest SST's) are observed at isotope stages 16 and 12, and the coldest alkenone-based SST's occurred during isotope stage 12. Lateral SST differences within the Benguela Current region can be linked to incursions of the relatively warm Agulhas Current. We suggest that the trend in $\delta^{18}O$ toward lighter values for the last 0.65 m.y. is associated with a warming of the eastern South Atlantic as a response to a weakening of the cross-equatorial heat transport from the South to the North Atlantic.

INTRODUCTION

The Benguela system in the southeast Atlantic is one of the five largest upwelling areas of the world. The strength of coastal upwelling is a function of the strength of along-shore winds, which in turn are closely tied into the trade-wind system (Berger and Wefer, 2001). The Benguela Current is influenced by relatively warm water masses of the Angola Current from the north and the Agulhas Current from the south. Therefore, changes in SST can provide information about past variations in the oceanic surface circulation and wind-driven coastal upwelling in the eastern South Atlantic. Several marine sediment records have been used to study the variations of surface circulation and wind-driven coastal upwelling in the southeast Atlantic during the late Quaternary (Kirst et al., 1999; Little et al., 1997a; b; Bickert and Wefer, 1999). Reconstruction is based on paleontological and organic geochemical tracers, such as foraminifera, alkenones, and total organic carbon. These proxies indicate that upwelling maxima during the last 150 k.y. are linked to enhanced southeast trade winds off Namibia.

In the case of the Benguela Current and the associated coastal upwelling, the heat transfer toward the equator is of special interest, because of the substantial movement of heat from the South to the North Atlantic. This investigtion involves several oceanic processes, including the migration of the Intertropical Convergence Zone (ITCZ), the transport of heat from the Indian Ocean around the Cape of Good Hope in the Agulhas Retroflection, warming of the Benguela Current on its way

north, and entrainment of warm surface waters from the central gyre, as well as advection within the thermocline (Gordon, 1985; Lutjeharms and van Ballegooyen, 1988). According to Berger and Wefer (1996) northern heat piracy was greatly reduced under glacial conditions, presumably because the ITCZ migrated toward the equator (as it does now during northern winter).

Over the last two decades, a technique for reconstruction of past sea-surface temperatures (SST) has been developed, based on the ratio of di-unsaturated to the sum of di- and tri-unsaturated C_{37}-alkenones ($U^{k'}_{37}$ index; Brassell et al., 1986; Prahl and Wakeham, 1987; Prahl et al., 1988). These long-chain ketones are synthesized by haptophyte algae, such as *Emiliania huxleyi* and *Gephyrocapsa oceanica* (e.g., Conte et al., 1993; Volkman et al., 1995). Most of the studies (e.g., Prahl et al., 1995; Schneider et al., 1995; Emeis et al., 1995) focus on late Quaternary sediments, the time range over which the two principal modern alkenone-synthesizing species, *E. huxleyi* and *G. oceanica,* have both existed. In most cases, field and laboratory culture studies assume that *E. huxleyi* is the dominant alkenone-producing species in open-ocean sediments (Brassell, 1993). Marlowe et al. (1990) suggested that species of the genus *Gephyrocapsa* are also likely contributors of alkenones to Cenozoic marine sediments, while extinct genera of the family *Gephyrocapsaceae* were the most likely sources of alkenones in the Tertiary and early Pleistocene (Conte et al., 1993; Volkman et al., 1995). The lipids of the species *G. oceanica* contain the same series of long-chain alkenones and other related compounds as *E. huxleyi* (Volkman et al., 1980; 1995). A nannoplankton study covering the last 200 k.y. showed that the two coccolithophorids *E. huxleyi* and *G. oceanica* coexist in sediments from Walvis Ridge, with a pronounced predominance of *G. oceanica* for the interval from 200 to 50 ka. Only for the last 50 k.y. does *E. huxleyi* indicate a slight predominance (e.g., Müller et al., 1997; Winter and Siesser, 1994; Giraudeau, 1992; Thierstein et al., 1977). Müller et al. (1997) have shown that alkenone SST's for the last 200 k.y. are reliable in the eastern Atlantic upwelling system, but prior to 200 ka a systematic error may possibly occur because the alkenone producers have changed. To control this effect, we applied the independent SST proxy of $\delta^{18}O$.

In the present study, we reconstruct climate variations in the Benguela system for the last 1.2 m.y. and discuss possible connections to the global ocean circulation and implications for trans-equatorial heat transport. One of the crucial elements in the upper circulation system of the South Atlantic is the Benguela Current area. This region monitors properties of the gyre margin. Temperatures in the southern portion of the Benguela Current reflect the Agulhas contribution, and hence the opening or closing of the Cape Valve. We present alkenone-based SST records and isotope data from two sediment cores along the south-to-north-flowing Benguela Current (ODP Site 1082 and core GeoB 1722-1).

ODP Site 1082 was drilled on the shelf edge off Namibia during Leg 175 (21.5° S, 11.5° E; 1290 m water depth; R.V. *Joides Revolution*; Wefer et al., 1998) and core GeoB 1722-1 from the deep sea during the Meteor expedition M20/2 (29.3° S, 11.5° E; 3973 m water depth; R.V. *Meteor*; Schulz et al., 1992). We want to reveal changes in sea-surface circulation in the southeast Atlantic associated with Northern Hemisphere glaciation. We therefore established a continuous SST record that

encompassed the mid-Pleistocene Revolution (MPR), tracing the transition from the 41-k.y. obliquity cycle to the dominant 100-k.y. eccentricity cycle of Earth's climate. An increase in the difference between ice mass buildup and melting associated with the dominance of the 100-k.y. cycle changed the global climate pattern at about 0.9 Ma (e.g., Raymo et al., 1997; Berger and Jansen, 1994).

Modern Oceanographic Settings

As part of the subtropical gyre system in the South Atlantic, the Benguela Current (BC) is divided into the Benguela Coastal Current (BCC), which forms its eastern limb, and the Benguela Ocean Current (BOC), which turns to the northeast at about 17° S (Fig. 1). This complex current system brings relatively cold, low-salinity water to the tropics, and also exerts a strong influence on the climate of southwest Africa (for a detailed hydrography see, e.g., Shannon, 1985; Peterson and Stramma, 1991; Lutjeharms, 1996). The southern part of the BC system receives a periodical supply of heat and salt from the subtropical gyre in the South Indian Ocean. The leakage of water from the South Indian Ocean to the South Atlantic is primarily driven by the Agulhas Current and results in the presence of anomalous warm water to the coastal ocean off southwestern Africa (e.g., Lutjeharms, 1996, Lutjeharms et al., 1994; de Ruijter et al., 1995; Rigg et al., 1992). The interaction of an Agulhas ring with the South Atlantic is probably driven by intense, seaward, berg winds that move upwelling filaments as well as warm and cold eddies (Duncombe Rae et al., 1992; Lutjeharms, 1991).

The upwelling regime in the southeast Atlantic occurs preferentially in eight well-defined upwelling cells (e.g., Lutjeharms et al., 1991). The central and most intense of these upwelling cells is off Lüderitz (27°S). On the average its surface water is colder than that in other upwelling cells, it extends farther offshore, and it exhibits active upwelling more frequently than any of the other cells (Lutjeharms and Meeuwis, 1987). Core GeoB 1722-1 (29°S) is located in the deep-sea, outside of the extensive upwelling cells off Lüderitz and Namaqua, whereas ODP Site 1082 is located at the upper continental margin close to the intense upwelling cell off Walvis Bay (22°S) (Fig. 1). The seasonal variability of modern SST's at the location of the two sediment cores is shown in Figure 2a. The seasonal variation is nearly identical, but temperatures at 22°S (ODP Site 1082) average around 1°C lower than those at 29°S (GeoB 1722-1), indicating the stronger influence of cold upwelled surface waters at Site 1082. The coldest SST's occur during austral winter and spring, from June to November.

METHODS

Oxygen Isotopes

Foraminiferal samples from ODP Site 1082 and core GeoB 1722-1 were taken at 25-cm and 5-cm intervals, respectively. The oxygen-isotope compositions of hand-picked specimens of the

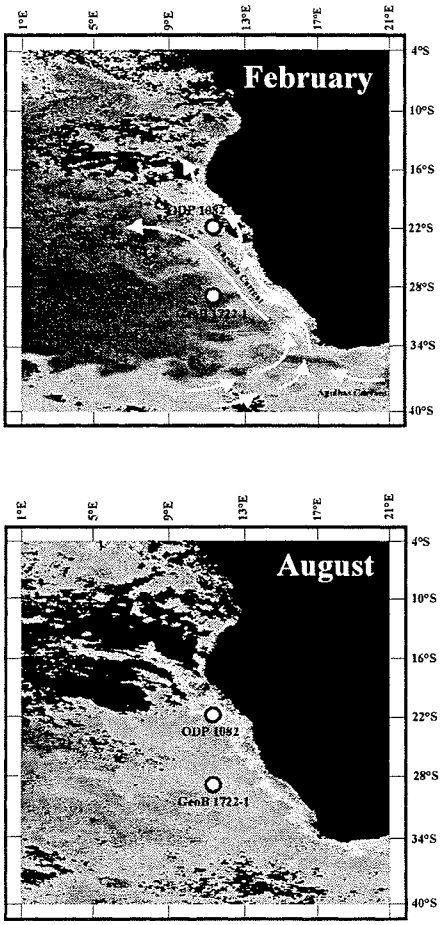

Figure 1: Productivity maps of the southeast Atlantic Ocean with the locations of Site 1082 in the northern Cape Basin and core GeoB 1722-1 in the mid Cape Basin, together with the surface circulation.

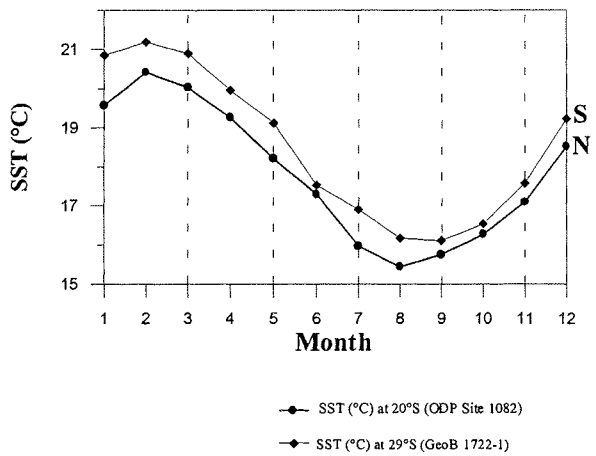

Figure 2: Annual variability of sea surface temperature (SST; Oceanographic Atlas; Conkright et al., 1998) for Site 1082 (21.5°S, 11.5°E) and core GeoB 1722-1 (29.3°S, 11.5°S). The Atlas was extracted from the web site http://ingrid.ldgo.columbia.edu.

foraminiferal species *Globorotalia inflata* were analyzed using a Finnigan MAT 251 micromass spectrometer coupled with a Finnigan automated carbonate device. The carbonate was reacted with 100% orthophosphoric acid at 75°C. The reproducibility (1σ) based on replicate measurements of a laboratory internal carbonate standard (Solnhofen limestone) is ± 0.07 ‰.

Stratigraphy

The planktonic $\delta^{18}O$ record of *G. inflata* for ODP Site 1082 was graphically correlated with the benthic foraminiferal $\delta^{18}O$ record from ODP Site 659 (Tiedemann et al., 1994) and provides the stratigraphic framework for the last 1.2 m.y. *G. inflata* does not occur continuously throughout the investigated sediment sequence at Site 1082, causing data gaps in MIS (Marine Isotope Stages) 47, 43, 33, and 25. A reliable determination of MIS 21 to 17 was also difficult based on the isotope data. Paleomagnetic data (Wefer et al., 1998) and assigned magnetochrons were employed to help solve the MIS 21 to 17 problem and to identify the well-dated boundaries of the Brunhes/Matuyama (0.78 Ma) and the top and bottom of the Jaramillo (0.99 and 1.06 Ma).

For core GeoB 1722-1 we used the $\delta^{18}O$ curve of the planktonic foraminifera *Globorotalia inflata* to cover the last 0.55 m.y. The age model for core GeoB 1722-1 is based on the oxygen-isotope curve of the benthic foraminifera *Cibicides wuellerstorfi*. (Bickert, unpublished data). This benthic record was graphically correlated with the normalized SPECMAP standard record (Martinson et al., 1987; Imbrie et al., 1984). Marine isotopic events were identified for the last 0.78 m.y.

Alkenone Analysis

Alkenones were extracted from 0.25- to 0.5-ml aliquots of the freeze-dried sediment using a UP200H ultrasonication disruptor probe (S3 micropoint, amplitude 0.5, and pulse 0.5) and applying successively less polar solvent mixtures of methanol and methylene chloride (MeOH, MeOH/CH_2Cl_2 (1:1), CH_2Cl_2), each for 3 min. The extracts were combined, washed with demineralized water to remove sea salt and methanol, dried over Na_2SO_4, concentrated under N_2, and finally taken up in 25 µl of a 1:1 (volume) MeOH/CH_2Cl_2 mixture.

3 µl aliquots of the final extracts were analyzed by capillary gas chromatography using an HP 5890 Series II gas chromatograph (GC). Further analytical details are given elsewhere (e.g. Kirst et al., 1999; Müller et al., 1998). The quantification of C_{37} alkenones was achieved by using an internal standard (octacosane acid methyl ester (OCSME)). $U^{k'}_{37}$ values were converted into temperatures applying the global core-top calibration of Müller et al. (1998), which is in good agreement with the calibration of Prahl and Wakeham (1987) based on laboratory cultures of a single strain of *E. huxleyi*.

RESULTS

Northern Cape Basin (Site 1082)

The Site 1082 $\delta^{18}O$ record of the planktonic foraminifera *G. inflata*, a species proliferating under gyre water conditions (Ufkes et al., 2000; Little et al., 1997a; Oberhänsli, 1991), clearly exhibits glacial-interglacial variations (Fig. 3a). The interval from 1.2 to 0.78 Ma is characterized by $\delta^{18}O$ values varying between 2.8 ‰ and 1.2 ‰, and poorly expressed glacial-interglacial cycles. During the subsequent interval, from 0.78 to 0.6 Ma, the onset of pronounced 100-k.y. glacial-interglacial cycles is evident, and oxygen isotopes increase to their heaviest values for interglacial and glacial periods, in MIS 17 and 16, respectively. However, this is two glaciations earlier (200 k.y.) than for the alkenone SST record, which exhibits the coldest glacial temperatures during MIS 12 (Fig. 3b). Apparently, this interval of increasing isotope values is a response to the mid-Pleistocene climatic shift, starting at the boundary of MIS 22/20, when the oscillations in many marine $\delta^{18}O$ records changed from a shorter cyclicity dominated by the 41-k.y. obliquity period to the saw-tooth shaped larger amplitude 100-k.y. cycles characteristic of the late Pleistocene (e.g., Mudelsee and Stattegger, 1997). The interval after 0.6 Ma, extending to modern conditions, exhibits the 100-k.y. glacial-interglacial cycles with $\delta^{18}O$ values ranging from 3.7 ‰ to 0.5 ‰. The warm stages 11, 9, and 5, as well as the Holocene, are characterized by the lowest $\delta^{18}O$ values. Interestingly, the *G. inflata* $\delta^{18}O$ record displays a continuous trend toward ever decreasing glacial values for the last 0.4 m.y. The decrease in mean glacial $\delta^{18}O$ values over this period is about 1 ‰ (4°C).

Three pronounced long-term trends can also be observed in the alkenone-based SST record of the northern Cape Basin (Fig. 3b). The first interval, from 1.2 to 0.8 Ma, is characterized by SST values varying between 16 and 22.8°C, and glacial-interglacial differences are less pronounced compared to the late Pleistocene SST record. This is due to smaller glacial-interglacial temperature differences and the dominant 41-k.y. cyclicity. During the second interval, from 0.8 to 0.45 Ma, a strong decrease in the mean temperature by about 2 to 3°C is obvious. After MIS 12, a third interval from 0.45 to 0 Ma reflects pronounced 100-k.y. cycles in glacial-interglacial SST changes with a warming trend of 2°C for the interval from MIS 12 to MIS 4. An exception is seen at MIS 2/3 with much colder temperatures than expected based on the trend set by the other glacial periods during that interval.

Mid Cape Basin (Core GeoB 1722-1)

The oxygen-isotope curve of *G. inflata* illustrates that the trend to lighter isotopes over the last 0.65 m.y. seen at ODP Site 1082 is also present in core GeoB 1722-1 covering the last 0.55 m.y. The planktonic $\delta^{18}O$ record in 1722-1 also reflects glacial-interglacial cycles with a periodicity of 100 k.y. for the last 0.55 m.y. (Fig. 3a) with values ranging from 3.42 ‰ to 0.82 ‰. The most positive isotope values occurred during glacial stages 12 and 2, while the most negative values were observed during the interglacial stages 11, 9, 7, 5, and the Holocene. From stage 12 to stage 4, a similar long-

term trend toward lighter glacial oxygen-isotope values by 1 ‰ (4°C) is indicated. The $\delta^{18}O$ record of core GeoB 1722-1 closely matches that of ODP Site 1082, with exceptions at isotope stages 10, 3, and 2 where the $\delta^{18}O$ values are heavier by 0.5 to 1 ‰ (Fig. 3a).

The warmest alkenone SST's (over 21°C) in core GeoB 1722-1 are observed during interglacial stages 9 and 5, whereas the lowest glacial SST's (ca. 13.5°C) occurred during glacial stages 12 and 10 (Fig. 3b). The SST values for interglacial stages 9 and 5 exceed Holocene alkenone temperatures of around 19.8°C, which is slightly higher than the modern annual mean value of 18.5°C (Conkright et al., 1998).

In summary, we focus on the following results: a.) General patterns at both sites include the cooling trend in the alkenone SST in glacial and interglacial periods by 2°C for the interval from 0.8 to 0.45 Ma, and the subsequent warming trend of glacial periods where temperatures increase by 2°C over the last 0.45 m.y. At both sites, however, the estimated temperature at MIS 2 breaks this late Quaternary warming trend in glacials with somewhat cooler values than would be expected. b.) In the interval from 0.8 to 0.45 Ma there are significant differences in the alkenone SST values between the two locations, with temperatures averaging about1.5°C warmer at Site 1082 than at GeoB 1722-1. c.) Alkenone SST records from Site 1082 and core GeoB 1722-1 reveal SST patterns that are in conformity with their respective planktonic $\delta^{18}O$ records, with the coldest glacial temperatures occurring simultaneously with ice-volume maxima at the end of the glacial periods.

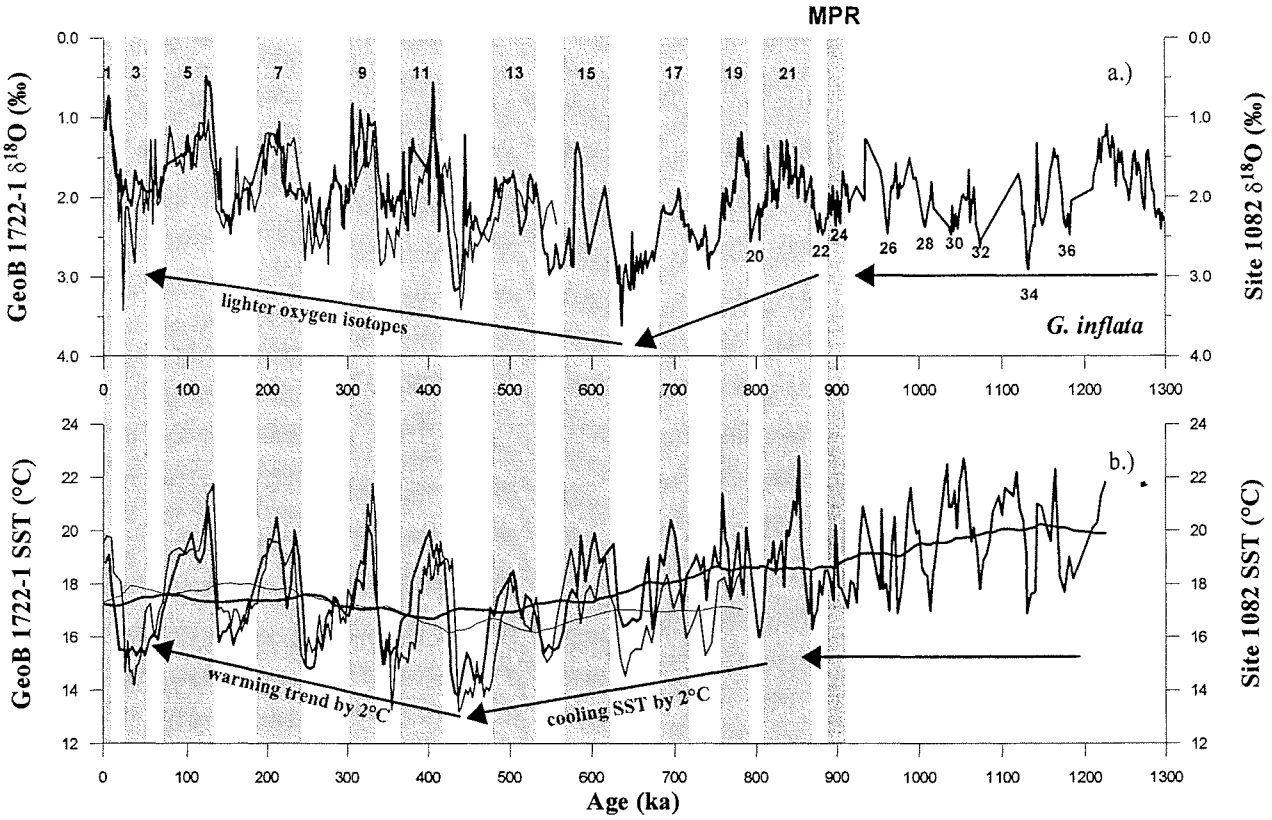

Figure 3: Comparisons of Site 1082 (bold line) with core GeoB 1722-1 (thin line) from the southeast Atlantic. a) $\delta^{18}O$ records of the planktonic foraminifera *G. inflata* and b) SST records derived from alkenones and 60 point running mean. Note the generally good agreement between $\delta^{18}O$ and SST.

DISCUSSION

Mid-Pleistocene Climate Step

Alkenone SST values and $\delta^{18}O$ isotopes of ODP Site 1082 in the northern Benguela system indicate that the change in Earth's cyclicity occurred at around 0.9 Ma and was characterized by an increase in ice volume (Mudelsee and Stattegger, 1997). This climate change at around 0.9 Ma marks the transition from the dominant 41-k.y. cycle to the dominant 100-k.y. cycle of the late Quaternary. Based on the alkenone SST and $\delta^{18}O$ curves, the well-defined typical sawtoothed pattern of 100-k.y. cycles can be seen at Site 1082, beginning at about 0.65 Ma, around 250 k.y. after the mid-Pleistocene Revolution (MPR). This is in agreement with results from previous studies (e.g., Mudelsee and Stattegger, 1997; Berger and Jansen, 1994; DeBlonde and Peltier, 1991; Prell, 1982). From 0.9 to 0.65 Ma (MIS 24 to 16) Site 1082 shows a decrease in the $\delta^{18}O$ values by ca. 0.7 ‰ during glacial and interglacial periods with the heaviest $\delta^{18}O$ values noted during MIS 16. The SST's of Site 1082 exhibit a similar trend to colder temperatures by ca. 2°C, but for a significantly longer interval from 0.9 to 0.45 Ma. The coldest SST's are reached during MIS 12, 250 k.y. later than the heavy peak of the $\delta^{18}O$ isotopes. The delay interval between the termination of this trend for the $\delta^{18}O$ isotopes from 0.9 to 0.65 Ma and the SST record from 0.9 to 0.45 Ma is described by Mudelsee and Stattegger (1997) as a transition in the climate system to find the two-modal solution (from a principally linear to a complex, nonlinear climate system) after the initial disturbance in the form of increased ice volume. The late Pleistocene ice ages started at about 0.65 Ma with the sawtooth shaped 100-k.y. cycle and strong glacial and interglacial periods, indicating a climate system with a strong nonlinear character (Mudelsee and Stattegger, 1997).

The Influence of the Agulhas Current on the SST's of the Adjacent Benguela Current

From 0.8 to 0.45 Ma, the SST's within glacial-interglacial cycles average 1.5°C lower at station GeoB 1722-1 than at ODP Site 1082 in the Benguela system. However, modern SST's at the GeoB 1722-1 location average 1°C higher compared to Site 1082 (Fig. 2). One possible explanation for this could be that the SST pattern is related to changes in upwelling at the northern Site 1082. As shown in Figure 1, however, both core sites are located outside of the main upwelling cells and are thus not directly influenced by coastal upwelling. We therefore assume that the reversal in the SST difference is probably caused by other mechanisms than upwelling, namely by the influence of relatively warm surface waters on the northern Benguela Current, which receives warm surface waters of equatorial origin from the Angola Current (Shannon and Nelson, 1996; Fig. 1). Core GeoB 1722-1 is probably more influenced by the relatively warm Agulhas Retroflection, originating in the tropical Indian Ocean (Lutjeharms, 1996; Fig. 1). Thus, a reversal in the difference of SST's between the two core sites within the Benguela Current region could be due to a difference in the alternating influence of the warm water masses from the Angola and the Agulhas Current before and after 0.45 Ma. According to Wefer et al. (1996) the southern region of the Benguela Current is more strongly influenced by the Agulhas Current during interglacial periods, whereas during glacial

periods the effect of the warm Agulhas Current on the southern Benguela Current region is diminished because of the northern advancement of the subantarctic frontal zone. In this situation, the Benguela Current is more strongly influenced by cold subantarctic water. This would mean that from 0.8 to 0.45 Ma, the relatively colder SST's of core GeoB 1722-1 result either from a more northerly position of the subpolar frontal system causing cooler temperatures in the southern Benguela Current and/or the ITCZ linked to Northern Hemisphere glaciation shifted southward, allowing the warm waters of the Angola Current to influence the SST's at ODP Site 1082 in the northern Benguela Current, particularly during glacial periods.

However, it is more likely that the almost identical SST's in the two cores for the last 0.45 m.y. originate from protrusions of the relatively warm water masses of the Agulhas Retroflection to the position of core GeoB 1722-1, and that this is subsequently transported within the Benguela Current farther to the north, influencing ODP Site 1082. According to Giraudeau et al. (2001) the delivery of warm waters from the Indian Ocean continued throughout the last 0.46 m.y. based on the presence of the warm-water foraminifer *G. menardii* at ODP Site 1087 in the southern Benguela Current. They propose that inter-ocean exchange was most effective at glacial terminations. The trend to warmer SST's in both sediment cores is more evident during glacial periods over the last 0.45 m.y., suggesting a southward migration of the subpolar front and an intensification of the influence of warm Agulhas Current on the Benguela Current region during glacial stages 10, 8, 6, and 4. A comparison of the SST record of Site 1082 with that of core GeoB 1722-1 also shows a slight phase shift, with core GeoB 1722-1 leading during MIS 13, 12, 11, and 2, probably the result of an inaccuracy in the oxygen-isotope stratigraphy of core GeoB 1722-1.

Mechanisms Potentially Related to Warming of the Benguela Current Region

ODP Site 1082 shows a trend to lighter $\delta^{18}O$ values by about 1 ‰ (representing a warming of approximately 4°C, whereby 0.22‰ = 1°C), (Fig. 3a) over the last 0.65 m.y., and the available isotope data for GeoB 1722-1 (covering the past 0.56 Ma) follows this curve closely, except for a heavier peak at MIS 2. Alkenone SST variations in both sediment cores show a similar trend to warmer SST's by around 2°C for the last 0.45 m.y. (Fig. 3b). An additional factor that could contribute to continuous warming of the BC system is the degree of cross-equatorial heat transport. Immense amounts of tropical heat are delivered from the South to the North Atlantic by the transport of warm surface waters across the equator (Hastenrath, 1982). An interruption or reduction of the northward heat transport would lead to a general warming of the South Atlantic as observed for millennial-scale climate events during the last glacial and subsequent deglaciation (Charles et al., 1996; Arz et al., 1999; Rühlemann et al., 1999; Vidal et al., 1999). Warmer surface-water temperatures and a gradual increase in the distribution of % *G. inflata* during late Quaternary glacial periods are also indicated in sediment core PS2076-1/3 (Niebler, 1995) from the Agulhas Ridge at 40°S in the Southern Ocean. This suggests that the polar and subpolar frontal systems had probably reached their northernmost position during MIS 12 related to minimal penetration of the Agulhas waters into the South Atlantic (Berger and Wefer, 1996). According to Wefer et al. (1996)

the latitudinal position of the maximum gradient (subtropical-subpolar convergence) can change on a glacial-interglacial scale, and it is commonly assumed that it migrates equatorward during glacial conditions. As we have mentioned, the alkenone SST's are in good agreement with the $\delta^{18}O$ values ,indicating that the tendency towards lighter oxygen isotopes for the last 0.65 m.y. is mainly caused by a warming of the eastern South Atlantic.

Other mechanisms that could potentially modify the $\delta^{18}O$ signal in subsurface waters include, e.g., the ice effect, salinity, the habitant depth, and the seasonal contrast of *G. inflata*. The benthic $\delta^{18}O$ curve of *C. wuellerstorfi* from core GeoB 1722-1 (Bickert, unpublished data) does not reflect the warming trend in the planktonic $\delta^{18}O$ curve of *G. inflata* from the same sediment core (Fig. 4). Hence, we assume that the ice effect does not play a major role in the variations of the $\delta^{18}O$ records in the BC system. This supports the assumption that the *G. inflata* $\delta^{18}O$ signals are primarily driven by changes in sea-surface temperature.

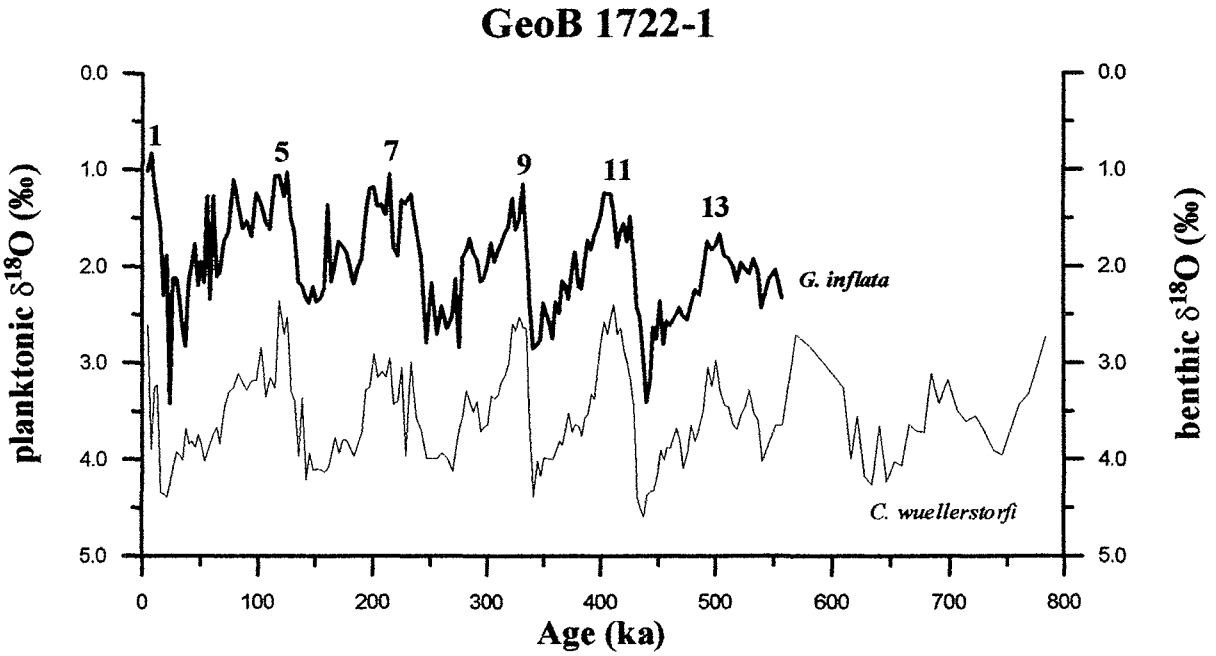

Figure 4: Comparison of the planktonic $\delta^{18}O$ record of *G. inflata* with the benthic $\delta^{18}O$ record of *C. wuellerstorfi* (Bickert, unpublished data) from core GeoB 1722-1.

Oxygen isotope values can also be affected by salinity (Wefer et al., 1996). The trend to lighter oxygen isotopes for the last 0.65 m.y. in the BC system may also reflect variations in salinity of the subsurface waters. For the last 0.65 m.y., this would mean that salinity slowly decreased in the BC system, except for MIS 3 and 2 of Site 1722-1. Variations in salinity can also help to understand the climatic changes on the adjacent continent. As yet, the question of whether the glacial climatic periods in the Namib Desert were more arid during the late Quaternary compared to modern conditions is still open, because correct interpretations of late Quaternary paleoclimatic terrestrial signals are missing. If the interpretation of an increase in salinity during the late Quaternary at sites 1082 and 1722-1 is correct, evaporation in the eastern South Atlantic has increased and climatic

conditions in the Namib Desert have become more arid for the last 0.65 m.y.

Oxygen-isotope measurements from Site 1082 and core 1722-1 sediments are based on the planktonic foraminiferal species *G. inflata*, a species proliferating between 100 and 300 m water depth with its maximal occurrence near the thermocline (Fairbanks et al., 1982). Consequently, a trend towards lighter $\delta^{18}O$ values of Site 1082 and core GeoB 1722-1 during glacial periods might reflect a rise in the SST and, therefore, a lowering of the thermocline. Wefer et al. (1996) have investigated changes in the temperature gradient between surface water and the thermocline in the Benguela Current. For this purpose, they used the isotope differences between cool-water (*G. inflata*) and warm-water (*Globigerinoides ruber*) species , considering this to be mainly an estimate of seasonal temperature differences. At the southwest Walvis Ridge (sediment cores GeoB 1031 and GeoB 1220) they found a gradual decrease of the seasonal contrast as indicated by the $\delta^{18}O$ difference between *G. inflata* and *G. ruber* over the last 120 k.y. From these results they suggested a gradual deepening of the thermocline, documenting an increased advection of warm surface water in the gyre through time. Thus, the processes responsible for the buildup of the gyre's warm water lens act over the entire Cape Basin. Furthermore, they interpreted this observation as a spin-up in the intensity of gyre-margin circulation with a southwestward migration of the gyre margin, and hence an overall increase in meridional heat transport.

Another consideration is the previously mentioned southward expansion of the northern ice shields, which weakens cross-equatorial heat transport and results in higher glacial SST's in the subtropical area of the eastern South Atlantic. This raises the following question : Could large freshwater melting events in the Northern Hemisphere during glacial periods also contribute to increased SST's in the BC system?

Manabe and Stouffer (1997) introduced a coupled ocean-atmosphere model that investigated the effect of freshwater input into high North Atlantic latitudes on a scale of centuries. In their experiment the thermohaline circulation (THC) in the Atlantic Ocean weakens rapidly with increased freshwater supply, and surface atmospheric temperatures are reduced from the North Atlantic to the Circumpolar Ocean and the Antarctic continent. The development of the negative surface-temperature anomalies is also associated with a change in the reverse circulation cell in the deep Pacific Ocean (Manabe and Stouffer, 1997). The weakening of the overturning circulation raises temperatures in the upper layers of both the Atlantic and Pacific Oceans in low to middle latitudes (Manabe and Stouffer, 1997; Fig. 5). The THC not only weakens, but also becomes much shallower and leads to a lowering of the thermocline in the South Atlantic. As a result, the decrease of $\delta^{18}O$ values of *G. inflata* in the sediment records of Site 1082 and core GeoB 1722-1 could reflect a continuous lowering of the thermocline over the last 0.65 m.y. in the BC system in response to melt-water discharge from continental ice sheets, which may have destabilized the thermohaline circulation. To test this hypothesis of a warming trend in the BC system over the last 0.45 m.y. as a response to the weakening of thermohaline circulation during glacial periods, we compared the Site 1082 planktonic $\delta^{18}O$ values with a corresponding record of ODP Site 820 from the shallower water depths (280 m) of the Great Barrier Reef off the northeastern Australian continental margin (Peerdeman et al., 1993;

Fig. 6). $\delta^{18}O$ values of the planktonic species *G. ruber* permit the clear definition of isotope stages from MIS 19 to the Holocene. From MIS 16 to the Holocene, the $\delta^{18}O$ isotope curve of Site 820 illustrates the same progressive 4°C increase in surface-water temperature as was observed at Site 1082. Potential mechanisms for a warming in the Southern Hemisphere include the reduction of North Atlantic Deep Water flux and thus, a reduced delivery of heat to the Circumpolar Deep Water in the Southern Ocean associated with (boreally driven) ice ages and/or a drop of global sea level. This could have provided a powerful positive feedback through the carbon dioxide control and an increased probability of generating terminations by the collapse of marine ice sheets (Berger and Wefer, 1996).

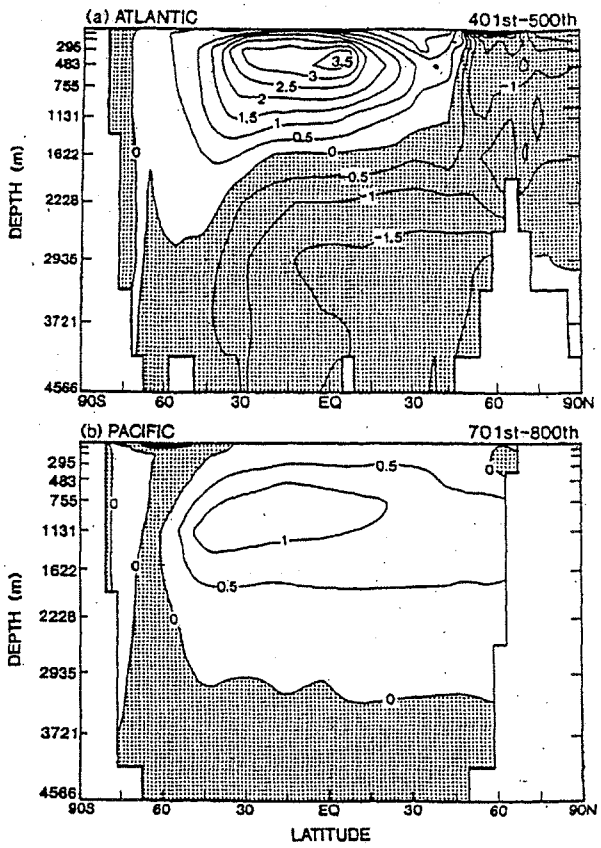

Figure 5: Coupled ocean-atmosphere model response to freshwater input (Manabe and Stouffer, 1997). a) Zonal mean temperature anomaly (°C) in the Atlantic Ocean averaged over the 401st-500th year. b) Zonal mean temperature anomaly (°C) in the Indo-Pacific Ocean averaged over the 701st-800th year.

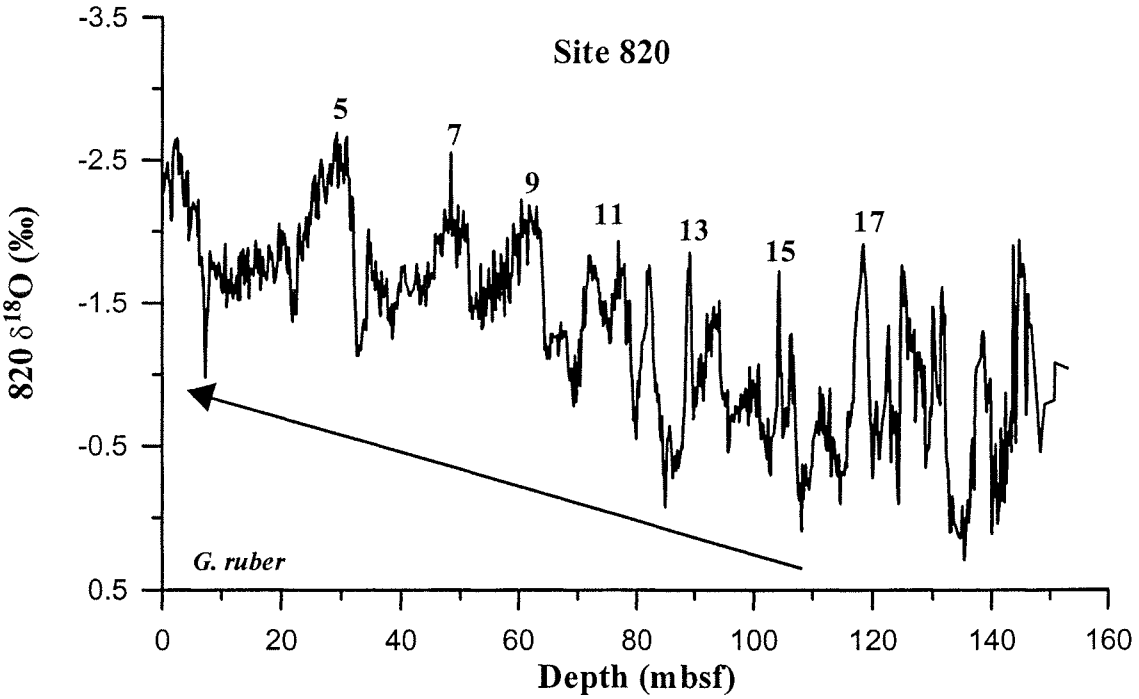

Figure 6: Planktonic oxygen isotope record of ODP Site 820 from the Great Barrier Reef off the northeastern Australian continental margin (Peerdeman et al., 1993). Note the trend toward lighter oxygen isotopes from MIS 16 to the Holocene.

CONCLUSIONS

Alkenone-based SST obtained from ODP Site 1082 and core GeoB 1722-1 in the southeast Atlantic roughly follow the pattern $\delta^{18}O$ variations of planktonic foraminifera. Both cores show warmer SST values during interglacial stages and colder SST values during glacial stages, and exhibit two significant long-term trends: a decrease in SST values by 2°C from 0.8 to 0.45 Ma and an increase in SST's by 2°C for the last 0.45 m.y. The interval from 0.8 to 0.45 Ma is characterized by a temperature difference of 1 to 1.5°C between the two sites within the Benguela system. The two SST records are in good agreement for the last 0.45 m.y. SST values and $\delta^{18}O$ isotopes of Site 1082 in the northern Benguela system confirm the change in Earth's climatic cyclicity at about 0.9 Ma and the onset of the clearly dominant 100-ka cycle at about 0.65 Ma. One important result of this study is the observed warming trend in the BC system in the eastern South Atlanticover the last 0.45 m.y. Based on this trend, a weakening of the cross-equatorial heat transport from south-to-north and thus, a reduction in northern heat piracy is presumed. One mechanism that could be responsible for the decline in heat exchange is a weakening of the thermohaline circulation in response to large melt-water influx to the North Atlantic during glacial conditions. This would lead to a weakening in the overturning circulation and an increase in the SST's of both the Atlantic and Pacific Oceans in low to mid latitudes. Support for this hypothesis has so far only been provided by an ocean-atmosphere model over relatively short time periods, and it has not been proved that the

same mechanism could work over millennial scales. Another possible process for inducing such a warming trend in the Benguela Current region is a stronger input of warm waters via the Agulhas Current, linked to an opening of the Cape Valve during glacial periods associated with a southward migration of the polar and subpolar frontal systems.

Acknowledgment

We thank Helge Arz, Lydie Dupont, and Henning Kuhnert for their discussions and suggestions and Dietmar Grotheer and Ralph Kreutz for assistance in the laboratory. We also thank Torsten Bickert for providing the unpublished oxygen-isotope data of Site 1722-1. The study was financially supported by the Deutsche Forschungsgemeinschaft (DSDP-ODP). Data are available at www.pangaea.de.

3. GENERAL CONCLUSIONS

Milankovitch (1930) followed Köppen and Wegener's (1924) view that the distribution of summer insolation at 65°N should be critical to the growth and decay of ice sheets. In the years since, numerous studies have solidified our understanding of Milankovitch climate cycles. For instance, we know that the 100-, 41-, and 23-k.y. orbital periods characterize variations in global ice volume (e.g., Imbrie et al., 1984), in the thermohaline circulation (e.g., Shackleton and Pisias, 1985), in continental aridity (e.g., Pokras and Mix, 1985), in sea surface temperature (SST) (e.g., Ruddiman et al., 1989), and in atmospheric CO_2 concentrations (e.g., Barnola et al., 1987). In a linear version of the Milankovitch theory, the two shorter cycles can be explained as responses to insolation cycles driven by precession and obliquity. But the 100-k.y. cycles (arising from eccentricity variation) is too small in amplitude and too late in phase to produce the corresponding climate cycle by direct forcing (Imbrie et al., 1993). During the mid-Pleistocene, climatic variability switched from a world dominated by the 41-k.y. obliquity (tilt) cycle (Prell, 1982; Raymo et al., 1989) to the more familiar 100-k.y. world of the late Pleistocene. Previous studies of the mid-Pleistocene transition (MPT), which occurred around 0.9 Ma, have focused almost on the constraints provided by oxygen-isotope records of global ice volume, temperature, and ocean carbon chemistry (e.g., Saltzman and Verbitsky, 1994; Berger and Jansen, 1994; Raymo et al., 1997).

Detailed evaluation of temporal relations of mid- to late-Pleistocene climate changes such as the mid-Pleistocene climate step in association with Northern Hemisphere glaciation may provide a clue to test exiting feedback mechanisms. Such approaches require high-resolution records with accurate geological chronology. Particularly, it is of the utmost significance to document high-resolution paleoclimate variations in the Southern Hemisphere, because well-dated marine climate records of the Pleistocene are scarce in this part of the globe. Thereby, one of the major problems has been in establishing the timing, duration, and thus spatial patterns of the MPT.

In this context, marine sediment cores from the northern Congo Fan area (ODP Site 1075) and the northern Benguela Current system (ODP Site 1082) drilled during Leg 175 in the eastern South Atlantic (Wefer et al., 1998) were investigated in this study. Moreover, we focus on the history of the Angola-Benguela Current system for the Pleistocene associated with long-term variations in terrestrial supply and paleoproductivity combined on the interplay between high- and low-latitude Milankovitch forcing (obliquity versus precession), and the role of the 100-k.y. oscillation. Changes in marine productivity and the terrigenous input by eolian and fluvial transport of iron are supposed to reflect changes in regional climate.

The stratigraphic framework was derived from graphic correlation with marine oxygen isotope records. Sedimentation rates were calculated on the basis of the linear interpolation between the stratigraphic tie-points.

The evaluated total organic carbon content (TOC) was used for reconstruction of paleoproductivity variations in the Congo Fan area and in the northern Benguela Current system in relation to climate changes. For this purpose, the total organic carbon accumulation rate (TOC MAR) was investigated

in both sediment cores. To determine the isotopic signature of bulk organic carbon in the Congo Fan sediments, we used the stable organic carbon isotope ratio ($\delta^{13}C_{org}$) to receive basic information about the estimated portions of marine and terrestrial organic carbon content.

In sediments of the Congo Fan area the terrigenous supply of Fe by fluvial transport off the Congo River was used to examined variations in monsoonal intensity and weathering conditions of tropical Africa. We used the terrigenous supply of Fe by eolian transport from the Namib desert to the northern Benguela Current to reconstruct variations in the southeast trade winds and the weathering conditions on subtropical Africa.

In Manuscript I (*Terrigenous Climate Signals And Changes In Marine Productivity From Sediments Of The Congo Fan Region For The Last 1.7 m.y.*), marine paleoproductivity and terrigenous proxies in Quaternary sediments recovered from Site 1075 in the northern Congo Fan area show fluctuations, which response to regional and global orbital forcing. Fe intensity and TOC MAR variations are dominated by eccentricity, obliquity, and precession forcing. Band-pass filter of both paleoproductivity and the terrigenous input of Fe show strong influence of ice volume (eccentricity and obliquity) and a strong relation to precession, which controls the intensity of the monsoon over tropical Africa. We assume that glacial-interglacial boundary conditions may influence the magnitude of precessional climate variations in tropical latitudes. Strong glacial-interglacial cycles with a periodicity of 100 k.y. are observed in the TOC MAR_{100} filter and in the Fe_{100} filter for the last 0.6 m.y. Prior to 0.9 Ma, strong eccentricity occurred only in the Fe_{100} filter. From this observation we suggest that eccentricity modulation of the low-latitude insolation directly influenced the local climate and lead to changes in the southern African monsoon system. Thus have played an important role in the initiation of 100 k.y.

This idea is reinforced by results of ODP Site 1082 from the northern Benguela Current off Namibia (Manuscript II, *Variability Of Terrestrial Input And Marine Productivity In The Northern Benguela Current Associated With Orbital Cycles Over The Last 1.5 m.y.*). The environmental changes documented in the sediments of ODP Site 1082 cover several new aspects of the mid-Pleistocene Revolution in response to Northern Hemisphere glaciation. The proxies we used are $\delta^{18}O$, TOC MAR, and measurements of Fe intensities. Fe intensity is used as an indicator of eolian input from the Namib Desert and TOC MAR is taken as a proxy for paleoproductivity. Long-term variations of eolian input and paleoproductivity, indicating changes in the strengthening of upwelling winds in the northern Benguela Current. Filter results of Fe intensity and TOC MAR confirm our hypothesis that Northern Hemisphere glaciation is the dominant trigger for climate changes in the northern Benguela system.

Alkenone-derived sea-surface temperature estimates from the sediment cores of ODP Site 1082 and GeoB 1722-1 provide information about temperature changes of the northern and southern Benguela Current system in the eastern South Atlantic (Manuscript III, *Mid to Late Pleistocene Temperature Variability in the Benguela Current System Derived from Alkenones*). A comparison of the alkenone-derived sea-surface temperature estimates from the northern BC system with SSTs from the southern BC system are in a good agreement with each other and generally matches the climatic pattern revealed by

climatic pattern revealed by oxygen-isotope records of these sites. Two distinct long-term trends mark the SST records: 1.) a decrease in SST by 2°C from 0.8 to about 0.45 Ma BP and 2.) an increase in SST by 2°C, especially during glacial periods for the last 0.45 m.y. A comparison of the SST variability of both sites within the significant long-term trend from 0.8 to 0.45 Ma shows warmer temperatures by 1 to 1.5°C for Site 1082. For the last 0.45 m.y., the temperature difference within the glacial-interglacial cycles of both sites is much smaller by 0.5°C. $\delta^{18}O$ values show glacial-interglacial cycles with a periodicity of 100 k.y. associated to Northern Hemisphere glaciation over the last 0.65 m.y. The most positive $\delta^{18}O$ values (lowest SSTs) were observed during isotope stages 16 and 12 and coldest alkenone-based SSTs occurred during isotope stage 12. Variations in past sea-surface temperature in the Benguela Current off SW-Africa seem to have been controlled primarily by variations in the influence of the relatively warm water of the Agulhas Current. We suggest that the trend in $\delta^{18}O$ towards negative values over the last 0.65 m.y. is associated to a warming of the eastern South Atlantic as a response to a weakening of the cross-equatorial heat transport from the South to the North Atlantic.

3.1 Future Research

As already outlined in the general introduction, the interest in the reconstruction of productivity and terrigenous Fe supply off SW Africa lies in its potential implications for climate research.
The long-term climatic variations are a topic theme of modern climate research (e.g., the 100-k.y. oscillation). In this context we need a better understanding of the interaction between the ocean and the continent and the interplay between low- and high-latitude Milankovitch forcing. The reconstruction of further paleoenvironmental proxies on the sediment cores of this study (e.g., stable nitrogen isotope ratios as a proxy for productivity) as well as the synthesis of already employed calcium carbonate contents might be help for a better understanding of the Milankovitch climate variability in the tropical and subtropical areas in the Southern Hemisphere.
A detailed comparison of the results introduced in this study with other paleoceanographic studies of long-term climate variations in the eastern South Atlantic and out of the Atlantic Oçean is an important step in understanding the temporal and spatial radiation of long-term climate variability. Furthermore, the already employed X-ray flourescence data of Fe and Ca from the sediment core in the northern Benguela Current spans the interval of the late Pliocene to the Early Pleistocene and reveal together with palynological investigations the onset of the Northern Hemisphere glaciation at around 2.7 Ma ago. A detailed climate record in the subtropical area off SW Africa would be important to investigate the influence of the ocean circulation and the cooling events in the Southern Hemisphere related to Northern Hemisphere glaciation at the end of the Pliocene.

4. LITERATURE

Anderson, D.M. and Prell, W.L. A 300 kyr record of upwelling off Oman during the Late Quaternary: Evidence of the Asian southwest monsoon. *Paleoceanography 8*, 193-208, 1993.

Arrhenius GOS, Sediment cores from the east Pacific. *Swed. Deep-Sea Exped. Rep.*, 5, 1-227, 1952.

Arz, H.W. Dokumentation von kurzfristigen Klimaschwankungen des Spätquartärs in Sedimenten des westlichen äquatorialen Atlantiks, *Fachb. Geowiss.*, 124, 115 pp., Univ. Bremen, Bremen, Germany, 1998.

Arz, H.W., Pätzold, J., and Wefer G. The deglacial history of the western tropical Atlantic as inferred from high resolution stable isotope records off northeastern Brazil. *Earth and Planetary Science Letters*, 167, 105-117, 1999.

Berger, A. Milankovitch theory and climate. *Rev. Geophys.*, 26, 624-657, 1988.

Berger, A. and Loutre, M.-F. Insolation values for the climate of the last 10 million years. *Quaternary Science Reviews*, 10, 297-317, 1991.

Berger, W.H., and Keir, R.S. Glacial-Holocene changes in atmospheric CO_2 and the deep-sea record. *In*: Hansen, J.E., Takahashi, T. (Eds), *Climate processes and climate sensitivity*. AGU Geophys. Monogr., 29, 337-351, 1984.

Berger, W.H., Fischer, K., Lai, C., Wu, G. Ocean productivity and organic carbon flux (Part I. overview and maps of primary productivity and export production), University of California, San Diego, *SIO Reference*, Vol. 87-30, 67, 1987.

Berger, W.H. Global maps of ocean productivity. *In*: Berger, W.H., Smetacek, V.S., and Wefer, G. (Eds), *Productivity of the Ocean: Present and Past*. Dahlem Konferenzen. John Wiley, Chichester, 429-455, 1989.

Berger, W.H., and Wefer, G. Productivity of the glacial ocean: Discussion of the iron hypothesis. *Limnol. Oceanogr.*, 36, 1899-1918, 1991.

Berger, W.H. and Jansen, E. Mid-Pleistocene shift - The Nansen connection. *Geophysical Monograph* 84, 295-311, 1994.

Berger, W.H., and Wefer, G. Expeditions into the Past: Paleoceanographic Studies in the South Atlantic. *In*: Wefer, G., Berger, W.H., Siedler, G., Webb, D. (Eds), *The South Atlantic: Present and Past Circulation*, Springer, Berlin, 363-410, 1996.

Berger, W.H., Wefer, G., Richter, C., and Shipboard Scientific Party. Color Cycles in Quaternary Sediments From The Congo Fan Region (Site 1075): A Statistical Analysis. *In*: Wefer, G, Berger, W.H., Richter, C. et al., *Proceedings of the Ocean Drilling Program, Initial. Reports*, 175, 561-567, 1998.

Berger, W.H., Lange, C.B., and Wefer, G. Upwelling History of the Benguela-Namibia System: A Synthesis of Leg 175 Results. *In*: Wefer, G., Berger, W.H., and Richter, C. (Eds.), *Proc. of the Ocean Drill. Prog., Scientific Res.*, 175, (Online). Available from World Wide Web:<http://www-odp.tamu.edu/publications/175_SR/VOLUME/CHAPTERS/SR175_11.PDF>, 2001.

Berger, W.H., and Wefer, G. On the reconstruction of upwelling history: Namibia upwelling in context. *Marine Geology,* 2964, 1 - 26, 2001.

Bickert, T., and Wefer, G. South Atlantic and benthic foraminifer $\delta^{13}C$ deviations: Implications for reconstructing Late Quaternary deep-water circulation. *Deep-Sea Research II*, 46, 437-452, 1999.

Birch, G.F., Rodgers, J., Bremner, J.M., and Moir, G.J. *Proc. First Interdisciplinary Conf. Mar. Freshw. Res. Sth Afr.*, Fiche 20A, C1-D12, 1976.

Blackman, R.B. and Tukey, J.W. *The Measurement of Power Spectra from the Point of Communications Engineering*. Dover Press, Mineola, New York, 1958.

Bolly, H.M., Ryan, W.B.F. et al., *Initial Reports of the Deep Sea Drilling Project*, 40, U.S. Govt. Printing Office, Washington, 1978.

Boyle, E.A. and Keigwin, L.D. Deep circulation of the North Atlantic over the last 20 000 years linked to high-latitude surface temperature. *Nature*, 330, 35-40, 1987.

Brassell, S.C., Eglington, G., Marlowe, I.T., Plaumann, U., and Sarnthein, M. Molecular stratigraphy: a new tool for climatic assessment. *Nature*, 320, 129-133, 1986.

Brassell, S.C. Applications of biomarkers for delineating marine paleoclimatic fluctuations during the Pleistocene. *In*: Engel, M.H. and Macko, S.A. (Eds), *Org. Geochem.: Principles and Applications*: New York (Plenum), 699-738, 1993.

Broecker, W.S. Ocean chemistry during glacial time. *Cosmochim. Acta*, 46: 1689-1705, 1982.

Broecker, W.S. Terminations. *In*: Berger, A. and Imbrie, J. (Eds.). *Milankovitch and Climate*. D. Reidel Publ., Dordrecht, 687-698, 1984.

Charles, C., Lynch-Stieglitz, J., Ninnemann, U.S., Fairbanks, R.G. Climate connections between the hemispheres revealed by deep sea sediment core/ice core correlation. *Earth Planetary Science Letters*, 142, 19 - 27, 1996.

Clemens, S.C. and Prell, W.L. Late Pleistocene variability of Arabian Sea summer monsoon winds and continental aridity: Eolian records from the lithogenic component of deep-sea sediments. *Paleoceanography 5*, 109-145, 1990.

Clemens, S.C., Prell, W.L., Murray, D., Shimmield, G., and Weedon, G. Forcing mechanisms of the Indian Ocean monsoon. *Nature*, 353, 720-725, 1991.

Conkright, M., Levitus, S., O'Brian, T., Boyer, T., Antonov, J., and Stephens, C. World Ocean Atlas. Available online and on CD-ROM Data Set Documentation. *Tech. Rep.*, 15, NODC Internal Report, Silver Spring, MD, pp 16, 1998.

Conte, M.H., and Eglington, G. Alkenones and alkenoate distributions within the euphotic zone of the eastern North Atlantic: correlation with production temperature. *Deep-Sea Res.*, 40, 1935-1961, 1993.

Dean, W. and Gardner, J. Cyclic variations in calcium carbonate and organic carbon in Miocene to Holocene sediments, Walvis Ridge, South Atlantic Ocean. *In*: Hsü, K. J. & Weissert, H. J. (Eds) *South Atlantic Paleoceanography*. Cambridge University Press, 47-55, 1985.

DeBlonde, G., and Peltier, W.R. A one-dimensional model of continental ice volume fluctuations through the Pleistocene: implications for the origin of the mid-Pleistocene climate transition. *J. Climate*, 4, 318-

344, 1991.

DeMenocal, P.B., Ruddiman, W.F., and Pokras, E.M. Influences of high- and low-latitude processes on African terrestrial climate: Pleistocene eolian records from equatorial Atlantic Ocean Drilling Program Site 663. *Paleoceanography*, 8, 209-242, 1993.

De Ruijter, W.P.M., van Leeuwen, P.J., and Lutjeharms, J.R.E. Triggering mechanisms for Natal Pulses in the Agulhas Current. *J. Geophys. Res.*, 112-123, 1995.

Diester-Haass, L. and Schrader, H.J. Neogene coastal upwelling history off northwest and southwest Africa. Marine Geology, 29, 39-53, 1979.

Diester-Haass, L. Late Quaternary sedimentation on the eastern Walvis Ridge, SE Atlantic (HPC 532 and four piston cores). *Marine Geology*, 65, 145-189, 1985a.

Diester-Haass, L. Late Quaternary upwelling history off southwest Africa (DSDP Leg 75, HPC 532). *In*: Hsü, K.J. & Weissert, H.J. (Eds), *South Atlantic Paleoceanography*. Cambridge University Press, 47-55, 1985b.

Diester-Haass, L., Meyers, P.A., and Rothe, P. Light-dark cycles in opal-rich sediments near the Plio-Pleistocene boundary, DSDP Site 532, Walvis Ridge continental terrace. *Marine Geology*, 1-23, 1986.

Diester-Haass, L. and Rothe, P. Plio-Pleistocene sedimentation on the Walvis Ridge, southeast Atlantic (DSDP Leg 75, Site 532) - Influence of surface currents, carbonate dissolution and climate. *Marine Geology*, 77, 53-85, 1987.

Diester-Haass, L. Sea level changes, carbonate dissolution and history of the Benguela Current in the Oligocene-Miocene off southwest Africa. *Marine Geology*, 79, 213-242, 1988.

Diester-Haass, L., Meyers, P.A., and Rothe, P. Miocene history of the Benguela Current and Antartic ice volumes: Evidence from rhythmic sedimentation and current growth across the Walvis Ridge (Deep Sea Drilling Project Sites 362 and 532). *Paleoceanography*, 5, 685-707, 1990.

Diester-Haass, L., Meyers, P.A., and Rothe, P. The Benguela Current and associated upwelling on the southwest African Margin: a synthesis of the Neogene-Quaternary sedimentary record at DSDP Sites 362 and 532. *In*: Summerhayes, C.P., Prell, W.L. & Emeis, K.C. (Eds), Upwelling Systems: Evolution Since the Early Miocene. *Geological Society Special Publication,* 64, 331-342, 1992.

Duncombe Rae, C.M., Shillington, F.A., Agenbag, J.J., Taunton-Clark, J., and Gründlingh, M.L. An Agulhas Ring in the South Atlantic Ocean and its interaction with the Benguela upwelling frontal system. *Deep-Sea Res.*, 39 (11/12), 2009-2027, 1992.

Dupont, L.M. and Leroy, S. Steps toward drier conditions in north-western Africa during the Upper Pliocene. *In*: Vrba, E., Denton, G.H., Partridge, T. C., and Burckle, L. H. (Eds), *Paleoclimate and Evolution, with emphasis on human origins*, Yale University Press, New Haven, CT: 289-298, 1995.

Dupont, L.M., Schneider, R.R., Schmüser, A., and Jahns, S. Marine-terrestrial interaction of climate changes in West Equatorial Africa of the last 190,000 years. *Paleoecology of Africa*, 26, 61-84, 1999.

Dupont, L.M., Donner, B., Schneider R.R., Wefer, G. Mid-Pleistocene environmental change in tropical Africa began as early as 1.05 Ma. *Geology*, 29, 195-198, 2001.

Eisma, D, Kalf, J., and van der Gaast, S.J. Suspended matter in the Zaire estuary and the adjacent Atlantic Ocean. *Neth. J. Sea Res.*, 12, 382-406, 1978.

Emeis, K.-C., Anderson, D.M., Doose, H., Kroon, D., and Schulz-Bull, D. Sea-surface temperatures and the history of monsoon upwelling in the northwest Arabian Sea during the last 500,000 years. *Quat. Res.*, 43, 355-361, 1995.

Emiliani, C. Pleistocene temperatures. *J. Geol.*, 63, 538-578, 1955.

Fairbanks, R.G., Sverdlove, M., Free, R., Wiebe, P.H. and Bé, A.H.W. Vertical distribution and isotopic fractionation of living planktonic foraminifera from the Panama Basin. *Nature*, 298, 841-844, 1982.

Flohn, H. Climatic belts in the case of a unipolar glaciation. *In*: Mörner, N. A. and Karlen, J. (Eds) *Climatic Changes on a Yearly to Millenial Basis, Proceedings of the Second NATO Symposium on Climatic Changes and Related Problems*. D. Reidel, Dordrecht, 609-620, 1984.

Gingele, F.X. Holocene climatic optimum in Southwest Africa - evidence from the marine clay mineral record. *Palaeogeogr., Palaeoclim., Palaeoeco.*, 122, 77-87, 1996.

Gingele, F.X., Müller, P.J., and Schneider, R.R. Orbital forcing of freshwater input in the Zaire Fan area - clay mineral evidence from the last 200 kyr. *Palaeogeogr., Palaeoclim., Palaeoeco.*, 138, 17-26, 1998.

Giraudeau, J. Distribution of recent nannofossil beneath the Benguela system: southwest African continental margin. *Marine Geology,* 108, 219-237, 1992.

Giraudeau, J., Pierre, C., and Herve, L. A Late Quaternary, High-Resolution Record of Planktonic Foraminiferal Species Distribution in the Southern Benguela Region: Site 1087. In: Wefer, G., Berger, W.H., and Richter, C. (Eds.). *Proc. ODP, Sci. Results*, 175, 1-26 [Online]. Available from World Wide Web:<http://www-odp.tamu.edu/publications/175_SR/VOLUME/CHAPTERS/SR175_11.PDF>, 2001.

Gordon, A. Indian-Atlantic transfer of thermocline water at the Agulhas retroflection. *Science,* 227, 1030-1033, 1985.

Güntner, U. Geochemische Signale in Tiefseesedimenten des südwestafrikanischen Kontinentalrands: Indikatoren für paläoklimatische und paläoozeanographische Bedingungen. *Dissertation*, Carl von Ossietzky Universität Oldenburg, Oldenburg, pp 137, 2000.

Hagen, E., Schemainda, R., Michelsen, N., Postel, L., Schulz, S., and Below, M. Zur Küsten-senkrechten Struktur des Kaltwasserauftriebs vor der Küste Namibias. *Geodätische und geophysikalische Veröffentlichungen*, 36, 1-99, 1981.

Hart, T.J. and Currie, R.T. The Benguela Current. *Discovery Rep.*, 31, 123-298, 1960.

Hastenrath, S. On meridional heat transports in the world ocean. *J. Phys. Oceanogr.*, 12 (8), 922-927, 1982.

Hay, W.W., Sibuet, J.C. et al., *Initial Reports of the Deep Sea Drilling Project*, 75, Washington (U.S. Govt. Printing Office),1984.

Hay, W.W. and Brock, J.C. Temporal variation in intensity of upwelling off southwest Africa. *In*: Summerhayes, C.P., Prell, W.L. & Emeis, K.C. (Eds), *Upwelling Systems: Evolution since the Early*

Miocene. Geological Society Special Publication 63, 463-497, 1992.

Hays, J.D., Imbrie, J., and Shackleton, N.J. Variations in the Earth's Orbit: Pacemaker of the Ice Ages. *Science*, 194, 1121-1132, 1976.

Holtvoeth, J., Wagner, T., Horsfield, B, Schubert, C.B., Wand, U. Late-Quaternary supply of terrigenous organic matter to the Congo deep-sea fan (ODP site 175): implications for equatorial African paleoclimate. *Geo-Marine Letters*, 21, 23-33, 2001.

Imbrie, J, and Imbrie, K.P. Ice ages: solving the mystery. Enslow, Short Hills, New Jersey, 1979.

Imbrie; J., Hays J.D., Martinson, D.G., McIntyre, A., Mix, A.C., Morley, J.J., Pisias, N.G., Prell, W.L., and Shackleton, N.J. The orbital theory of Pleistocene climate: Support from a revised chronology of the marine $\delta^{18}O$ record. *In*: A.L. Berger et al. (Eds), *Milankovitch and Climate, Part 1*, 269-305, 1984.

Imbrie, J., McIntyre, A., and Mix, A. Oceanic Response To Orbital Forcing In The Late Quaternary: Observational and Experimental Strategies. *In*: A. Berger et al. (Eds), *Climate and Geo-Sciences*, 121 - 164, Kluwer Academic Publishers, 121-164, 1989.

Imbrie, J., Berger, A., and Shackleton, N.J. Role of orbital forcing: a two million year perspective. *In*: Eddy, J.A., and Oeschger, H. (Eds) *Global Changes in the Perspective of the Past*, Chichester, Wiley, 263-277, 1993.

Imbrie, J., Boyle, E.A., Clemens, S.C., Duffy, A., Howard, W.R., Kukla, G, Kutzbach, J., Martinson., D.G., McIntyre, A., Mix, A., Molfino, B., Morley, J.J., Peterson, L.C., Pisias, N.G., Prell, W.L., Raymo, M.E., Shackleton, N.J., and Toggweiler, J.R. On The Structure And Origin Of Major Glaciation Cycles 2. The 100,000-year cycle. *Paleoceanography*, 8, 699-735, 1993.

Jahnke, R.A. and Shimmield, G.B. Particle flux and its conversion to the sediment record: Coastal ocean upwelling systems. *In*: Summerhayes, C.P., Angle, M.V., Smith, R.L., Emeis, K.C., and Zeitschel, B. (Eds), *Upwelling in the oceans: Modern processes and ancient records*. Dahlem Workshop Rep., J. Wiley & Sons, 83-100, 1995.

Jansen, J.H.F., Van Weering, T.C.F., Gieles, R., and Van Iperen, J. Late Quaternary oceanography and climatology of the Zaire / Congo fan and the adjacent eastern Angola Basin. *Neth. J. Sea Res.*, 17, 201-249, 1984.

Jansen, J.H.F. Middle and Late Quaternary carbonate production and dissolution, and paleoceanography of the eastern Angola Basin, South Atlantic Ocean. *In*: Hsü, K.J., and Weissert, H.J. (Eds) *South Atlantic paleoceanography*. Cambridge (University Press), 25-46, 1985.

Jansen, J.H.F. Glacial-interglacial oceanography of the southeastern Atlantic Ocean and the paleoclimate of west central Africa. *In*: Lanfranchi, R. and Schwartz, D. (Eds), *Paysages quaternaires de l'Afrique centrale atlantique*, 110-123, Office de la Recherche Scientifique et Technique Outre-Mer., Paris, 1990.

Jansen, J.H.F. and Van Iperen, J.M. A 200,000-year climatic record for the east equatorial Atlantic Ocean and equatorial Africa: Evidence from diatoms and opal phytoliths in the Zaire (Congo) deep-sea Fan. *Paleoceanography*, 6, 573-591, 1991.

Jansen, J.H.F., Van der Gaast, S.J., Koster, B. and Vaars, A.J. CORTEX, a shipboard XRF-scanner

for element analyses in split sediment cores. *Marine Geology* 151, 143-153, 1998.

Jenkins, G.M. and Watts, D.G.. Spectral analysis and its applications. Holden Day, San Francisco, 525 pp, 1968.

Kirst, G., Schneider, R.R., Müller, P.J., von Storch, I., and Wefer, G. Late Quaternary temerature variability in the Benguela Current system derived from alkenones. *Quaternary Research*, 52, 92-103, 1999.

Köppen, W. and Wegener, A. Die Klimate der geologischen Vorzeit. Bornträger, Berlin, 1924.

Kutzbach, J.E. and Liu, Z. Response of the African monsoon to orbital forcing and ocean feedbacks in the middle Holocene, *Science*, 278, 440-443, 1997.

Lancaster, N. Paleoenvironmental implications of fixed dune systems in Southern Africa. *Palaeogeography, Palaeoclimatology, Palaeoecologogy*, 33, 327-346, 1981.

Lancaster, N. Development of linear dunes in the southwestern Kalahari, Southern Africa. *J. Arid Environments*, 14, 233-244, 1988.

Lange, C.B., Berger, W.H., Lin, H.-L., Wefer, G., and Shipboard Scientific Party Leg 175. The early Matuyama Diatom Maximum off SW Africa, Benguela Current System (ODP Leg 175). *Marine Geology* 161, 93-114, 1999.

Little, M.G., Schneider, R.R., Kroon, D., Price, B., Bickert, T., and Wefer, G. Rapid palaeoceanographic changes in the Benguela Upwelling System for the last 160,000 years as indicated by abundances of planktonic foraminifera. *Palaeogeography, Palaeoclimatology, Plalaeoecology*, 130, 135-161, 1997a.

Little, M.G., Schneider, R.R., Kroon, D., Price, B., Summerhayes, C.P., and Segl, M. Trade wind forcing and upwelling, seasonality, and Heinrich events as a response to sub-Milankovitch climate variability. *Paleoceanography*, 12, 568-576, 1997b.

Lutjeharms, J.R.E. and Stockton, P.L. Kinematics of the upwelling front off southern Africa. *In*: Payne, A.I.L., Gulland, J.A. and Brink, K.H. (Eds), *The Benguela and Comparable Ecosystems*. South African Journal of Marine Science 5, 51-62, 1987.

Lutjeharms, J.R.E. and Meeuwis, J.M. The extent and variability of southeast Atlantic upwelling, *In:* Payne, A.I.L., Gulland, J.A., and Brink, K.H. (Eds), The Benguela and Comparable Ecosystems, *S. Afr. J. mar. Sci.*, 5, 51-62, 1987.

Lutjeharms, J.R.E. and van Ballegooyen, R.C. The retroflection of the Agulhas Current. *J. Phys. Oceanogr.*, 18, 1570-1583, 1988.

Lutjeharms, J.R.E., Shilington, F.A., and Duncombe Rae, C.M. Observations of extreme upwelling filaments in the southeast Atlantic Ocean. *Science*, 253, 774-776, 1991.

Lutjeharms, J.R.E., Lucas, M.I., Perissinotto, R., van Ballegooyen, R.C., and Ronault, M. Oceanic processes at the Subtropical Convergence; report of research cruise SAAMES III. *S. A. J. Sci.*, 90, 367-370, 1994.

Lutjeharms, J.R.E. The exchange of water between the South Indian and South Atlantic ocean. *In*: Wefer, G., Berger, W.H., Siedler, G., Webb, D. (Eds), *The South Atlantic: Present and Past Circulation*, Springer, Berlin, 125-162, 1996.

Manabe, S. and Stouffer, R.J. Coupled ocean-atmosphere model response to freshwater input:

Comparison to Younger Dryas event. Paleoceanography, 12, 321-336, 1997.

Marlow, J.R., Lange, C.B., Wefer, G., Rosell-Mele, A.Upwelling Intensification as Part of the Pliocene-Pleistocene Climate Transition. *Science* 290, 2288-2291, 2000.

Marlowe, I.T., Brassell, S.C., Eglington, G., and Green, J.C. Long-chain alkenones and alkyl alkenoates and the fossil coccolith record of marine sediments. *Chem. Geol.*, 88, 349-375, 1990.

Martin, R.A. Benthonic foraminifera from the Orange-Lüderitz shelf, Southern African continental margin. *Bull. Mar. Geosci.* Unit, No. 11, Dep. Of Geol., Univ. Cape Town, Cape Town, 82 pp, 1981.

Martinson, D.G., Pisias, N.G., Hays, J.D., Imbrie, J., Moore, T.C., Shackleton, N.J. Age Dating and the Orbital Theory of the Ice Ages: Development of a High-Resolution 0 to 300,000-Year Chronostratigraphy. *Quatern. Res.*, 27, 1-29, 1987.

McIntyre, A., Ruddiman, W.F., Karlin, K., and Mix, A.C. Surface water response of the equatorial Atlantic Ocean to orbital forcing. *Paleoceanography*, 4, 19-55, 1989.

Meeuwis, J.M. and Lutjeharms J.R.E. Surface thermal characteristics of the Angola-Benguela front. *S Afr J Mar Sci.*, 9, 261-279, 1990.

Milankovitch, M. Mathematische Klimalehre und astronomische Theorie der Klimaschwankungen. *In*: Köppen, W. und Geiger, R. (Eds), *Handbuch der Klimatologie*, Bd. 1, Teil A, Gebr. Bornträger, 1930.

Moroshkin, K.V., Bubnov, V.A., and Bulatov, R.P. Water circulation in the eastern South Atlantic Ocean. *Oceanology*, 10, 27-37, 1970.

Mpounza, M. and Samba-Kimbata, M.J. Apercu sur le climat de l'Afrique centrale occidentale. *In*: Lanfranchi, R. and Schwartz, D. (Eds), *Paysages quaternaires de l'Afrique centrale atlantique*, 31-41, Office de la Recherche Scientifique et Technique Outre-Mer., Paris, 1990.

Mudelsee, M. and Stattegger, K. Exploring the structure of the mid-Pleistocene revolution with advanced methods of time-series analysis. *Geol. Rundschau*, 86, 499-511, 1997.

Müller, P.J., and Suess, E. Productivity, sedimentation rate, and sedimentary carbon content in the oceans. *Deep-Sea Res.*, 26A, 1347-1362, 1979.

Müller, P.J., and Schneider, R.R. An automated leaching method for the determination of opal in sediments and particulate matter. *Deep-Sea Res.*, 40, 425-444, 1993.

Müller, P.J., Schneider, R.R., and Ruhland, G. Late Quaternary pCO_2 variations in the Angola Current: Evidence from organic carbon $\delta^{13}C$ and alkenone temperatures. *In*: R. Zahn, M.A. Kaminski, L. Labeyrie and T.F. Pedersen (Eds), *Carbon cycling in the glacial ocean: Constraints on the oceans role in global change*. NATO ASI Ser., 117, Springer, Heidelberg, 343-366, 1994.

Müller, P.J., Cepek, M., Ruhland, G., and Schneider, R.R. Alkenone and coccolithophorid species changes in late Quaternary sediments from the Walvis Ridge: Implications for the alkenone paleotemperature method. *Palaeogeography, Palaeoclimatology, Palaeoecology*, 135, 71-96, 1997.

Müller, P.J., Kirst, G., Ruhland, G., von Storch, I, and Rosell-Melé, A. Calibration of the alkenone paleotemperature index $U_{37}^{k'}$ based on core-tops from the eastern South Atlantic and the global ocean (60°N-60°S). *Geochim. Cosmochim. Acta*, 62, 1757 - 1722, 1998.

Nelson, G., and Hutchings, L. The Benguela upwelling area. *Progr. Oceanogr.*, 12, 333-356, 1983.

Niebler, H.-S. Reconstruction of paleo-environmental parameters using stable isotopes and faunal assemblages of planktonic foraminifera in the South Atlantic Ocean. *Berichte zur Polarforschung*, 167, 198 pp, 1995.

Oberhänsli, H. Upwelling Signals At The Northeastern Walvis Ridge During The Past 500,000 Years. *Paleoceanography*, Vol. 6, No. 1, 53-71, 1991.

Paillard, D., Labeyrie, L., and Yiou, P. Macintosh program performs time-series analysis. *EOS Trans.*, AGU, 77: 379, 1996.

Partridge, T.C., DeMenocal, P.B., Lorentz, S.A., Paiker, M.J., and Vogel, J.C. Orbital forcing of climate over South Africa: A 200,000-year rainfall record from the Pretoria Saltpan. Quaternary *Science Reviews*, 16, 1125-1133, 1997.

Pastouret, L., Chamley, H., Delibrias, G., Duplessy, J.C., and Thiede, J. Late Quaternary climatic changes in western tropical Africa deduced from deep-sea sedimentation off Niger delta. *Oceanol. Acta I* (2), 217-232, 1978.

Peerdeman, F.M., Davies, P.J., Chivas, A.R. The stable oxygen isotope signal in shallow-water, upper-slope sediments off the Great Barrier Reef (Hole 820 A). In: McKenzie, J.A., Davies, P.J., Palmer-Julson, A. et al. (Eds.). *Proc. Ocean Drilling Program Sci. Results 133*, 163-173, 1993.

Petschick, R., Kuhn, G., Gingele, F.X. Clay mineral distribution in surface sediments of the South Atlantic sources transport and relation to oceanography. *Mar. Geol.*, 130, 203-229, 1996.

Peterson, R.G. and Stramma, L. Upper-level circulation in the South Atlantic Ocean. *Prog. Oceanogr.*, 26, 1-73, 1991.

Prahl, F.G. and Wakeham, S.G. Calibration of unsaturation patterns in long-chain ketone compositions for paleotemperature assessment. *Nature*, 330, 367-369, 1987.

Prahl, F.G., Muehlhausen, L.A., and Zahnle, D.L. Further evaluation of long-chain alkenones as indicators of paleoceanographic conditions. *Geochim. Cosmochim. Acta*, 52, 2203-2310, 1988.

Prahl, F.G., Pisias, N., Sparrow, M.A., and Sabin, A. Assessment of sea-surface temperature at 42°N in the California Current over the last 30,000 years. *Paleoceanography*, 10, 763-773, 1995.

Prell, W.L. Oxygen and carbon isotope stratigraphy for the Quaternary of hole 502B: evidence for two modes of isotopic variability. *In*: Prell, W.L., Gardner, J.V. et al. (Eds), *Init. Repts. DSDP*, 68, U.S. Govt. Printing Office, Washington DC, 455-464, 1982.

Raymo, M.E., Ruddiman, W.F., Backman, J., Clement, B.M., Martinson, D.G. Late Pliocene variation in northern hemisphere ice sheets and North Atlantic deep water circulation, *Paleoceanography* 4, 413-446, 1989.

Raymo, M.E., Oppo, D.W., and Curry, W. The mid-Pleistocene climate transition: A deep sea carbon isotopic perspective. *Paleoceanography* 12, 546-559, 1997.

Rigg, G.M., van Ballegooyen, R.C., Attwood, C., Newton, S., Lucas, M., and Lutjeharms, J.R.E. Data report on the first cruise of the South African Antarctic Marine Ecosystem study (SAAMES I), Univ. Cape Town Dept., *Oceanogr. Rep.*, pp 30, 1992.

Röhl, U. and Abrams, L.J. High-resolution, downhole and non-destructive core measurements from Sites 999 and 1001 in the Caribbean Sea: application to the Late Paleocene Thermal Maximum.

Proc. ODP, Scientific Results, 165, 191-203, 2000.

Ruddiman, W.F., McIntyre, A., and Raymo, M.E. Matuyama 41,000-year cycles: North Atlantic Ocean and northern hemisphere ice sheets. *Earth and Planet Sci. Lett.*, 80, 117-129, 1986.

Ruddiman, W.F., and Raymo, M.E. Northern hemisphere climate regimes during the past 3 Ma: possible tectonic connections. *Phil. Trans. R. soc. Lond. B* 318, 411-430, 1988.

Ruddiman, W.F., Raymo, M.E., Martinson, D.G., Clement, B., Backman, J. Pleistocene evolution: Northern hemisphere ice sheets and North Atlantic Ocean. *Paleoceanography* 4, 353-412, 1989.

Rühlemann, C., Müller, P.J., and Schneider, R.R. Organic carbon and carbonate as paleoproductivity proxies: Examples from high and low productivity areas of the tropical Atlantic. *In*: Fischer, G., and Wefer, G. (Eds), *Use of Proxies in Paleoceanography: examples from the South Atlantic*. Springer-Verlag, Berlin Heidelberg, 315-344, 1999.

Rutherford, S. and D'Hondt, S. Early onset and tropical forcing of 100,000-year Pleistocene glacial cycles. *Nature*, 408, 72-75, 2000.

Saltzman, B., and Maasch, K.A. A first-order global model of late Cenozoic climatic change, II. A simplification of CO_2 dynamics. *Clim. Dyn.* 5, 201-210, 1991.

Saltzman, B., and Verbitsky, M.Y. Multiple instabilities and modes of glacial rhythmicity in the Plio-Pleistocene: a general theory of late Cenozoic climatic change. *Clim. Dyn.*, 9, 1-15, 1994.

Sancetta, C., Heusser, L., and Hall, M.A. Late Pliocene climate in the Southeast Atlantic: Preliminary results from a multi-disciplinary study of DSDP Site 532. *Marine Micropaleontology*, 20, 59-75, 1992.

Sarnthein, M., Winn, K., and Zahn, R. Paleoproductivity of oceanic upwelling and the effect on atmospheric CO_2 and climatic change during deglaciation times. *In*: Berger, W.H., and Labeyrie, L.D. (Eds), *Abrupt Climatic Change: Evidence and Implications*. NATO ASI Series, C: Mathematical and Physical Sciences. D. Reidel Publishing Company, 311-337, 1987.

Schefuss, E., Versteegh, G.J.M., Jansen, J.H.F., Sinninghe Damste, J.S. Marine and terrigenous Lipids in Southeast Atlantic Sediments (Leg 175) as Paleoenvironmental Indicators: Initial Results. *In*: Wefer, G., Berger, W.H., and Richter, C. (Eds), *Proc. ODP, Sci. Results*, 175, 1-34 (Online). Available from World Wide Web:<http://www-odp.tamu.edu/publications/175_SR/VOLUME/CHAPTERS/SR175_11.PDF>, 2001.

Schlünz, B., Schneider, R.R., Müller, P.J., Showers, W.J., and Wefer, G. Terrestrial organic carbon accumulation on the Amazon deep sea fan during the last glacial sea level low stand. *Chem. Geol.*, 159 (1-4), 263-281, 1999.

Schneider, R.R. Spätquartäre Produktivitätsänderungen im östlichen Angola-Becken: Reaktion auf Variationen im Passat-Monsun-Windsystem und in der Advektion des Benguela-Küstenstroms, *Ber. Fachb. Geowiss. 21*, 198 pp., Univ. Bremen, Bremen, Germany, 1991.

Schneider, R. R., Müller, P. J., and Wefer, G. Late Quaternary productivity changes off the Congo deduced from stable carbon isotopes of planktonic foraminifera. *Palaeogeography, Palaeoclimatology, Palaeoecology*, 110: 255-274, 1994.

Schneider, R.R., Müller, P.J., and Ruhland, G. Late Quaternary surface circulation in the east

equatorial South Atlantic: Evidence from alkenone sea surface temperatures. *Paleoceanography*, 10, 197 - 219, 1995.

Schneider, R.R., Müller, P.J., Ruhland, G., Meinecke, G., Schmidt, H., Wefer, G. Late Quaternary surface temperatures and productivity in the east-equatorial South-Atlantic: Response to changes in trade/monsoon wind forcing and surface advection. *In* Wefer, G., Berger, W.H., Siedler, G., Webb, D.J. (Eds), *The South Atlantic: Present and Past Circulation*, Springer-Verlag Berlin Heidelberg, 527-551, 1996.

Schneider, R.R., Price, B., Müller, P.J., Alexander, I. Monsoon related variations in Zaire (Congo) sediment load and influence of fluvial silicate supply on marine productivity in the east equatorial Atlantic during the last 200,000 years. *Paleoceanography*, 12, 3, 463-481, 1997.

Schulz, H.D., Beese, D., Breitzke, M., Brück, L., Brügger, B., Dahmke, A., Dehning, K., Diekamp, V., Donner, B., Ehrhardt, I., Gerlach, H., Giese, M., Glud, R., Gumprecht, R., Gundersen, J., Henning, R., Hinrichs, S., Petermann, H., Richter, M., Sagemann, J., Schmidt, W., Schneider, R., Scholz, M., Segl, M., Werner, U., and Zabel, M. Bericht und Ergebnisse über die Meteor-Fahrt M 20/2 Abidjan-Dakar. *Berichte*, Fachbereich Geowissenschaften, Universität Bremen, Nr. 25, 1992.

Shackleton, N.J., Berger, A., Peltier, W.R. An alternative astronomical calibration of the lower Pleistocene timescale based on ODP Site 677. *Transactions Royal Society Edinburgh: Earth Sciences*, 81, 251-261, 1990.

Shackleton, N.J. The 100,000-Year Ice-Age Cycle Identified and Found to Lag Temperature, Carbon Dioxide, and Orbital Eccentricity. *Science*, 289, 1897-1902, 2000.

Shannon, L.V. The Benguela ecosystems: Part I. Evolution of the Benguela, physical features and processes. *Annual Review of Oceanography and Marine Biology*, 23, 105-182, 1985.

Shannon, L.V., Agenbag, J.J., and Buys, M.E.L. Large- and mesoscale features of the Angola-Benguela front. *In*: Payne, A.I.L., Gulland, J.A., and Brink, K.H. (Eds), *The Benguela and comparable ecosystems*. S Afr. J. Mar. Sci., 5, 11-34, 1987.

Shannon, L.V., and Nelson, G. The Benguela: Large Scale Features and Processes and System Variability. *In*: Wefer, G., Berger, W.H., Siedler, G., Webb, D.J. (Eds.). *The South Atlantic: Present and Past Circulation*, Springer-Verlag, Berlin, 163-210, 1996.

Shi, N. and Dupont, L.M. Vegetation and climate history of SW Africa: a marine palynological record of the last 300,000 years. *Veg. Hist. Archaeobot.*, 6, 117-131, 1997.

Simpson, E.S.W. The geology of the South-West African margin: a review. *In: The Geology of the East Atlantic Continental Margin*, ICSU/SCOR Working Party 31, Symp. Cambridge 1970, Inst. Of Geol. Sciences, London, Rep. No. 70/16, 153-170, 1971.

Siesser, W.G., Scrutton, R.A., and Simpson, E.S.W. *In*: Burke, C.A., and Drake, C.L. (Eds.) *The Geology of Continental Margins*. Springer-Verlag, New York, 641-654, 1974.

Siesser, W.G. Late Miocene origin of the Benguela upwelling system off northern Namibia, *Science* 208, 283-285, 1980

Stuut, J.-B., Prins, M.A., Schneider, R.R., Weltje, G.J., Jansen, J.H.F., and Postma, G. A 300 kyr record of aridity and wind strength in southwestern Africa: evidence from grain-size distributions

of sediments on Walvis Ridge, SE Atlantic. *Marine Geology*, in press.

Summerhayes, C.P., Kroon, D., Rosell-Melé, A., Jordan, R.W., Schrader, H.-J., Hearn, R., Villanueva, j., Grimalt, J.O., and Eglington, G. Variability in the Benguela Current upwelling system over the past 70,000 years. *Prog. Oceanog.*, 35, 207-251, 1995.

Thierstein, H.R., Geitzennauer, K.R., Molfino, B., and Shackleton, N.J. Global synchroneity of late Quaternary coccolith datum levels: Validation by oxygen isotopes. Geology, 5, 400-404, 1977.

Tiedemann, R., Sarntheim, M. and Shackleton, N.J. Astronomic Timescale for the Pliocene Atlantic $\delta^{18}O$ and dust flux records of Ocean Drilling Program Site 659. *Paleoceanography*, Vol. 9, No. 4, 619-638, 1994.

Tyson, R.V. Sedimentary organic matter. Chapman & Hall, London, 615 pp, 1995.

Ufkes, E., Jansen, J.H.F., Schneider, R.R. Anomalous occurrence of *Neogloboquadrina pachyderma* (left) in a 420-ky upwelling record from Walvis Ridge (SE Atlantic). *Marine Micropaleontology*, 40, 23-42, 2000.

Uliana, E., Lange, C.B., Donner, B., and Wefer, G. Siliceous phytoplankton productivity fluctuations in the Congo Basin over the past 460,000 years: marine vs. riverine influence, ODP Site 1077. *In:* Wefer, G., Berger, W.H., and Richter, C. (Eds.), *Proc. ODP, Sci. Results*, 175, 1-32 [Online]. Available from World Wide Web:<http://www-odp.tamu.edu/publications/175_SR/VOLUME/CHAPTERS/SR175_11.PDF>, 2001.

Van Andel, T.H., Heath, G.R. and Moore, T.C. Cenozoic history and paleoceanography of the central equatorial Pacific Ocean. *Geol. Soc. Am. Mem.*, 143: pp 134, 1975.

Van Bennekom, A.J. and Berger, G.W. Hydrography and silica budget of the Angola Basin. *Neth. J. Sea. Res.*, 17 (2-4), 149-200, 1984.

Van Bennekom, A.J. Silica signals in the South Atlantic. *In*: Wefer, G., Berger, W.H., Sieder, G, and Webb, D.J. (Eds), *The South Atlantic: Present and Past Circulation*. Springer-Verlag, Berlin, Heidelberg, 345-354, 1996.

Van der Gaast, S.J. and Jansen, J.H.F. Mineralogy, opal, and manganese of middle and late Quaternary sediments of the Zaire (Congo) deep-sea fan: Origin and climatic variation. *Neth. J. Sea Res.*, 17, (2-4), 313-341, 1984.

Van Iperen, J.M., van Weering, T.C.E., Jansen, J.H.F., and van Bennekom, A.J. Diatoms in surface sediments of the Zaire deep-sea fan (SE Atlantic Ocean) and their relation to overlying water masses. *Neth. J. Sea Res.*, 21 (3), 203-217, 1987.

Van Zinderen Bakker, E.M. A Late- and post-glacial pollen record from the Namib Desert. *Palaeoecology of Africa and its surrounding islands*, 16, 1984.

Vidal, L., Schneider, R.R., Marchal, O., Bickert, T., Stocker, T.F., Wefer, G. Link between the North and South Atlantic during the Heinrich events of the last glacial period. *Climate Dynamics*, 15, 909 - 919, 1999.

Vincent, E. and Berger, W.H. Carbon dioxide and polar cooling in the Miocene: the Monterey hypothesis. *In*: Sundquist, E.T., and Broecker, W.S. (Eds), *The Carbon Cycle and Atmospheric CO_2: Natural Variations Archeon to Present*, Amer. Geophys. Union Geophys. Monogr., 32, 455-468, 1985.

Volkman, J.K., Eglington, G., Corner, E.D.S, and Forsberg, T.E.V. Long-chain alkanes and alkenones in the marine coccolithophorid *Emiliania huxleyi*. *Phytochemistry* 19, 2619-2622, 1980.

Volkman, J.K., Barrett, S.M., Blackburn, S.I., and Sikes, E.L. Alkenones in Gephyrocapsa oceanica: implications for studies of paleoclimate. *Geochim. Cosmochim. Acta*, 59, 513-520, 1995.

Wagner, T. Control of organic carbon accumulation in the late Quaternary equatorial Atlantic (Ocean Drilling Program sites 664 and 663): Productivity versus terrigenous supply. *Paleoceanography, 15*, 181-199, 2000.

Ward, J.D., Seely, M.K., and Lancaster, N. *S. Afr. J. Sci.*, 80, 72-77, 1983.

Wefer, G., Berger, W.H., Bickert, T., Donner, B., Fischer, G., Kemle-v. Mücke, S., Meinecke, G., Müller, P.J., Mulitza, S., Niebler, H.-S., Pätzold, J., Schmidt, H., Schneider, R.R., and Segl, M. Late Quaternary Surface Circulation of the South Atlantic: The Stable Isotope Record and Implications for Heat Transport and Productivity. *In*: Wefer, G., Berger, W.H., Siedler, G., Webb, D. (Eds.), *The South Atlantic: Present and Past Circulation*, Springer, Berlin, 363-410, 1996.

Wefer, G., Berger, W.H., Richter, C. and Shipboard Scientific Party. Facies patterns and authigenic minerals of upwelling deposits off southwest Africa. *In*: Wefer, G., Berger, W.H., and Richter, C., et al., *Proc. ODP, Init. Repts.*, 175: College Station, TX (Ocean Drilling Program), 273-312, 1998.

Wigley, T.M.L. Spectral analysis and the astronomical theory of climatic change. *Nature*, 264, 629-631, 1976.

Winter, A. and Siesser, W. Coccolithophores, Cambridge University Press, Cambridge, pp 1-242, 1994.

Zabel, M, Schneider, R.R., Wagner, T., Adegbie, A.T., de Vries, U., Kolonic, S. Documentation of Late Quaternary Climate Changes in Central Africa by Variations of Terrigenous Input to the Niger Fan. *Quaternary Res.*, 56, 207-217, 2001.

APPENDIX

1. Presentations at international conferences

Jahn, B., Donner, B., Müller, P., Röhl, U., Schneider, R. & Wefer, G. Environmental Changes in the Benguela Upwelling for the last 1.5 Ma (ODP Site 1082). 2.NEBROC-Workshop, Februar 1999, Texel, Netherland.

Jahn, B., Donner, B., Müller, P., Röhl, U., Schneider, R. & Wefer, G. Environmental Changes in the Benguela Upwelling for the last 1.5 Ma (ODP Site 1082). ODP-Kolloquium, März 1999, Bremerhaven, Germany.

Jahn, B., Donner, B., Müller, P., Röhl, U., Schneider, R. & Wefer, G. Environmental Changes in the Benguela Upwelling for the last 1.5 Ma (ODP Site 1082). 10th Euopean Union of Geoscience, März-April 1999, Straßbourg, France.

Jahn, B., Donner, B., Müller, P., Röhl, U., Schneider, R. & Wefer, G. Late Pleistocene Paleoclimatology in the Benguela Upwelling System for the last 1.5 Ma. AGU Fall-Meeting, Dezember 1999, San Francisco, USA

Jahn, B., Dupont, L., Donner, B., Müller, P., Röhl, U., Schneider, R., & Wefer, G. Changes in marine productivity and terrigenous climate signals in the Congo plume for the last 2 Ma (ODP Site 1075). 3. NEBROC-Workshop, Januar 2000, Bremen, Germany.

Jahn, B., Donner, B., Dupont, L., Müller, P., Röhl, U., Schneider, R.R. und Wefer, G. Frühpleistozäne marine Produktivitätsänderungen und terrigene Klimasignale aus Sedimenten des Kongo Fächers für die letzten 2 Mio. Jahre (ODP Site 1075). ODP-Kolloquium, März 2000, Jena, Germany.

Jahn, B., Donner, B., Müller, P., Röhl, U., Schneider, R. & Wefer, G. Paleoclimatology in the Benguela Upwelling System for the last 1.5 Ma: Results from ODP Leg 175. Quaternary Evolution of the Benguela Coastal Upwelling System: It's Responses to Local and Global Climate Changes, April 2000, Carcans, France.

Jahn, B., Donner, B., Müller, P., Röhl, U., Schneider, R. & Wefer, G. Paleoclimatology in the Benguela Upwelling System for the last 1.5 Ma: Results from ODP Leg 175. JGOFS, September 2000, Bremen, Germany.

DANKSAGUNG

Für die Betreung dieser Arbeit und Unterstützung bei deren Ausführung möchte ich mich an erster Stelle bei Herrn Professor Dr. Gerold Wefer bedanken. Er gab konstruktive Anregungen und schuf eine hervorragende wissenschaftliche Arbeitsumgebung.
Für die freundliche Übernahme des zweiten Gutachtens danke ich Herrn Professor Dr. Rüdiger Henrich.
Priv. Doz. Dr. Ralph R. Schneider hat mich bei der Ausführung der Arbeit sorgfältig betreut.
Meine Kolleginnen und Kollegen aus der Arbeitsgruppe "Meeresgeologie" sorgten für ein gutes Arbeitsklima. Dr. Helge W. Arz, Dr. Barbara Donner, Dr. Lydie Dupont, Dr. Christopher Moos, Dr. Ursula Röhl, Dr. Sonja Schulte und Dr. Eleonora Uliana danke ich für die fachlichen Diskussionen und Kommentare. Dr. Monika Segl und Birgit Meyer-Schack führten die Isotopenmessungen durch und Dr. Peter J. Müller und Hella Buschoff unterstützten mich bei der Durchführung der Elementaranalysen. Für die tatkräftige Unterstützung bei der Alkenonanalyse danke ich Dietmar Grotheer und Ralph Kreutz. Götz Ruhland danke ich für die fachkundliche Hilfe bei Computerproblemen. Für die Korrektur der englischen Sprache bedanke ich mich vor allem bei Walter Hale. Mein Dank gilt auch dem Team aus dem Bremer ODP-Kernlager, die mir die langen Stunden während des Messens im „Container" erträglicher gemacht haben.
Werner Schmidt und vor allem meiner Tochter Rabea, die während der arbeitsreichen Wochen immer zu kurz kamen gilt mein ganz besonderer Dank. Ich bedanke mich auch bei meinen Freunden für die netten Ablenkungen und anhaltenden Aufmunterungen und hier vor allem bei Janneth Pachon de Heller.
Die Arbeit wurde von der Deutschen Forschungsgemeinschaft im Rahmen des Ocean Drilling Programs und im Rahmen des Sonderforschungsbereiches 261 "Der Südatlantik im Spätquartär: Rekonstruktion von Stoffhaushalt und Stromsystemen" finanziell unterstützt.